

Electronic Supporting Information

The Application of Perfluoroheteroaromatic Reagents in the Preparation of Modified Peptide Systems

Diana Gimenez,^a Caitlin A. Mooney,^a Anica Dose,^a Graham Sandford,^a Christopher R. Coxon^{b†} and Steven L. Cobb^{†a}

^a*Department of Chemistry, Durham University, South Road, Durham, DH1 3LE, U.K.*

^b*School of Pharmacy and Biomolecular Sciences, Byrom Street Campus, Liverpool John Moores University, Liverpool, L3 3AF, U.K.*

†Corresponding Authors E-Mail: s.l.cobb@durham.ac.uk and c.r.coxon@ljmu.ac.uk

| | |
|----------------------------------------------------------------------------------------------------|-----------|
| Materials and general methods | 5 |
| Solid phase synthesis of model peptides pep1-3: | 5 |
| General experimental procedure..... | 5 |
| LC/MS characterisation of crude peptides pep1-3 | 6 |
| Model peptide tagging and stapling with perfluoroaromatics: | 9 |
| General procedure for solution phase peptide tagging and stapling | 9 |
| LC/MS analysis of small scale reactions, Entries 1-22 | 9 |
| Pyridine based systems vs. hexafluorobenze. Table 1, Entries 1-5 | 9 |
| Effect of ArF/peptide ratio, concentration and temperature..... | 13 |
| Effect of the nucleophile: Serine and Lysine based peptides. Table 2, Entries 6-9 | 17 |
| Effect of the base: DIPEA vs Cs ₂ CO ₃ . Table 4, Entries 10-15 | 19 |
| Isolation and characterization of compounds 11-23 | 23 |
| General methods..... | 23 |
| Product 11 | 24 |
| General structure and characterization data..... | 24 |
| ¹⁹ F-NMR..... | 25 |
| Product 12 | 26 |
| General structure and characterization data..... | 26 |
| QToF-LC/MS | 26 |
| QToF-MS/MS..... | 27 |
| ¹⁹ F-NMR..... | 27 |

| | |
|--------------------------------------------------|----|
| Product 13 | 28 |
| General structure and characterization data..... | 28 |
| QToF-LC/MS | 28 |
| QToF-MS/MS..... | 29 |
| ¹⁹ F-NMR..... | 29 |
| Product 14 | 30 |
| General structure and characterization data..... | 30 |
| QToF-LC/MS | 30 |
| QToF-MS/MS..... | 31 |
| ¹⁹ F-NMR..... | 31 |
| Product 15 | 32 |
| General structure and characterization data..... | 32 |
| QToF-LC/MS | 32 |
| QToF-MS/MS..... | 33 |
| ¹⁹ F-NMR..... | 33 |
| Product 16 | 34 |
| General structure and characterization data..... | 34 |
| QToF-LC/MS | 34 |
| QToF-MS/MS..... | 35 |
| ¹⁹ F-NMR..... | 35 |
| Product 17 | 36 |
| General structure and characterization data..... | 36 |
| QToF-LC/MS | 36 |
| QToF-MS/MS..... | 37 |
| ¹⁹ F-NMR..... | 37 |
| Product 18 | 38 |
| General structure and characterization data..... | 38 |
| QToF-LC/MS | 38 |
| QToF-MS/MS..... | 39 |
| ¹⁹ F-NMR..... | 39 |
| Product 19 | 40 |
| General structure and characterization data..... | 40 |
| QToF-LC/MS | 40 |
| QToF-MS/MS..... | 41 |

| | |
|----------------------------------------------------------------------------------------------------------|-----------|
| ¹⁹ F-NMR..... | 41 |
| Product 20 | 42 |
| General structure and characterization data..... | 42 |
| QToF-LC/MS | 42 |
| QToF-MS/MS..... | 43 |
| ¹⁹ F-NMR..... | 43 |
| Product 21 | 44 |
| General structure and characterization data..... | 44 |
| QToF-LC/MS | 44 |
| QToF-MS/MS..... | 45 |
| ¹⁹ F-NMR..... | 45 |
| Product 22 | 46 |
| General structure and characterization data..... | 46 |
| QToF-LC/MS | 46 |
| QToF-MS/MS..... | 47 |
| ¹⁹ F-NMR..... | 47 |
| Product 23 | 48 |
| General structure and characterization data..... | 48 |
| QToF-LC/MS | 48 |
| QToF-MS/MS..... | 49 |
| ¹⁹ F-NMR..... | 49 |
| <u>Effect of perfluoro-tagging over Vasopressin and Oxytocin bio-stability</u> | 50 |
| General procedure for solution phase peptide tagging | 50 |
| LC/MS analysis | 50 |
| Oxytocin arylation using pentafluoropyridine (1) and tetrafluoropyridazine (3)..... | 50 |
| Vasopressin arylation using pentafluoropyridine (1) and tetrafluoropyridazine (3)..... | 51 |
| Characterization of tetrafluoropyridazine-tagged analogs 26 and 27 | 53 |
| Product 26 | 54 |
| General structure and characterization data..... | 54 |
| QToF-LC/MS | 54 |
| QToF-MS/MS..... | 55 |
| ¹⁹ F-NMR..... | 55 |
| Product 27 | 56 |
| General structure and characterization data..... | 56 |

| | |
|---------------------------------------------------------------|----|
| QToF-LC/MS | 55 |
| QToF-MS/MS..... | 57 |
| ¹⁹ F-NMR..... | 57 |
| General procedure for digestions using chymotrypsin..... | 58 |
| Bio-stability of non-tagged oxytocin 24 | 60 |
| Bio-stability of perfluoro-tagged oxytocin 26 | 61 |
| Bio-stability of non-tagged vasopressin 25 | 62 |
| Bio-stability of perfluoro-tagged vasopressin 27 | 63 |
| Control digestions using no enzyme | 64 |

Materials and general methods

All chemicals and solvents were analytical grade and used without further purification. Liquid chromatography (LC)-mass spectrometry (ESI+) analyses were performed on a Acquity UPLC BEH C18 column (1.7 μm , 2.1 mm x 50 mm) using a Waters Acquity UPLC system equipped with a photodiode array detector, providing absorbance data from 210 nm to 400 nm. A gradient with eluent I (0.1% HCOOH in water) and eluent II (0.1% HCOOH in acetonitrile) rising linearly from 5 to 95% of II during $t=0.2\text{--}4.0$ min was applied at a flow rate of 0.6 ml/min after 0.2 min of 95% solvent I equilibration. High-resolution QToF-LC/MS and QToF-MS/MS analyses were performed on a Acquity UPLC BEH C18 column also (1.7 μm , 2.1 mm x 50 mm) using a Waters Acquity UPLC system coupled in this case to a Micromass QToF Premier mass spectrometer, also equipped with a photodiode array detector providing absorbance data from 210 nm to 400 nm. A gradient with eluent I (0.1% HCOOH in water) and eluent II (0.1% HCOOH in acetonitrile) rising linearly from 0 to 99% of II during $t=0.0\text{--}5.0$ min was applied at a flow rate of 0.6 ml/min. ^{19}F NMR spectra studies were recorded at 376 MHz in a Bruker Advance spectrometer at 298 K, using 8 scans with a relaxation delay of 1s. All data has been processed using Mestrenova® software.

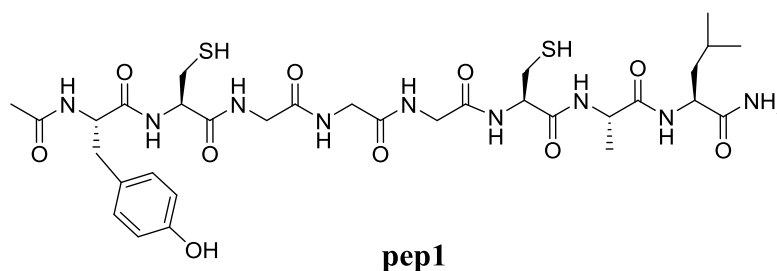
Solid phase synthesis of model peptides pep1-3:

General experimental procedure:

Each of the described peptide sequences was prepared using automated Fmoc-SPPS methods on a Liberty 1 peptide synthesiser (CEM) with microwave-assisted couplings (single coupling per amino acid; 10 min, 75 °C (50 °C for Fmoc-Cys(Trt)-OH coupling). Solid phase synthesis was conducted using Rink amide resin (0.7 mol/g loading) on a 0.1 mmol scale, employing HBTU and DIPEA as the activator and base respectively. Standard acid-sensitive amino acid side chain protecting groups e.g. Boc, tBu, trityl were employed. Following the on-resin growing of the appropriate sequence, N-terminal acetylation was achieved by using a solution of Ac_2O in DMF (20% v/v, 5 mL) while shaking at room temperature for 15 min. Once completed, the beads were washed with DMF three times and the acetylation step repeated. The resin was then carefully washed with DMF, MeOH and CH_2Cl_2 (3 x 10 mL). Finally, peptides were cleaved from the resin as the corresponding C-terminal amides by treatment with a mixture of TFA/TIPS/ H_2O 95:5:5% v/v (2 mL) at room temperature for 4 h. After removal of volatiles in vacuum, the product was triturated and carefully washed with Et_2O (3 x 10 mL). The final precipitated solid residue was then re-dissolved in H_2O /TFA 99:1 (15 ml) and lyophilised affording the corresponding peptides as a white/yellow powder. The crude peptides were used without further chromatographic purification. LC/MS data is given next.

LC/MS characterization of crude peptides **pep1-3**:

Pep1: Ac-YCGGGCAL-NH₂



LC/MS: Calculated m/z : 783.30, observed m/z : 784.12 $[M+H]^+$. Retention time: 2.237 min. Elemental composition: C₃₂ H₄₉ N₉ O₁₀ S₂.

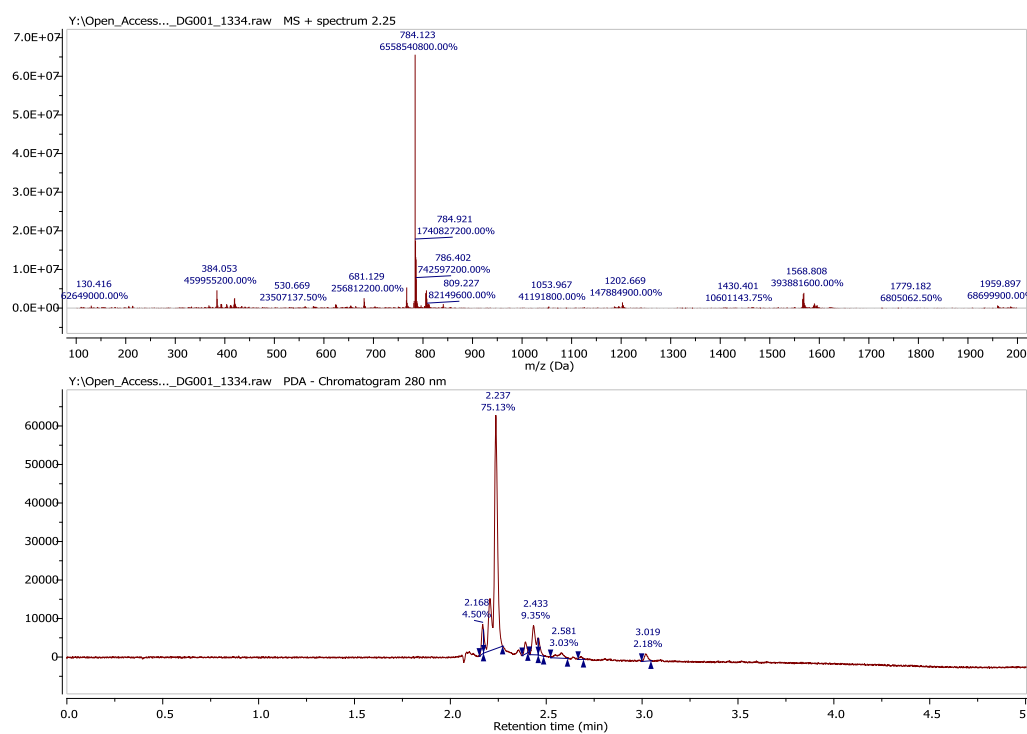
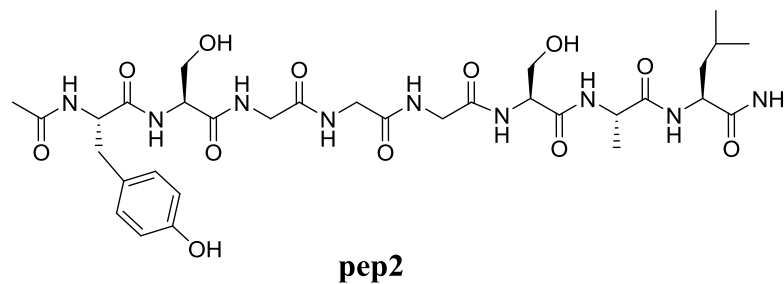


Figure SI01. LC/MS trace at $\lambda = 280$ nm of crude peptide **pep1**.

Pep2: Ac-YSGGGSAL-NH₂



LC/MS: Calculated m/z : 751.35, observed m/z : 752.03 [M+H]⁺. Retention time: 2.045 min. Elemental composition: C₃₂ H₄₉ N₉ O₁₂.

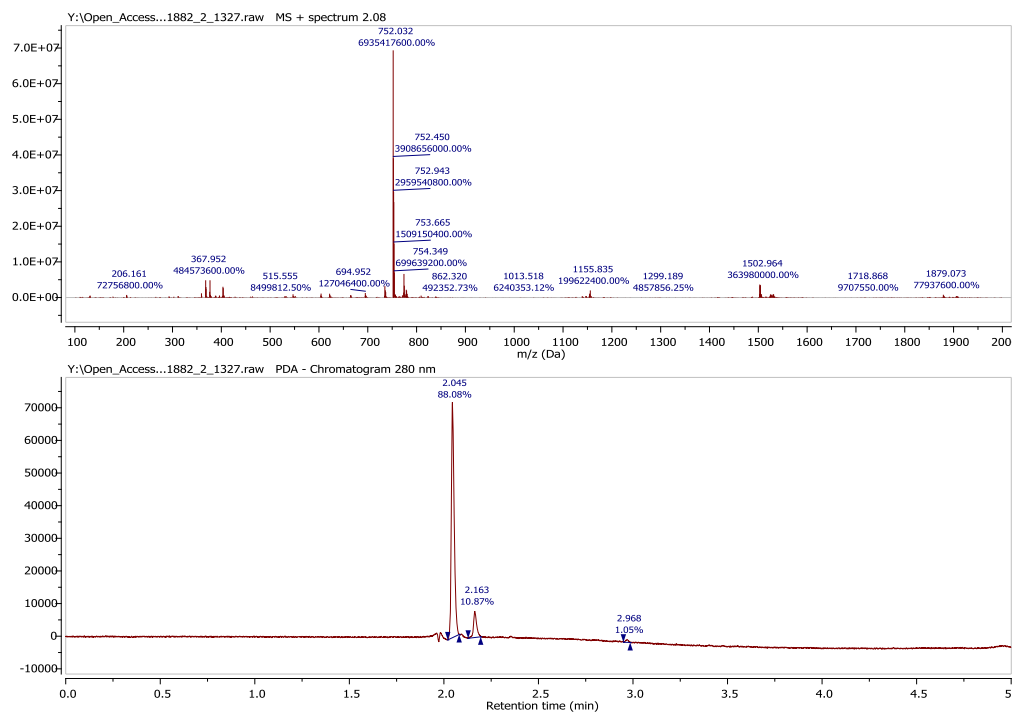
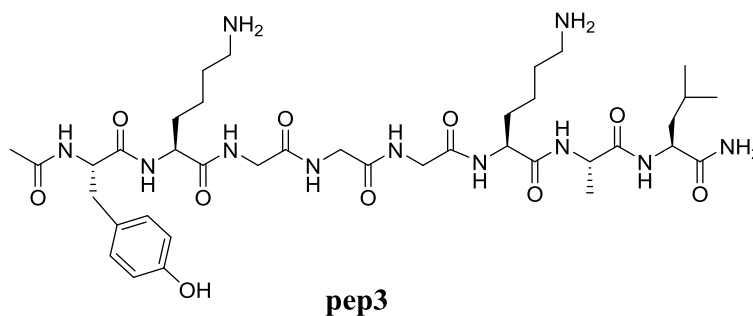


Figure SI02. LC/MS trace at $\lambda=280$ nm of crude peptide **pep2**.

Pep3: Ac-YKGGGKAL-NH₂



LC/MS: Calculated m/z : 833.47, observed m/z : 834.33 [M+H]⁺. Retention time: 1.732 min. Elemental composition: C₃₈ H₆₃ N₁₁ O₁₀.

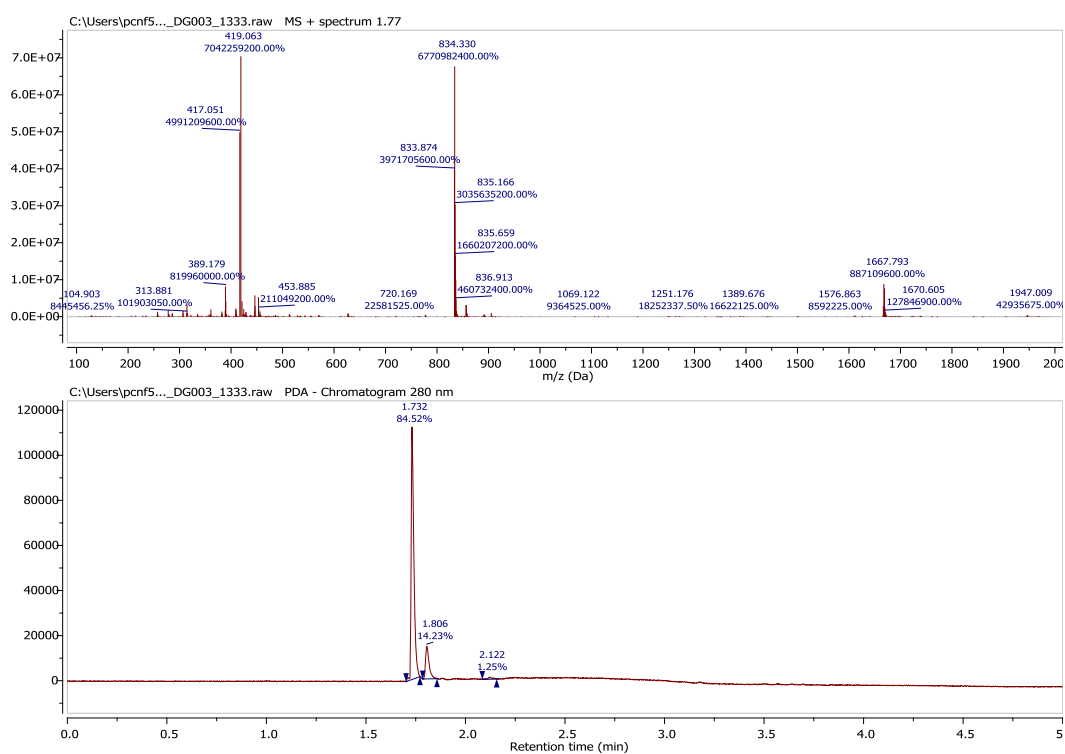


Figure SI03. LC/MS trace at $\lambda=280$ nm of crude peptide **pep3**.

Model peptide tagging and stapling with perfluoroaromatics:

General procedure for solution phase peptide tagging and stapling

Solid crude peptides **pep1-3** (2 mg, approx. 2.5 μmol) were dissolved in the DMF (0.5 mL) in a 1.5 ml plastic Eppendorf tube, to which a Cs_2CO_3 or DIPEA stock solution (50 mM in appropriate solvent, 0.5 mL) was then added. 25 equivalents of the corresponding perfluoroaromatic were slowly added and the tube was shaken vigorously at room temperature for 4.5 h (*method A*, unless otherwise stated). After removal of volatiles under vacuum, all products were dissolved in an 8:1:1 mixture of DMF/ H_2O /MeCN (1 mL) and characterised by LC/MS (ESI+). When formation of novel compounds was observed, 10-fold scaled reactions were employed in all cases for product isolation in order to afford a complete characterization. Scaled reactions were run under exactly the same exposed conditions but in argon flushed syringes, to avoid air bubbles where volatile aromatic compounds could concentrate. LC/MS data for crude reactions is provided next.

LC/MS analysis of small scale reactions

Pyridine based systems vs. hexafluorobenzene. Table 1, Entries 1-5

Entry 1: Ac-YCGGGCAL-NH₂ + **hexafluorobenzene** (1:25) in DMF/DIPEA:

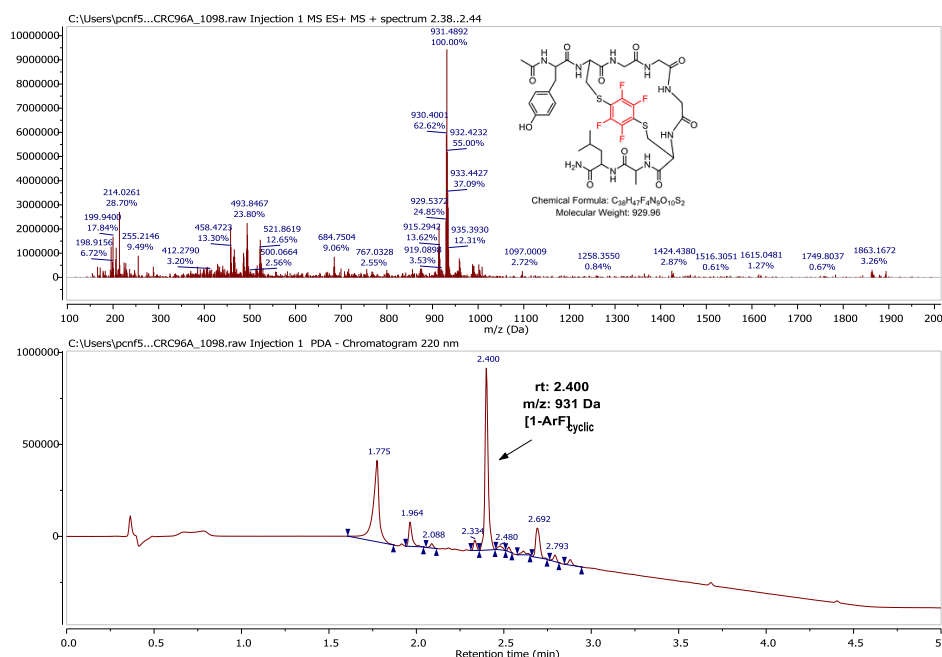


Figure S104. LC/MS traces at $\lambda=220$ nm of crude reaction of peptide **pep1** with hexafluorobenzene when using DIPEA as a base in DMF.

Entry 2: Ac-YCGGGCAL- NH₂ + *pentafluoropyridine* in (1:25) DMF/DIPEA:

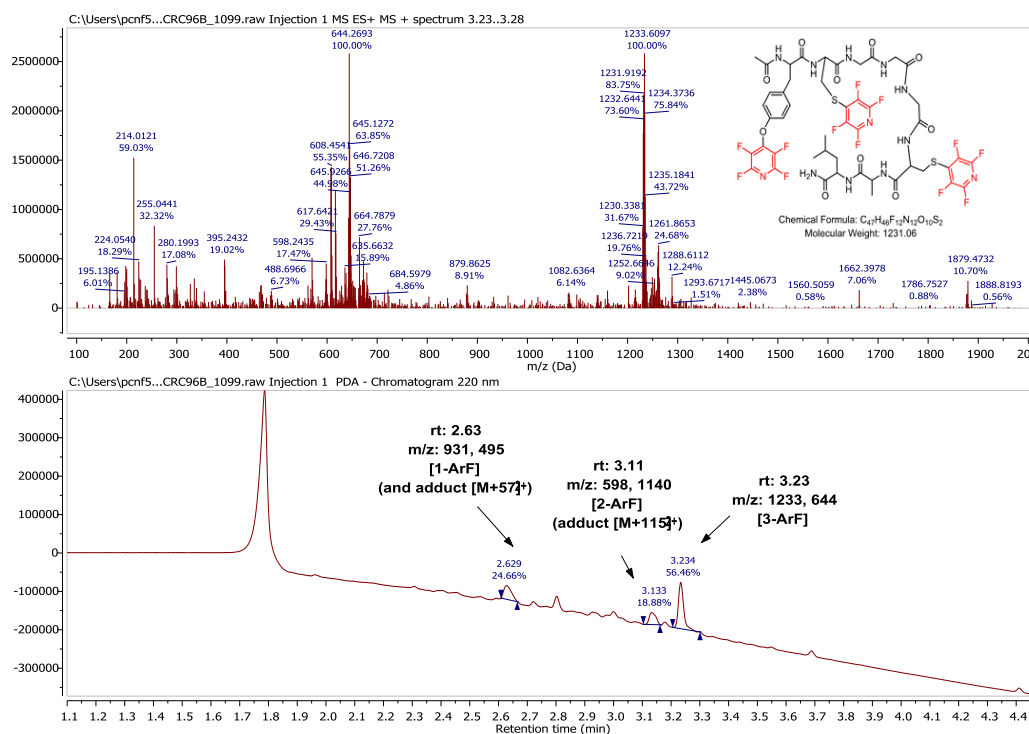


Figure SI05. LC/MS traces at $\lambda=220$ nm of crude reaction of peptide **pep2** with pentafluoropyridine when using DIPEA as a base in DMF.

Entry 3: Ac-YCGGGCAL- NH₂ + *4-aminotetrafluoropyridine* (1:25) in DMF/DIPEA:

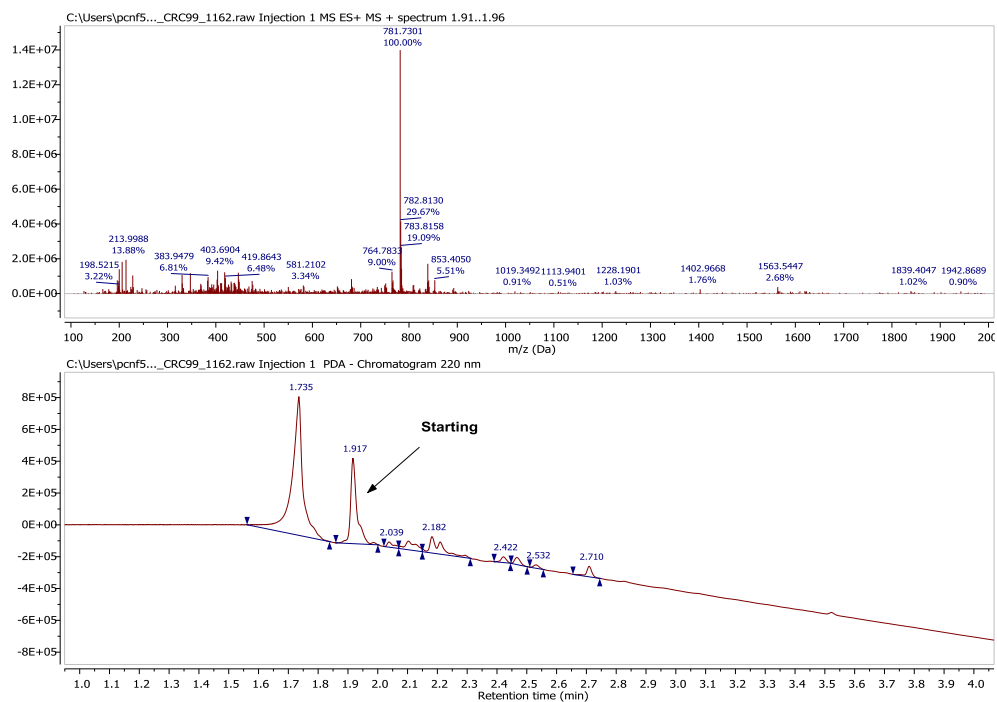


Figure SI06. LC/MS traces $\lambda=220$ nm of crude reaction of peptide **pep3** with hexafluorobenzene when using DIPEA as a base in DMF.

Entry 4: Ac-YCGGGCAL- NH₂ + **4-amino-2-methoxy-3,5,6-trifluoropyridine** (1:25) in DMF/DIPEA:

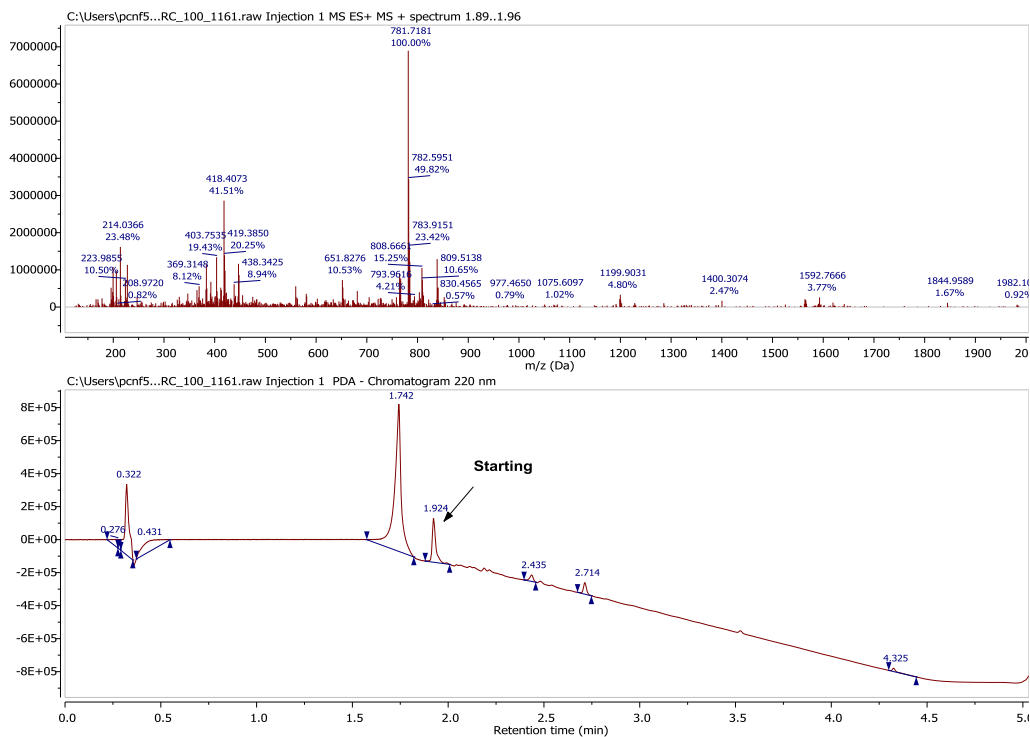


Figure S107. LC/MS traces at $\lambda=220$ nm of crude reaction of peptide **pep1** with pentafluoropyridine when using DIPEA as a base in DMF.

Entry 5: Ac-YSGGGSAL- NH₂ + 4-Amino-3,5-dichloro-2,6-difluoropyridine (1:25) in DMF/DIPEA:

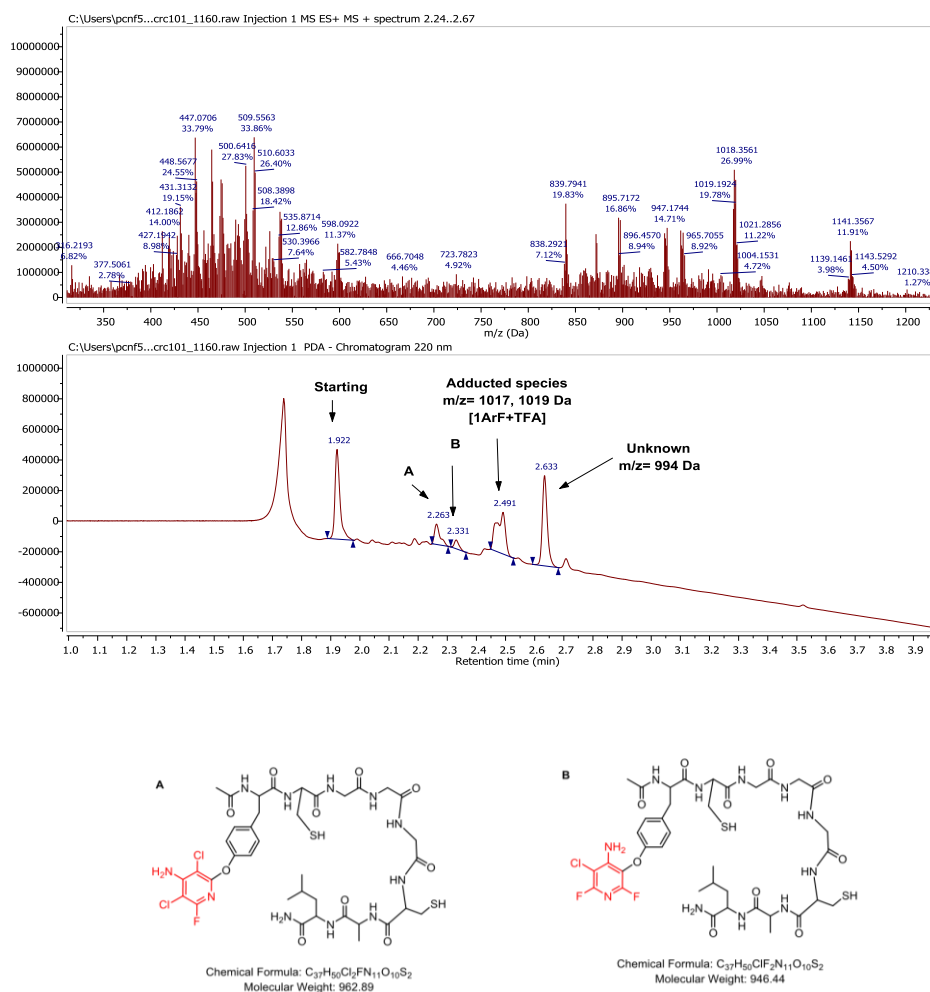
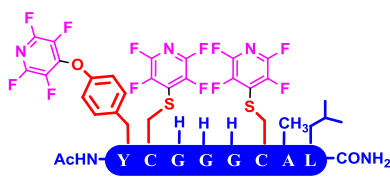
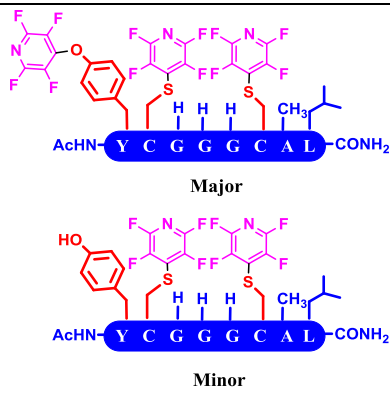
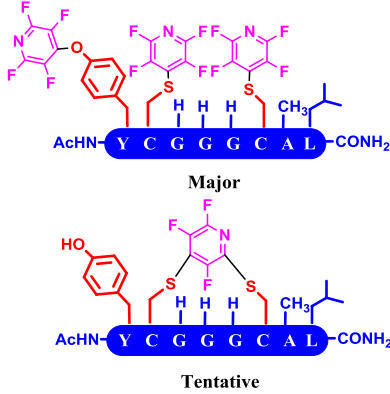


Figure S108. LC/MS traces at $\lambda=220$ nm of crude reaction of peptide **pep2** with pentafluoropyridine when using DIPEA as a base in DMF.

Effect of ArF/peptide ratio, concentration and temperature

In order to explore the impact of changing different reaction parameters alternative methods have been employed based in the above mentioned general procedure A, in all cases employing **pep1** as the model nucleophile. Main results and modifications are summarized in following **Table SI_001**. No other changes aside of those exposed were made to the reactions, work-up or analysis methods.

| Procedure | Conditions | Comments/ Products formed |
|----------------|------------------------------------------------------------|--------------------------------------------------------------------------------------------------------------------|
| A (Entry 2) | PFP 25 equivalents DIPEA 25 mM Vf= 1 mL RT |  |
| B | PFP 5 equivalents DIPEA 25 mM Vf= 1 mL RT |  <p>Major</p> <p>Minor</p> |
| C | PFP 25 equivalents DIPEA 25 mM Vf= 5 mL RT |  <p>Major</p> <p>Tentative</p> |

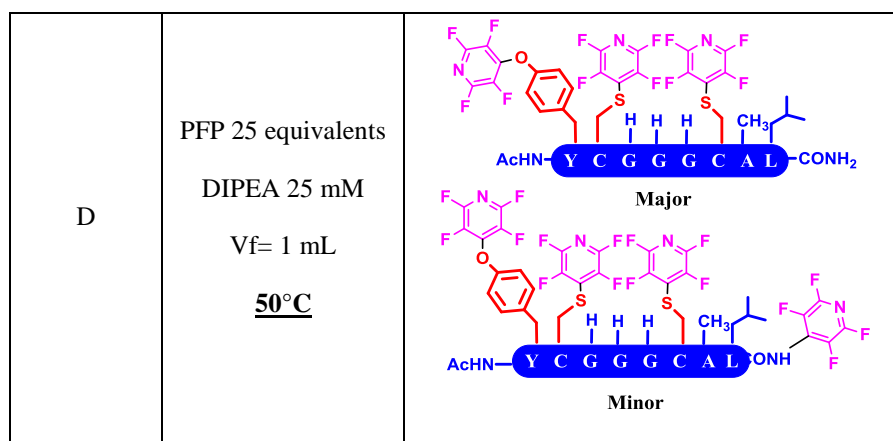


Table SI01: Procedures and overall observed effect of changing some reaction conditions over the SNAr of pentafluoropyridine by the model di-cysteine nucleophilic peptide **pep-1**.

Reactions in Table SI-001

REACTION Ac-YSGGGSAL- NH₂ (2 mg/mL) + pentafluoropyridine (**1:25**) at rt :

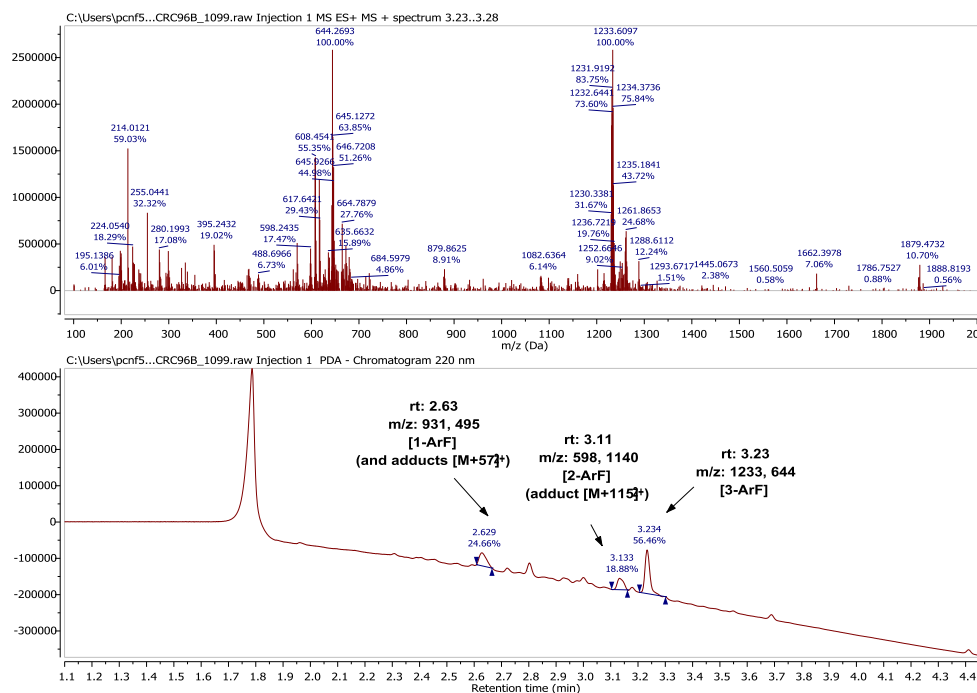
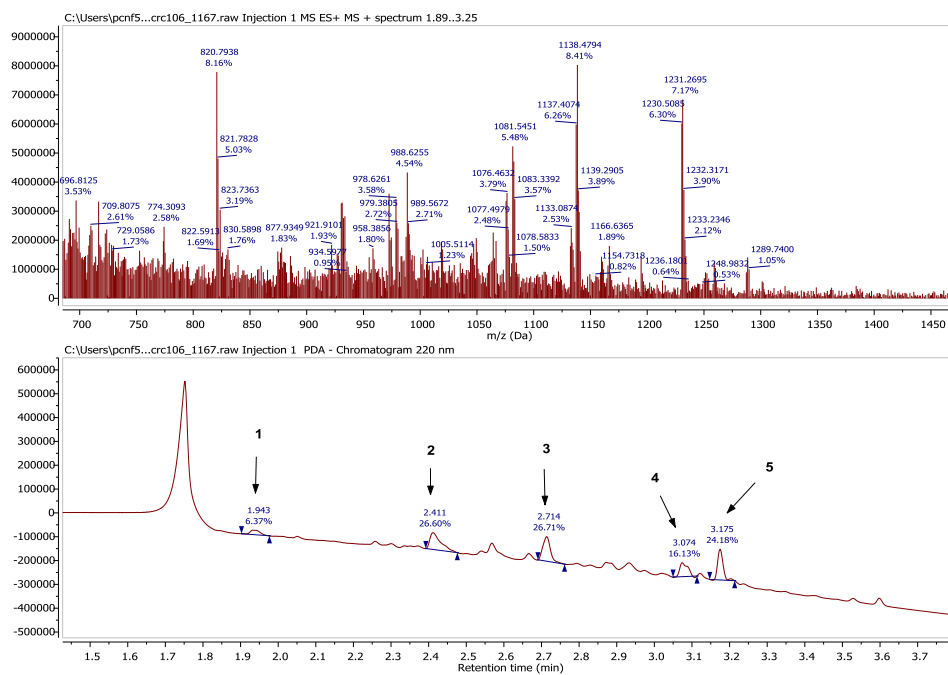


Figure SI09. LC/MS traces at $\lambda=220$ nm of crude reaction of peptide **pep1** with pentafluoropyridine in a ratio 1:25, when using DIPEA as a base in DMF.

REACTION Ac-YCGGGCAL- NH₂ (2 mg/mL) + pentafluoropyridine (**1:5**) at rt:



| Peak | Retention time | <i>m/z</i> | Identity |
|------|----------------|------------|-------------------------------------------|
| 1 | 1.946 | 820 | Starting peptide MeCN adduct |
| 2 | 2.411 | 1076, 1134 | Unknown |
| 3 | 2.714 | 1082 | Double ArF addition |
| 4 | 3.074 | 1138 | [2(M+2ArF)+TFA] ₂ ⁺ |
| 5 | 3.175 | 1231 | Triple ArF addition |

Figure SII0. LC/MS traces at $\lambda=220$ nm of crude reaction of peptide **pep1** with pentafluoropyridine in a ratio 1:5, when using DIPEA as a base in DMF.

REACTION Ac-YSGGGSAL- NH₂ (0.4 mg/mL) + pentafluoropyridine (1:25) at rt

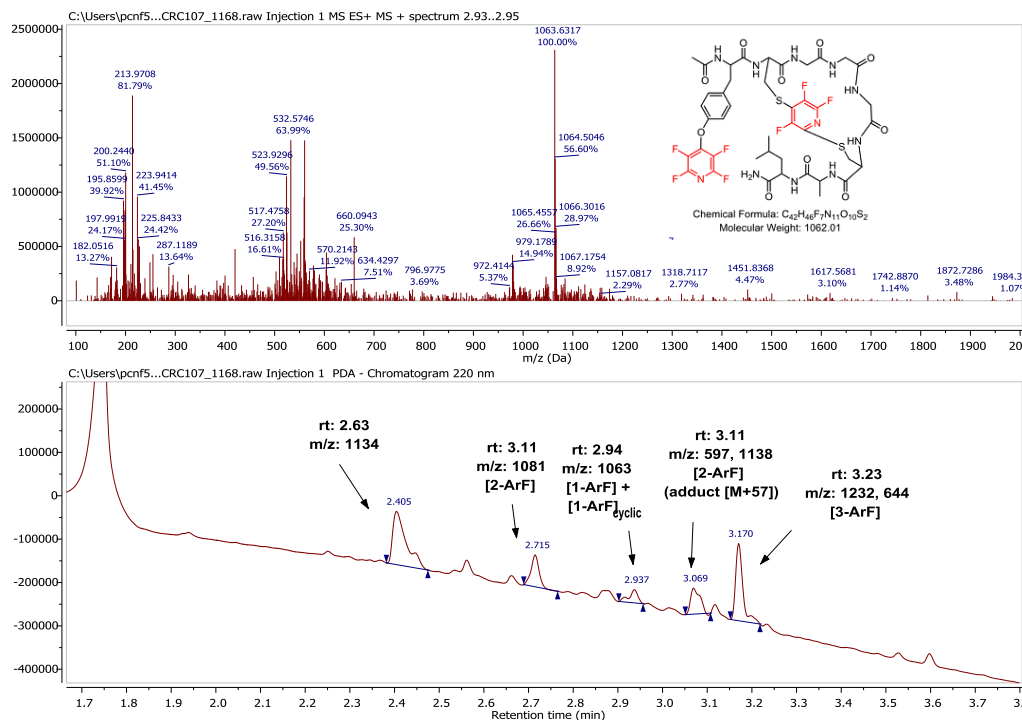


Figure SI11. LC/MS traces at $\lambda=220$ nm of crude reaction of peptide **pep1** with pentafluoropyridine in 5x more diluted conditions, when using DIPEA as a base in DMF.

REACTION Ac-YSGGGSAL- NH₂ (2 mg/mL) + pentafluoropyridine (1:25) at 50°C:

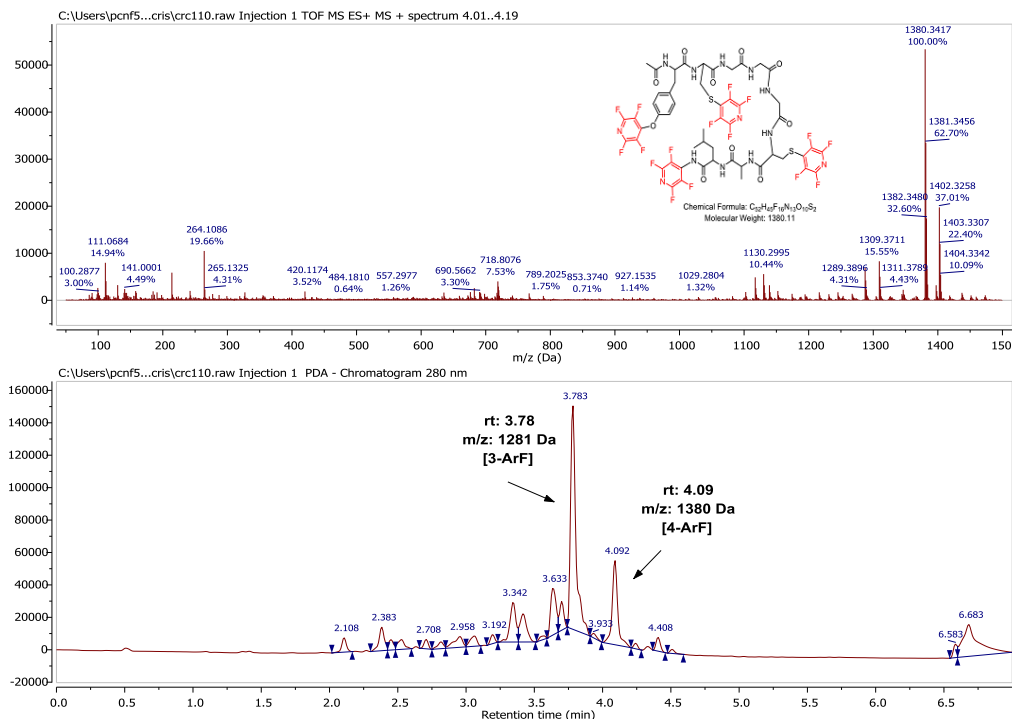


Figure SI12. LC/MS traces at $\lambda=280$ nm of crude reaction of peptide **pep1** with pentafluoropyridine in a ratio 1:25 at 50°C, when using DIPEA as a base in DMF.

Effect of the nucleophile: Serine and Lys based peptides. Table 2, Entries 6-9

Entry 6: Ac-YCGGGCAL- NH₂ + *hexafluorobenzene* (1:25) in DMF/DIPEA:

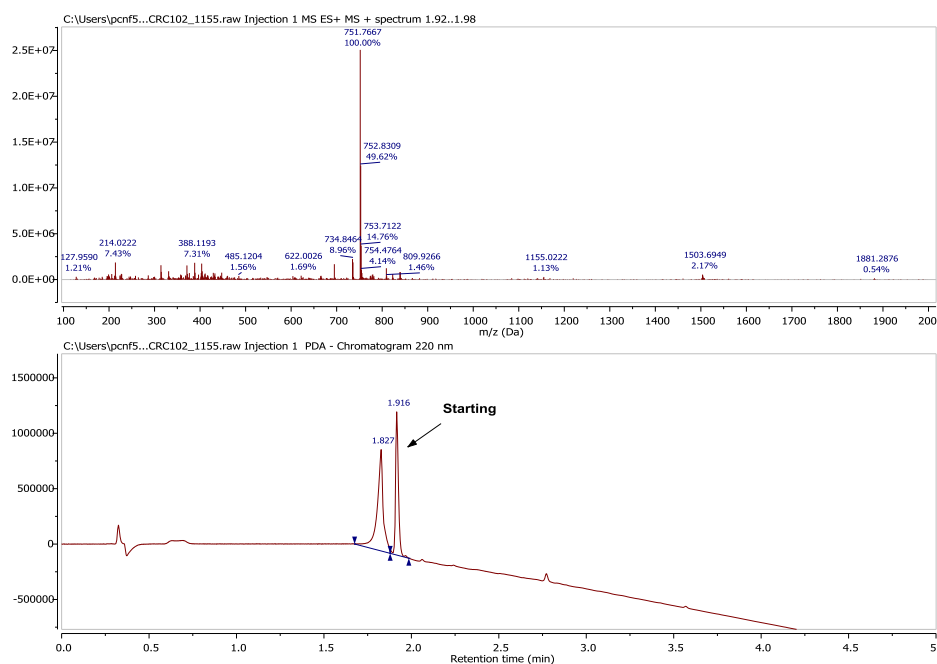


Figure SI13. LC/MS traces at $\lambda=220$ nm of crude reaction of peptide **pep2** with hexafluorobenzene when using DIPEA as a base in DMF.

Entry 7: Ac-YKGGGKAL- NH₂ + *hexafluorobenzene* (1:25) in DMF/DIPEA:

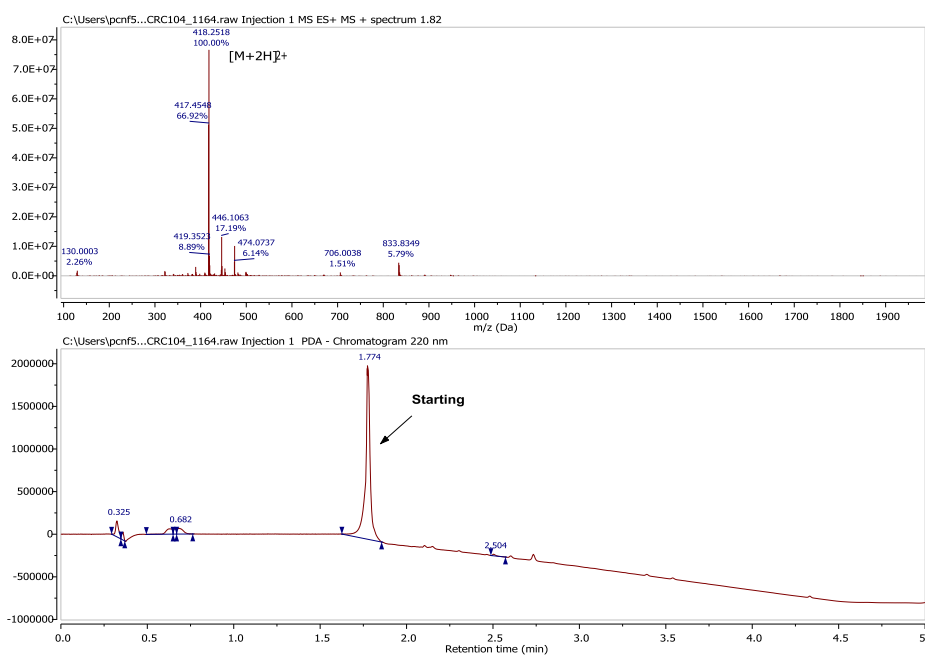


Figure SI14. LC/MS traces at $\lambda=220$ nm of crude reaction of peptide **pep3** with hexafluorobenzene when using DIPEA as a base in DMF.

Entry 8: Ac-YSGGGAL- NH₂ + pentafluoropyridine (1:25) in DMF/DIPEA:

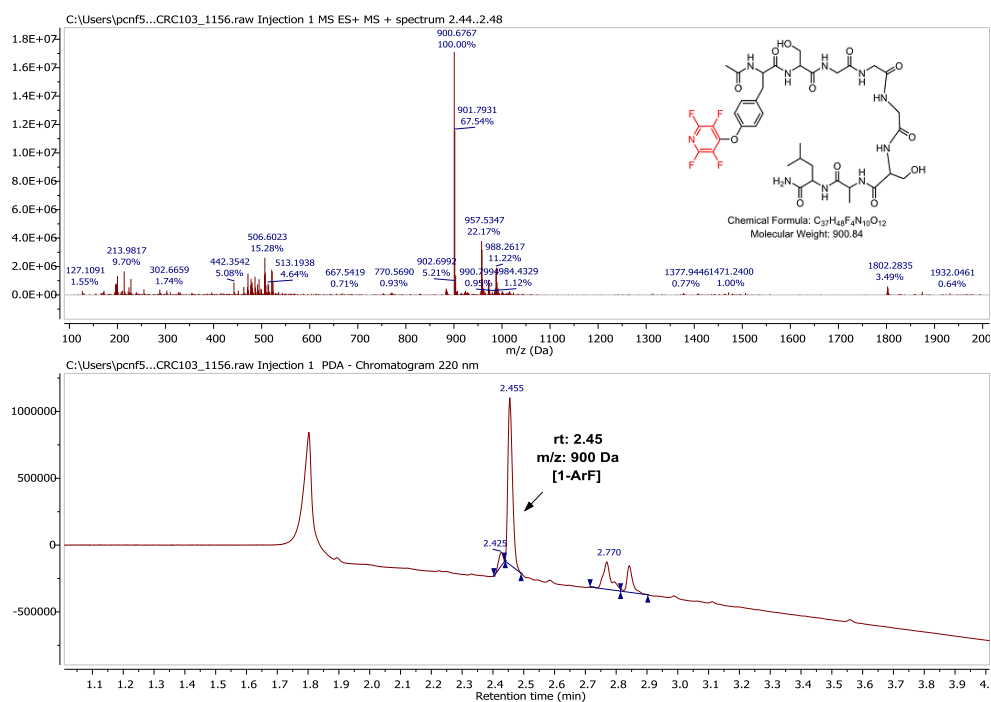


Figure SI15. LC/MS traces at $\lambda=220$ nm of crude reaction of peptide **pep2** with pentafluoropyridine when using DIPEA as a base in DMF.

Entry 9: Ac-YKGGGKAL- NH₂ + pentafluoropyridine (1:25) in DMF/DIPEA:

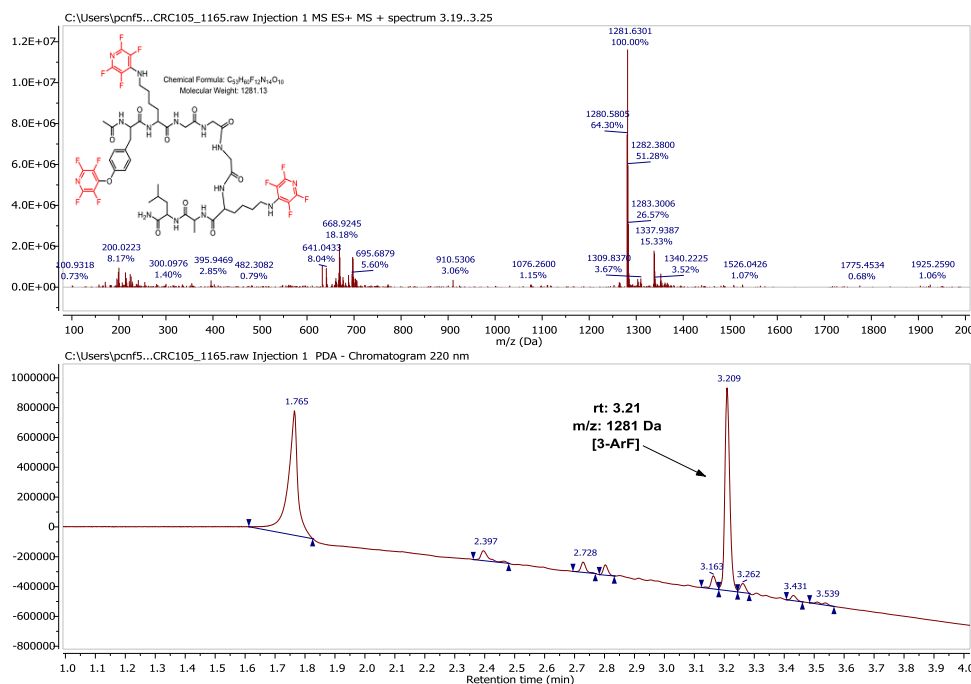


Figure SI16. LC/MS traces at $\lambda=220$ nm of crude reaction of peptide **pep3** with pentafluoropyridine when using DIPEA as a base in DMF.

Effect of the base: DIPEA vs Cs₂CO₃. Table 4, Entries 10-15

Entry 10: Ac-YCGGGCAL-NH₂ + **hexafluorobenzene** (1:25) in DMF/Cs₂CO₃:

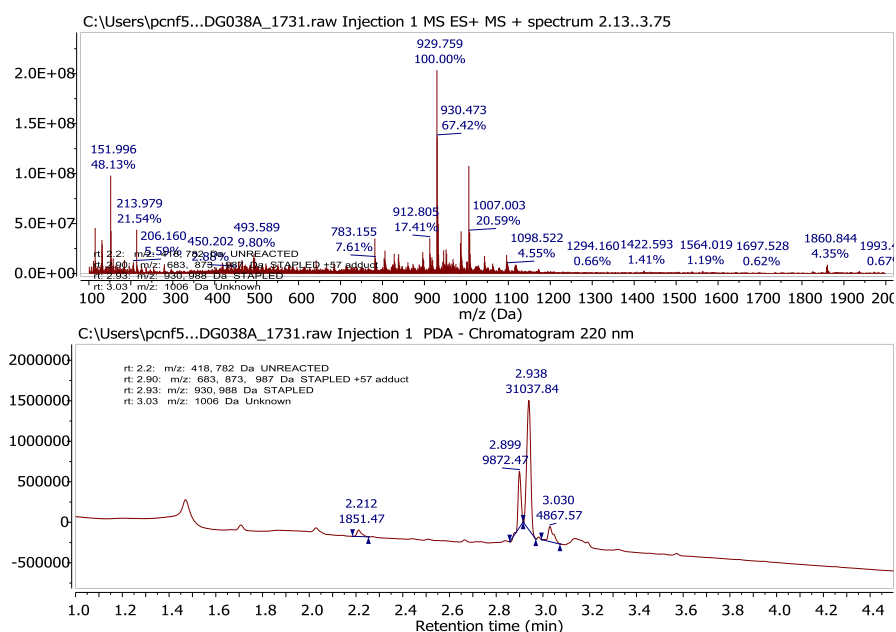


Figure SI17. LC/MS traces at $\lambda=220$ nm of crude reaction of peptide **pep1** with pentafluoropyridine when using Cs₂CO₃ as a base in DMF.

Entry 11: Ac-YSGGGGSAL-NH₂ + **hexafluorobenzene** (1:25) in DMF/Cs₂CO₃:

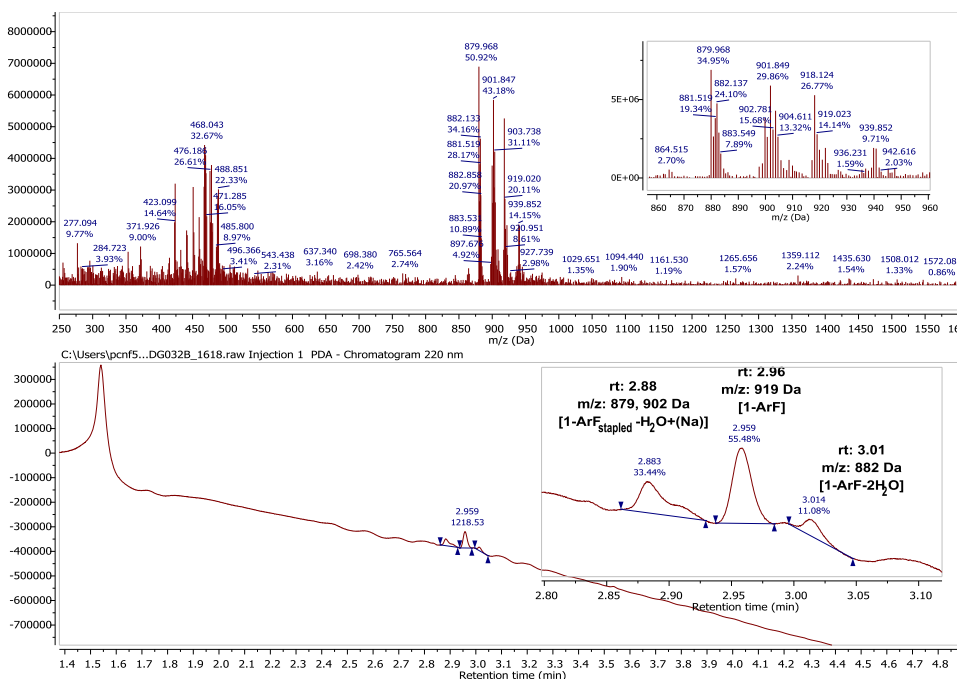


Figure SI18. LC/MS traces at $\lambda=220$ nm of crude reaction of peptide **pep2** with pentafluoropyridine when using Cs₂CO₃ as a base in DMF

Entry 12: Ac-YKGGGKAL- NH₂ + *hexafluorobenzene* (1:25) in DMF/Cs₂CO₃:

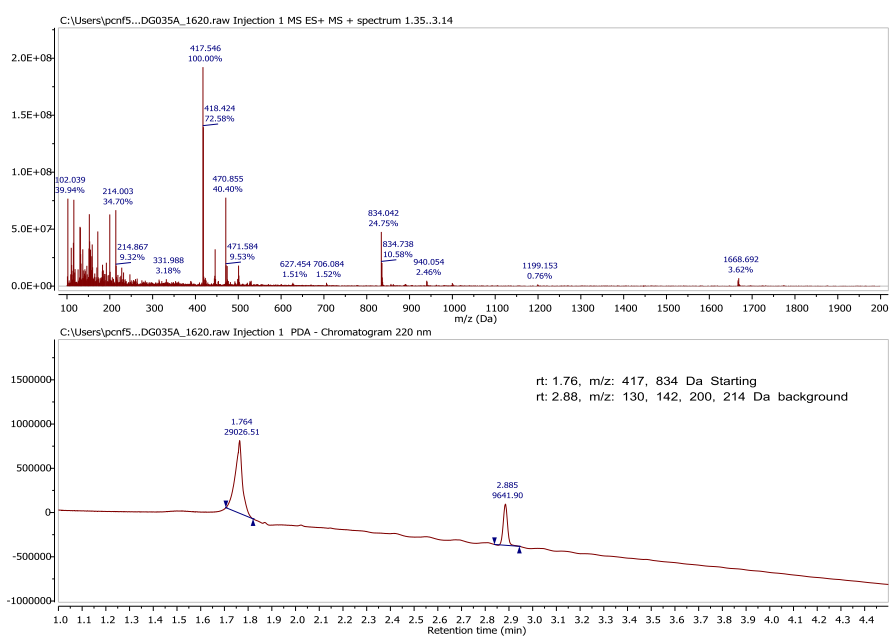


Figure SI19. LC/MS traces at $\lambda=220$ nm of crude reaction of peptide **pep3** with hexafluorobenzene when using Cs₂CO₃ as a base in DMF.

Entry 13: Ac-YCGGGCAL- NH₂ + *pentafluoropyridine* (1:25) in DMF/Cs₂CO₃:

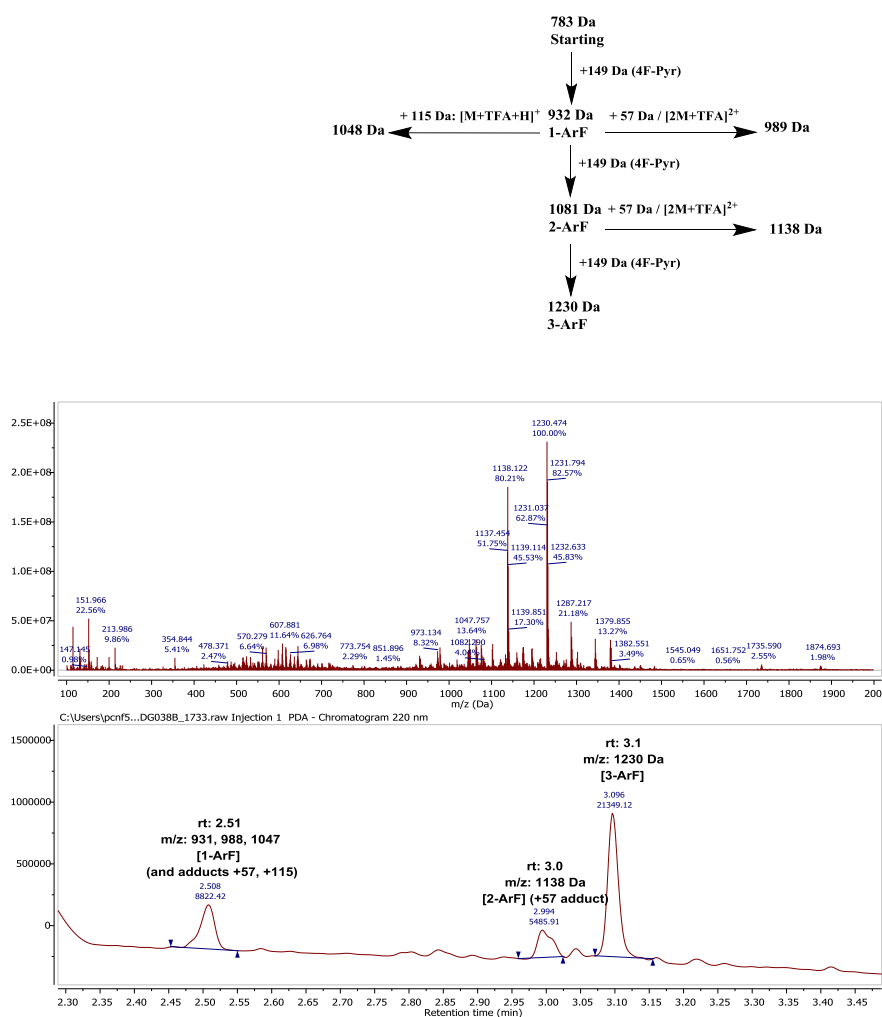


Figure SI20. LC/MS traces at $\lambda=220$ nm of crude reaction of peptide **pep1** with hexafluorobenzene when using Cs₂CO₃ as a base in DMF. Inset showing the scheme corresponding to adduct formation in the basis of the observed masses.

Entry 14: Ac-YSGGGSAL- NH₂ + *pentafluoropyridine* (1:25) in DMF/Cs₂CO₃:

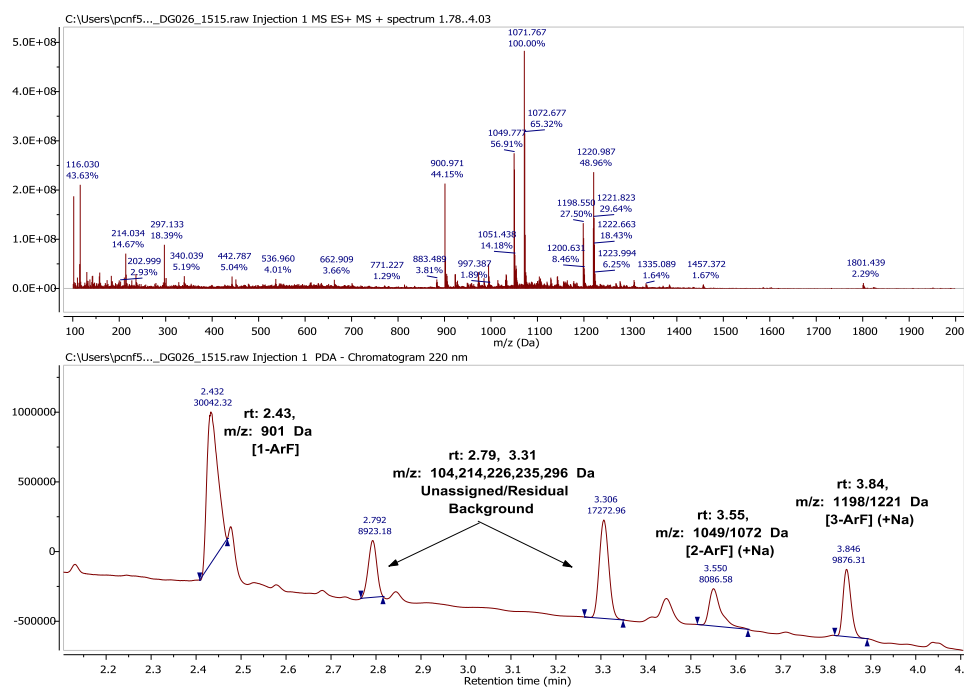


Figure SI21. LC/MS traces at $\lambda=220$ nm of crude reaction of peptide **pep2** with hexafluorobenzene when using Cs₂CO₃ as a base in DMF.

Entry 15: Ac-YKGGGKAL- NH₂ + *pentafluoropyridine* (1:25) in DMF/Cs₂CO₃:

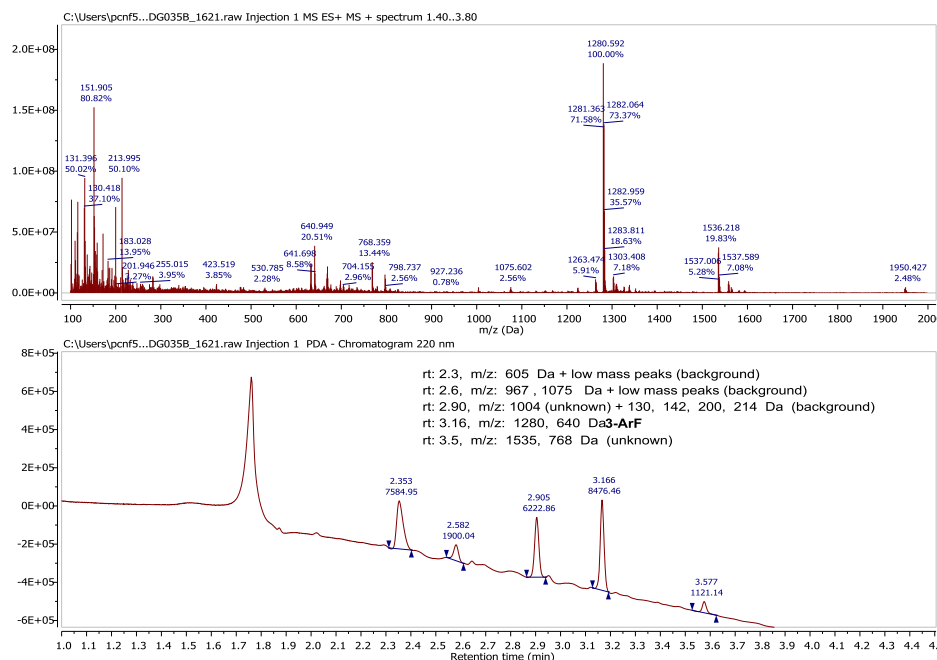


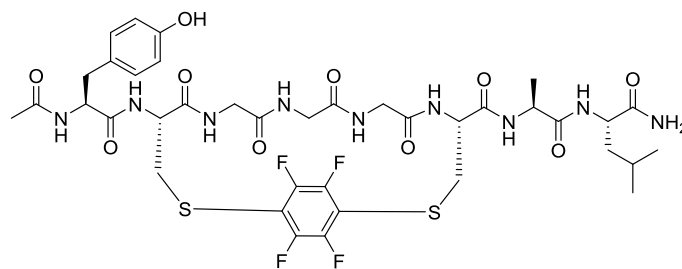
Figure SI22. LC/MS traces at $\lambda=220$ nm of crude reaction of peptide **pep3** with pentafluoropyridine when using Cs₂CO₃ as a base in DMF.

Isolation and characterization of compounds 11-23

General methods:

Products from large-scale reactions were purified and isolated by semi-preparative reverse phase HPLC performed on a Discovery Bio wide pore C₁₈-5 column from Supelco (5 μ m, 25 cm \times 10 mm), using a Pelking-Elmer 200 lc pump coupled to a Waters 486 tunable absorbance detector settled up at $\lambda=220$ nm. A gradient with eluent A (95:5:0.1% H₂O:MeCN:TFA) and eluent B (5:95:0.1% H₂O:MeCN:TFA) was applied, where solvent B was firstly rose linearly from 0 to 100% during $t=60$ min and finally maintained isocratically for 5 min at a flow rate of 2 mL/min. Purified pooled fractions were then freeze-dried and the identity and purity of the different compounds verified by LC/MS. The desired pure compounds were then further characterised by ¹⁹F NMR (2 mg/mL in H₂O/CD₃CN 1:1, unless otherwise stated), high resolution LC/MS-QToF and ion directed tandem mass spectrometry (MS/MS), allowing to obtain the characteristic rupture profile for each product. In MS/MS fragmentation analysis we have made use of the accepted nomenclature for fragment ions firstly proposed by Roepstorff and Fohlman (P. Roepstorff and J. Fohlman, *Biol. Mass Spectrom.* 1984, **11**, 601–601.), and subsequently modified by Johnson *et al.* (R. S. Johnson, S. A. Martin, K. Biemann J. T. Stults and J. T. Watson, *Anal. Chem.*, 1987, **59**, 2621–2625). Note that, in peptides and proteins, ions arising from fragmentation series γ or b are expected to be predominant.

Product 11.



Isolated mass: 6.2 mg (26%).

QToF LC/MS: Calculated m/z : 929.96, observed m/z : 931.49 $[M+H]^+$. Retention time: 2.400 min. Elemental composition: $C_{38}H_{47}F_4N_9O_{10}S_2$.

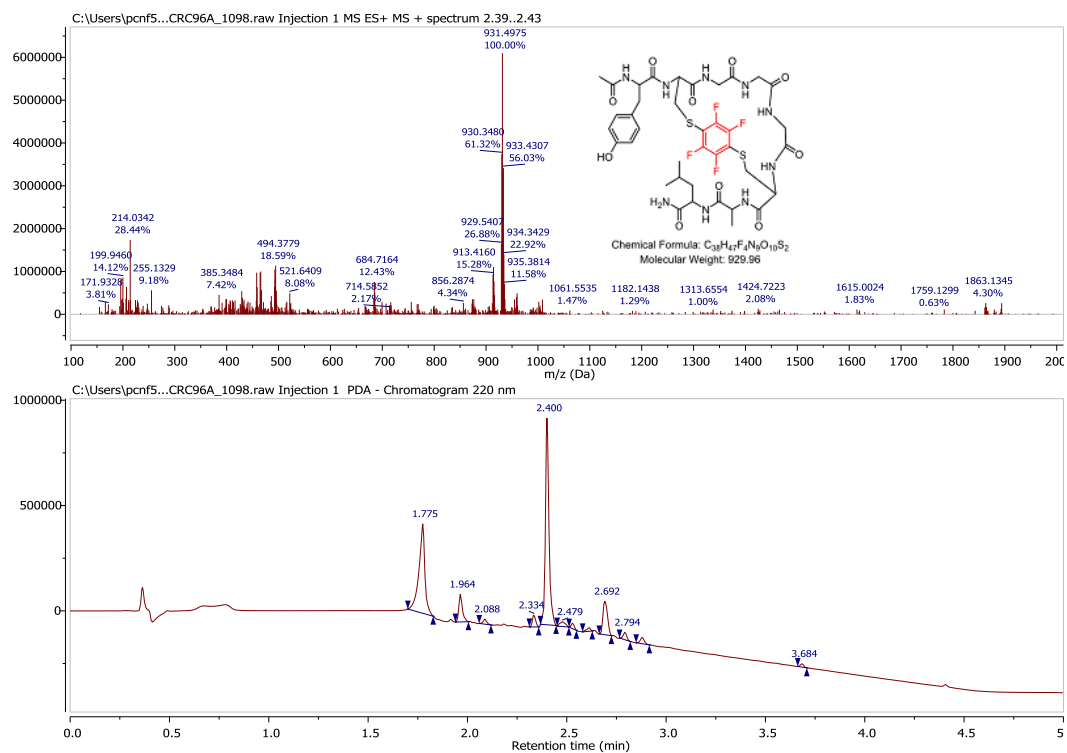


Figure SI23. Structure, high resolution QToF-LC/MS trace at $\lambda=280$ nm and composition of isolated compound **11**.

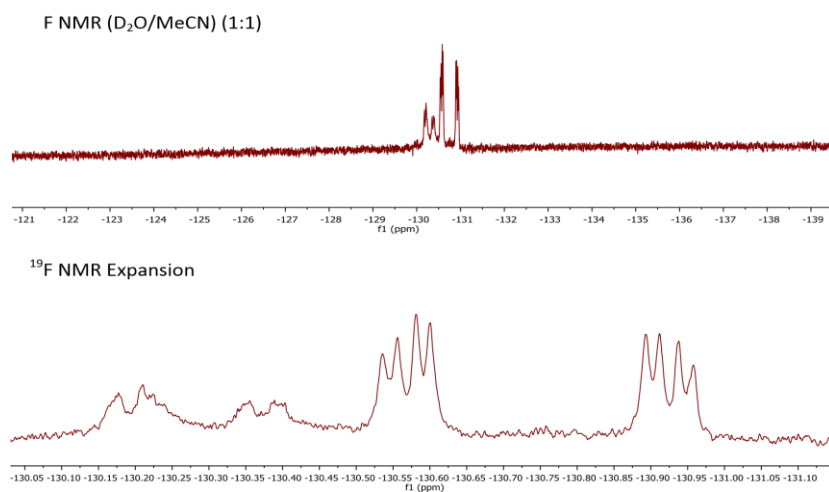
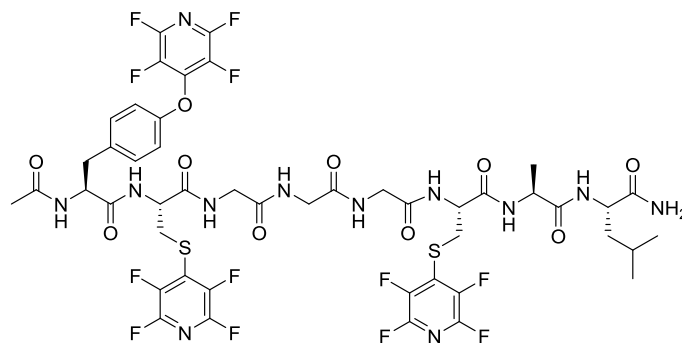


Figure SI024. ¹⁹F NMR spectrum of compound **11** as recorded in H₂O/ACN-d₃ 1:1 at room temperature.

Product 12.



Isolated mass: 6.4 mg (20%).

QToF LC/MS: Calculated m/z : 1230.27, observed m/z : 1231.28 $[M+H]^+$. Retention time: 3.442 min. Elemental composition: $C_{47}H_{46}F_{12}N_{12}O_{10}S_2$.

QToF-MS/MS: Calculated m/z : 1103.18 $[b7+H]^+$, 1032.13 $[b6+H]^+$, 779.14 $[b5+H]^+$, 722.11 $[b4+H]^+$, 665.09 $[b3+H]^+$, 608.07 $[b2+H]^+$, 356.07 $[b1+H]^+$, 495.15 $[z4+H]^+$ Da.

Observed m/z : 1103.21 $[b7+H]^+$, 1032.18 $[b6+H]^+$, 780.17 $[b5+H]^+$, 722.14 $[b4+H]^+$, 665.12 $[b3+H]^+$, 608.13 $[b2+H]^+$, 355.08 $[b1+H]^+$, 495.14 $[z4+H]^+$ Da.

^{19}F NMR (376 MHz, $DMSO-d_6$) δ -91.20 (m, 2F), -93.42 (m, 4F), -137.49 (m, 4F), -155.63 (m, 2F).

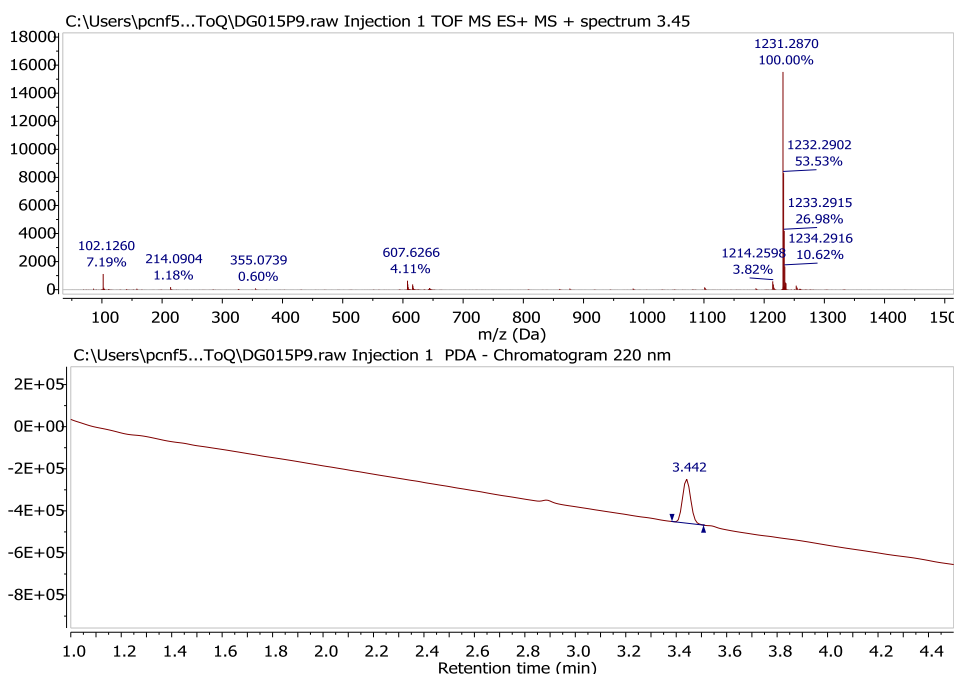


Figure SI25. Structure, high resolution QToF-LC/MS trace at $\lambda=220$ nm and composition of isolated compound **12**.

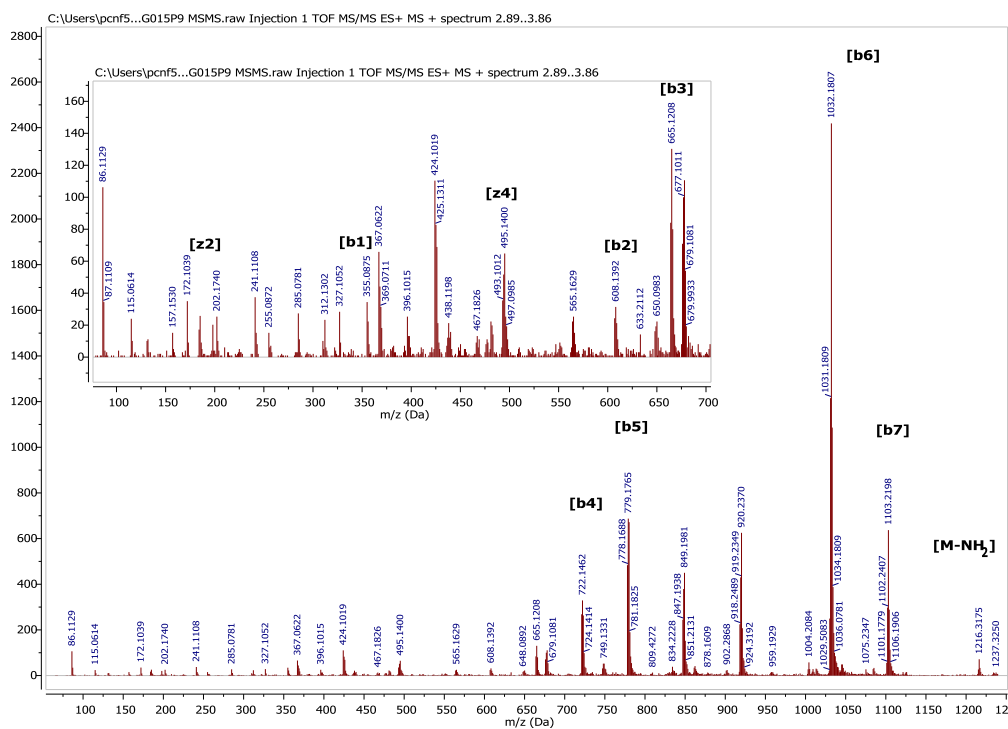


Figure SI26. MS/MS analysis of compound **12** showing its characteristic rupture pattern and the assignation of the main ions observed.

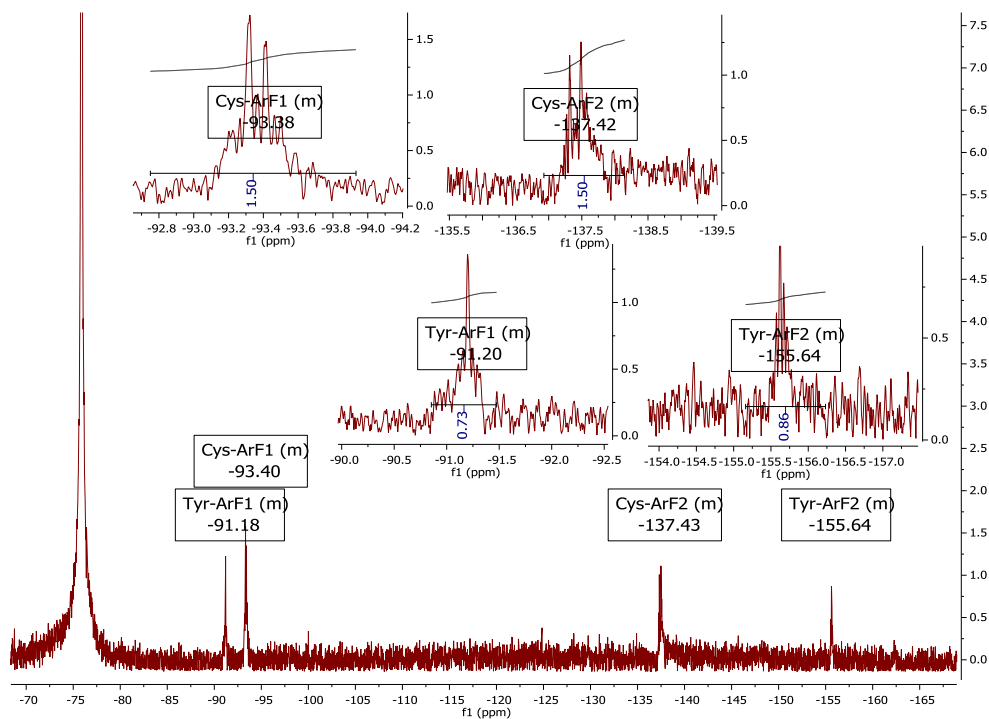
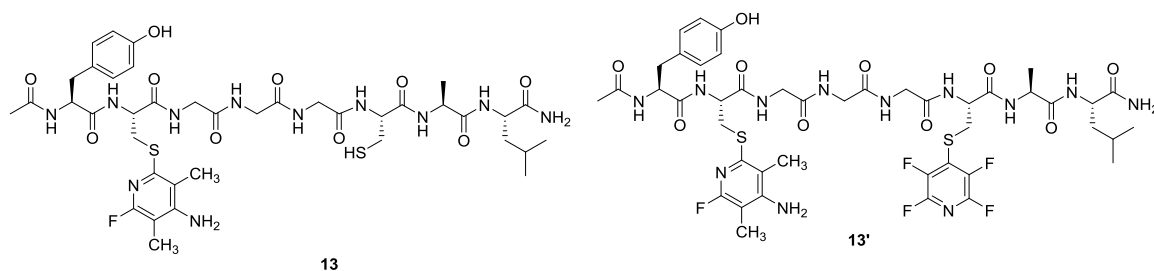


Figure SI27. ¹⁹F-NMR spectrum of compound **12** as recorded in DMSO-d₆ at room temperature.

Product 13.



Isolated mass: 2.7 mg (11%).

QToF LC/MS: Calculated m/z : 961.25, observed m/z : 1018.33 $[2M+TFA]^{2+}$. Retention time: 2.425 min. Elemental composition: $C_{37}H_{50}Cl_2FN_{11}O_{10}S_2$.

QToF-MS/MS: Calculated m/z : 889.65 $[b7/b7'+TFA+H]^+$, 818.65 $[b6/b6'+TFA+H]^+$, 730.32 $[b5+TFA+H]^+$, 658.58 $[b4+TFA+H]^+$, 601.08 $[b3+TFA+H]^+$, 537.66 $[b5'+TFA+H]^+$, 480.16 $[b4'+TFA+H]^+$, 423.13 $[b3'+TFA+H]^+$, 366.11 $[b2'+TFA+H]^+$, 331 $[x3+H]^+$ Da.

Observed m/z : 890.19 $[b7/b7'+TFA+H]^+$, 819.20 $[b6/b6'+TFA+H]^+$, 729.13 $[b5+TFA+H]^+$, 660.12 $[b4+TFA+H]^+$, 603.08 $[b3+TFA+H]^+$, 536.23 $[b5'+TFA+H]^+$, 479.20 $[b4'+TFA+H]^+$, 422.17 $[b3'+TFA+H]^+$, 365.14 $[b2'+TFA+H]^+$, 332.12 $[x3+H]^+$ Da.

^{19}F NMR (376 MHz, $H_2O/MeCN-d_3$ 1:1) δ -73.68 (m, 1F), -73.80 (m, 1F).

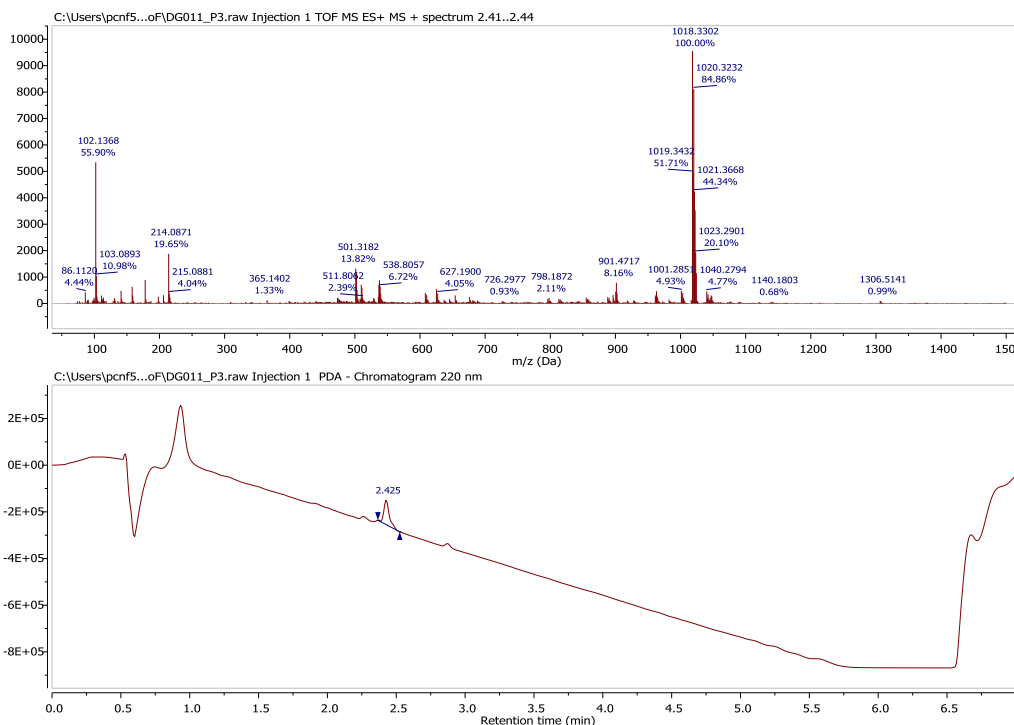


Figure SI28. Structure, high resolution QToF-LC/MS trace at $\lambda=220$ nm and composition of isolated compound 13.

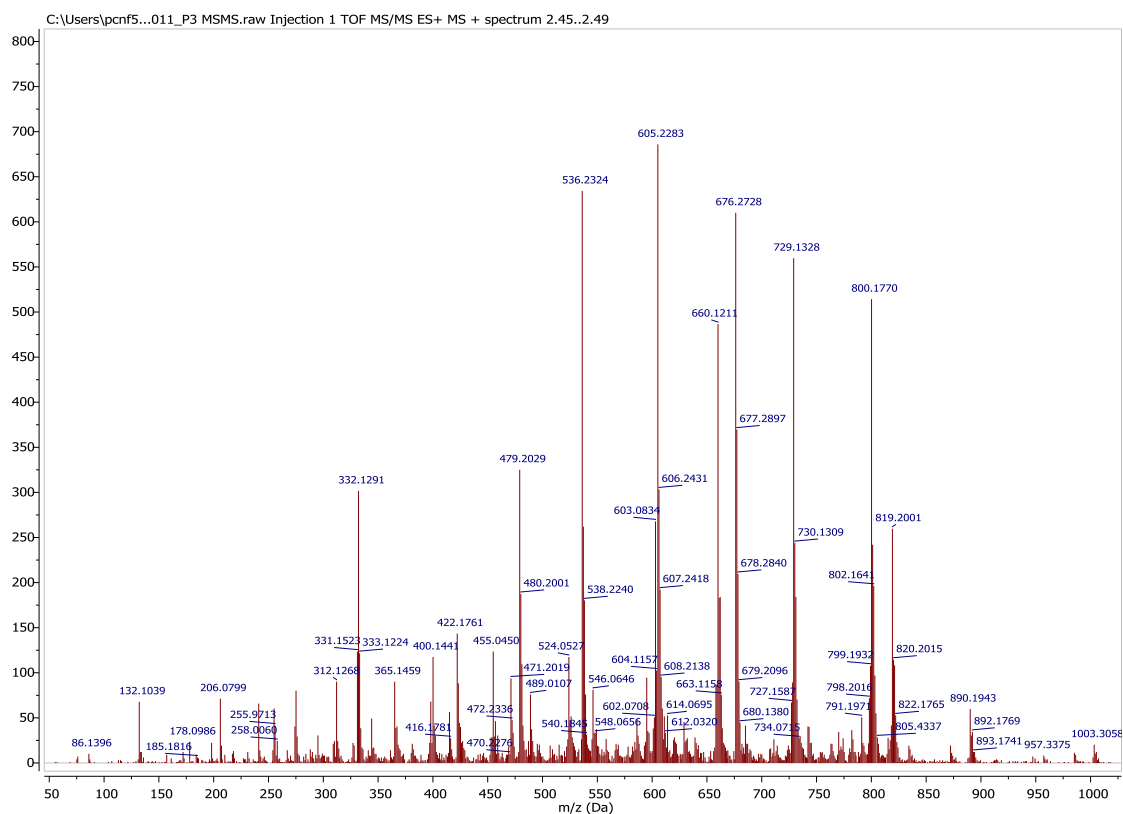


Figure SI29. MS/MS analysis of compound **13** showing its characteristic rupture pattern and the main ions observed.

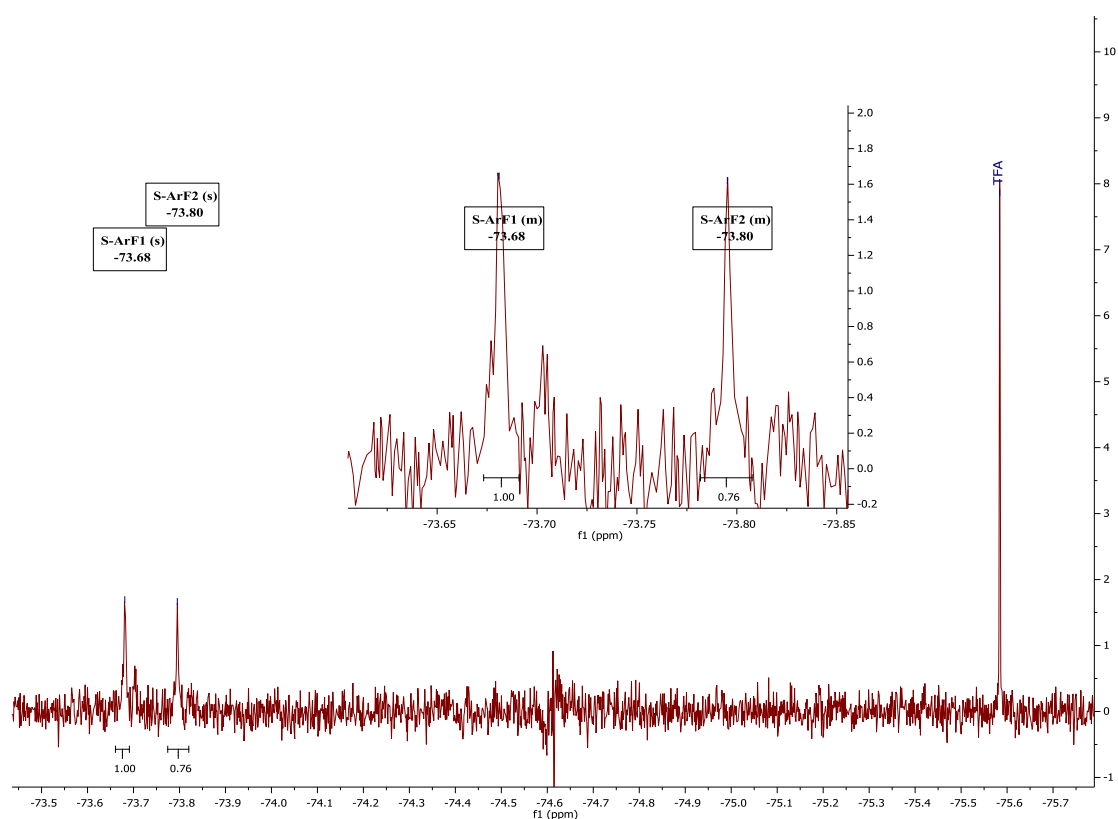
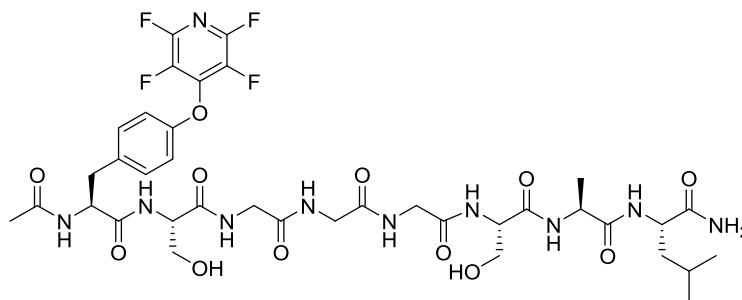


Figure SI30. ^{19}F NMR spectrum of compound **13** as recorded in $\text{H}_2\text{O}/\text{MeCN-d}_3$ 1:1 at room temperature.

Product 14.



Isolated mass: 6.1 mg (25%).

QToF LC/MS: Calculated m/z : 900.34, observed m/z : 901.34 $[M+H]^+$. Retention time: 2.375 min. Elemental composition: $C_{37}H_{48}F_4N_{10}O_{12}$.

QToF-MS/MS: Calculated m/z : 771.24 $[b7]^+$, 700.20 $[b6]^+$, 613.17 $[b5]^+$, 499.12 $[b3]^+$, 442.35 $[b2]^+$, 355.07 $[b1]^+$ Da.

Observed m/z : 771.27 $[b7]^+$, 700.24 $[b6]^+$, 613.19 $[b5]^+$, 499.10 $[b3]^+$, 442.08 $[b2]^+$, 355.11 $[b1]^+$ Da.

^{19}F NMR (376 MHz, $H_2O/MeOD$ 1:1) δ -91.32 (m, 2F), -155.98 (m, 2F).

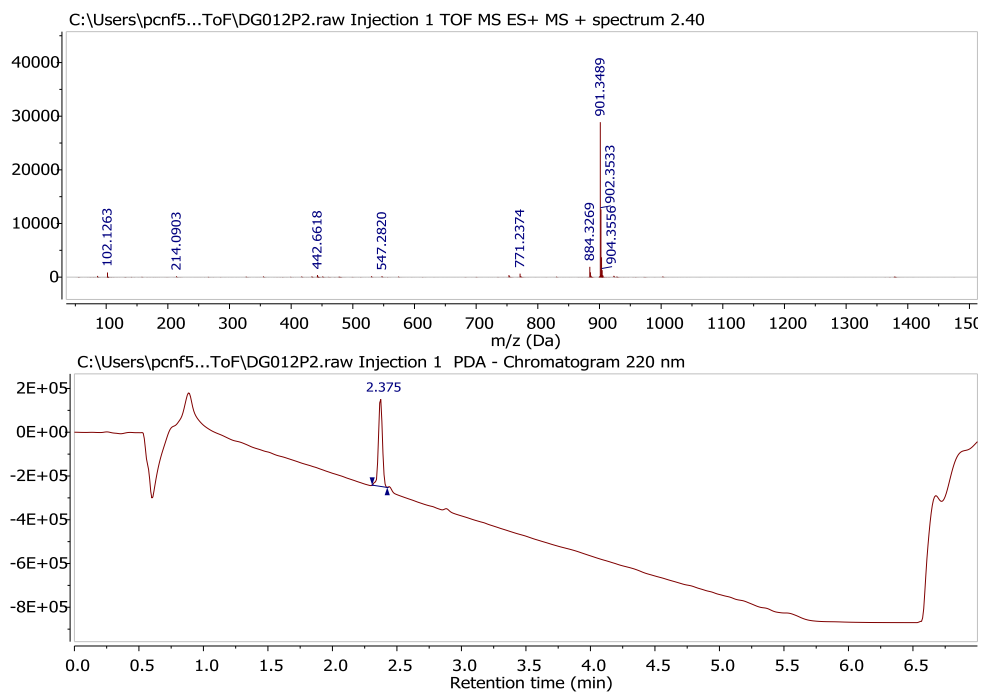


Figure SI31. Structure, high resolution QToF-LC/MS trace at $\lambda=220$ nm and composition of isolated compound 14.

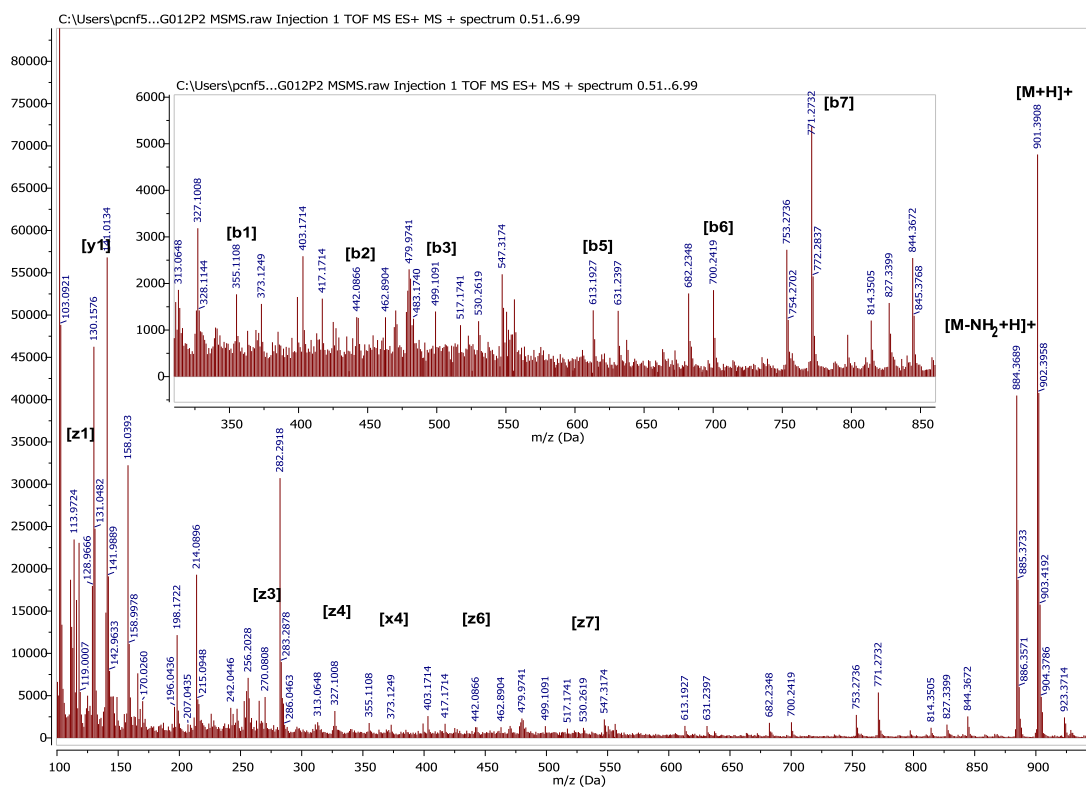


Figure SI32. MS/MS analysis of compound **14** showing its characteristic rupture pattern and the assignment of the main ions observed.

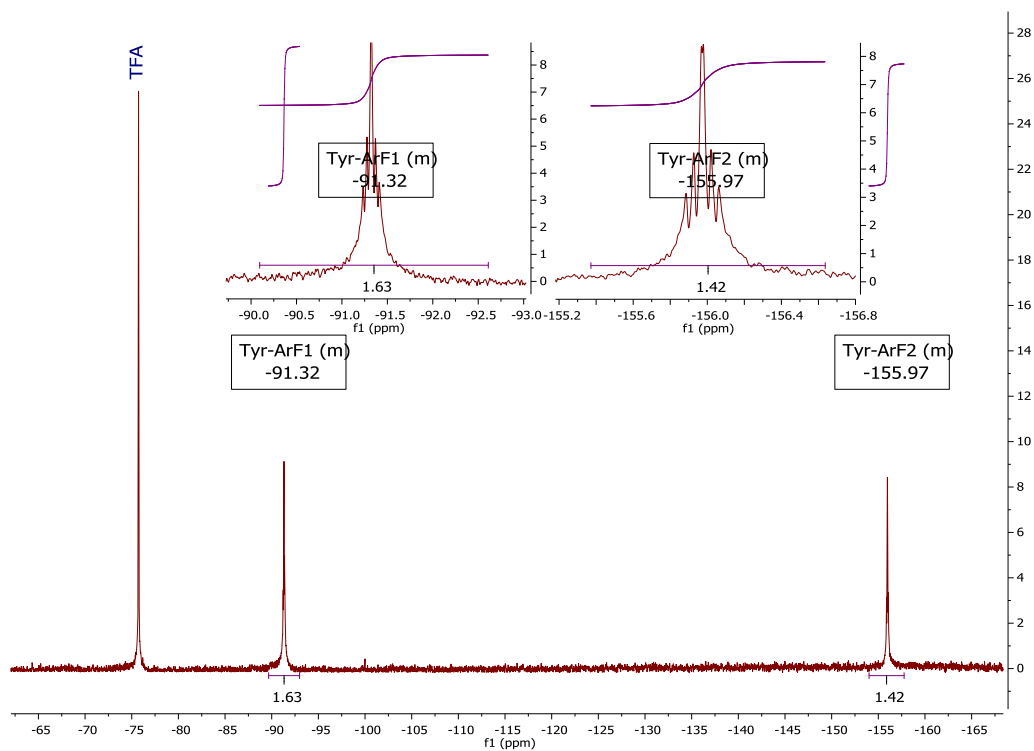
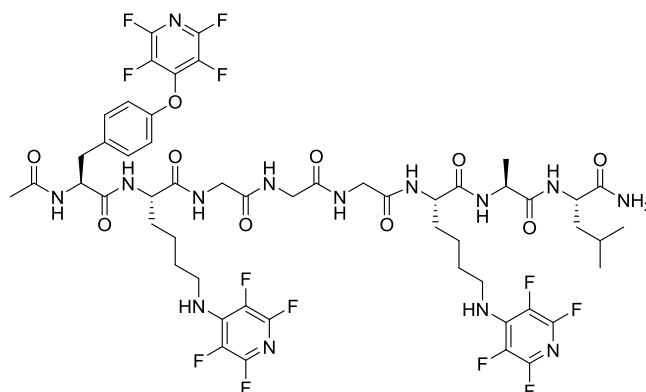


Figure SI33. ¹⁹F NMR spectrum of compound **14** as recorded in H₂O/MeOD 1:1 at room temperature.

Product 15.



Isolated mass: 7.2 mg (23%).

QToF LC/MS: Calculated m/z : 1280.44, observed m/z : 1281.45 $[M+H]^+$. Retention time: 3.492 min. Elemental composition: $C_{53}H_{60}F_{12}N_{14}O_{10}$.

QToF-MS/MS:

Calculated m/z : 1152.34 $[b7+H]^+$, 1081.30 $[b6+H]^+$, 804.22 $[b5+H]^+$, 691.2337 $[b3+H]^+$, 747.20 $[b4+H]^+$, 911.36 $[z7+H]^+$, 634.28 $[z6+H]^+$, 520.23 $[z4+H]^+$ Da.

Observed m/z : 1152.40 $[b7+H]^+$, 1082.36 $[b6+H]^+$, 804.26 $[b5+H]^+$, 690.23 $[b3+H]^+$, 747.24 $[b4+H]^+$, 911.36 $[z7+H]^+$, 634.29 $[z6+H]^+$, 520.23 $[z4+H]^+$ Da.

^{19}F NMR (376 MHz, $H_2O/MeOD$ 1:1) δ -91.66 (m, 2F), -98.17 (m, 4F), -156.29 (m, 4F), -165.54 (m, 2F).

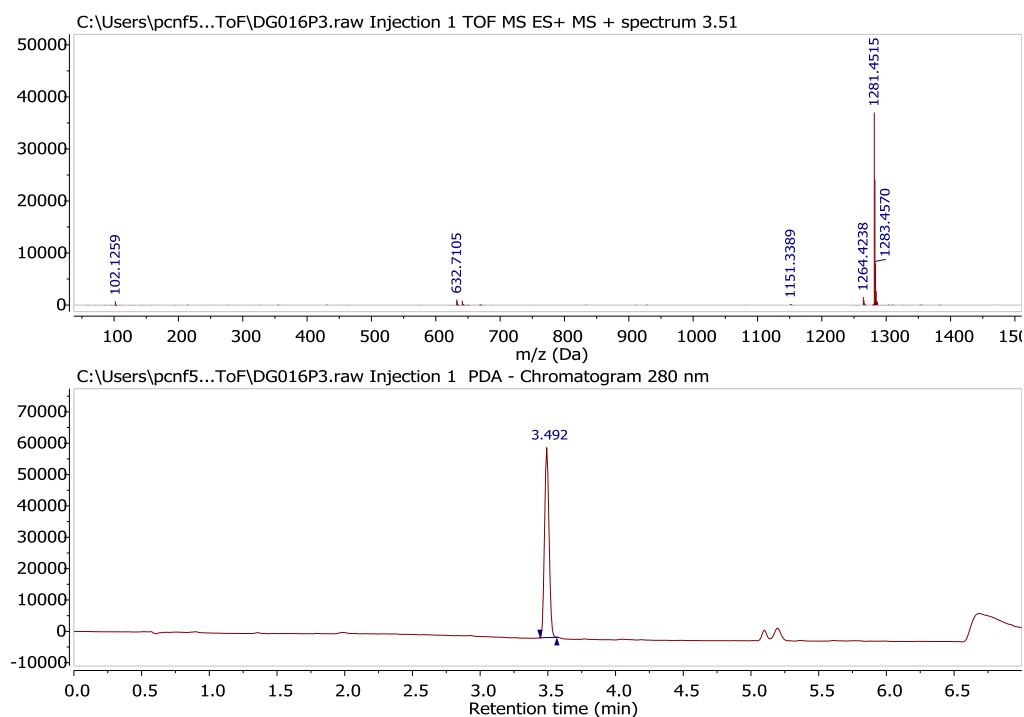
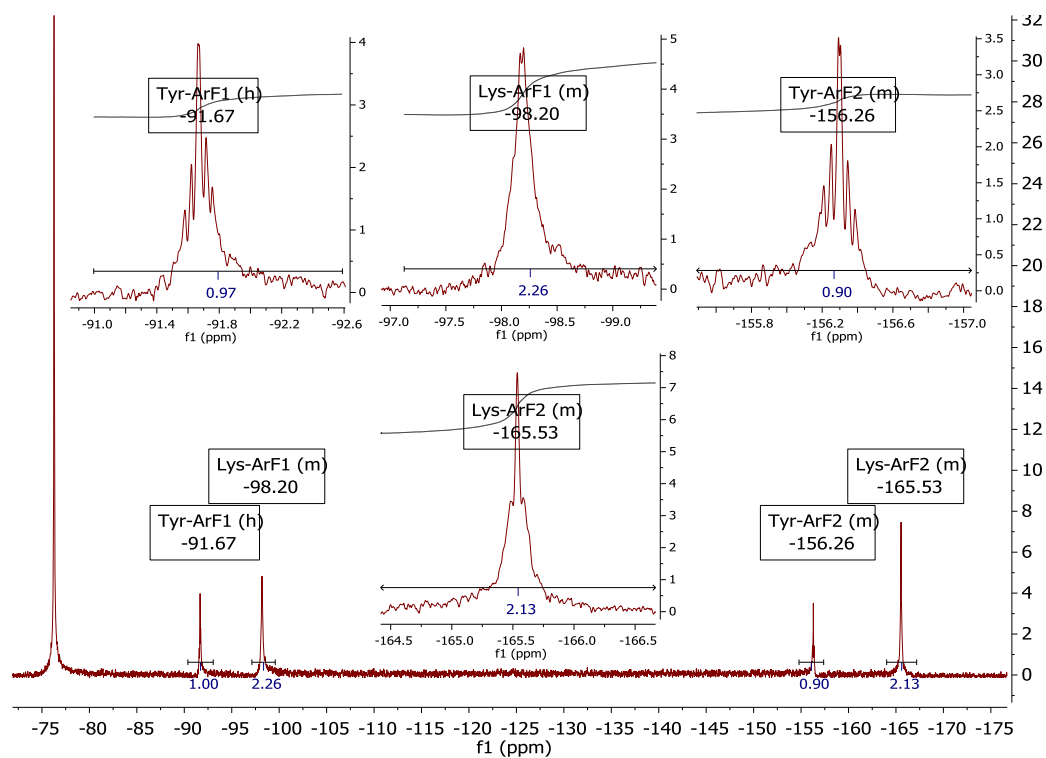
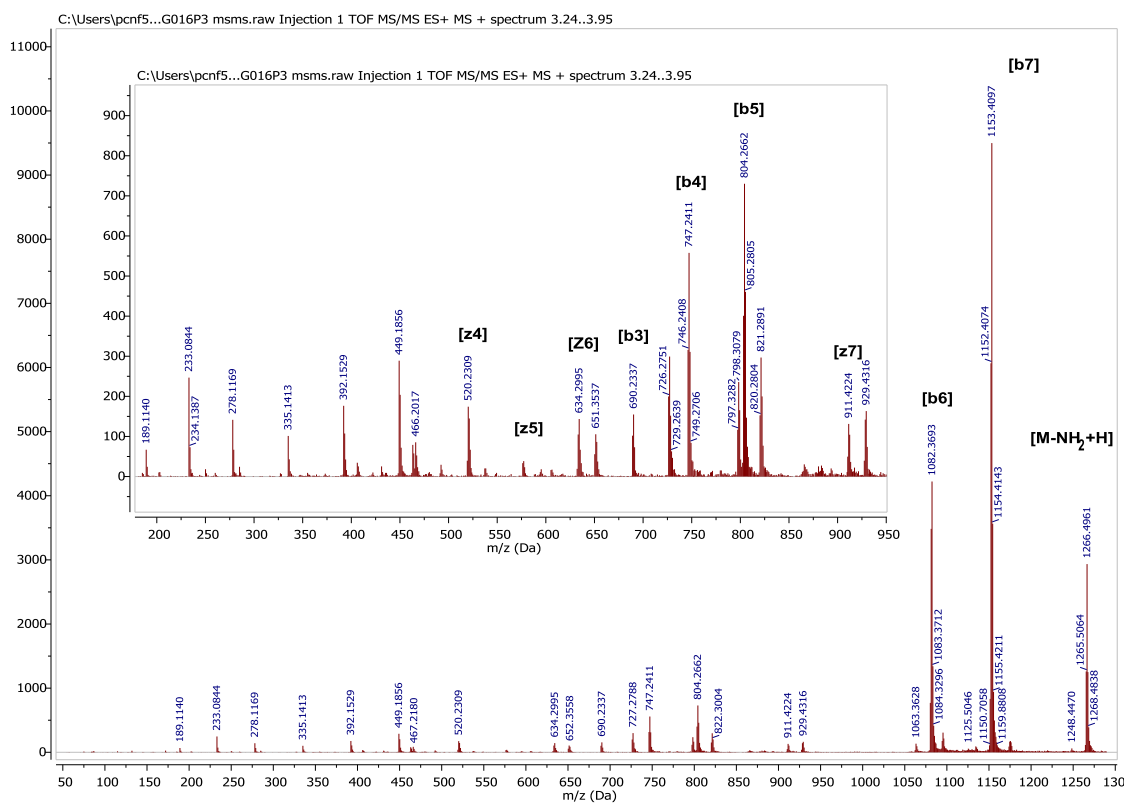


Figure SI34. Structure, high resolution QToF-LC/MS trace at $\lambda=220$ nm and composition of isolated compound 15.



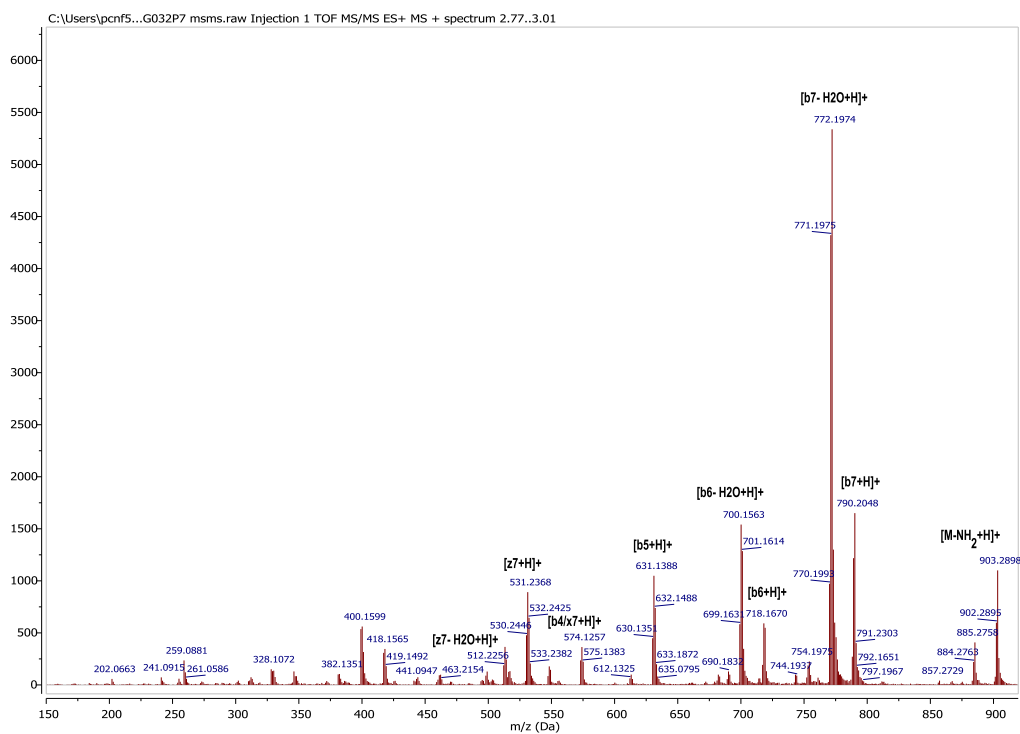


Figure SI38. MS/MS analysis of compound **16** showing its characteristic rupture pattern and the assignment of the main ions observed.

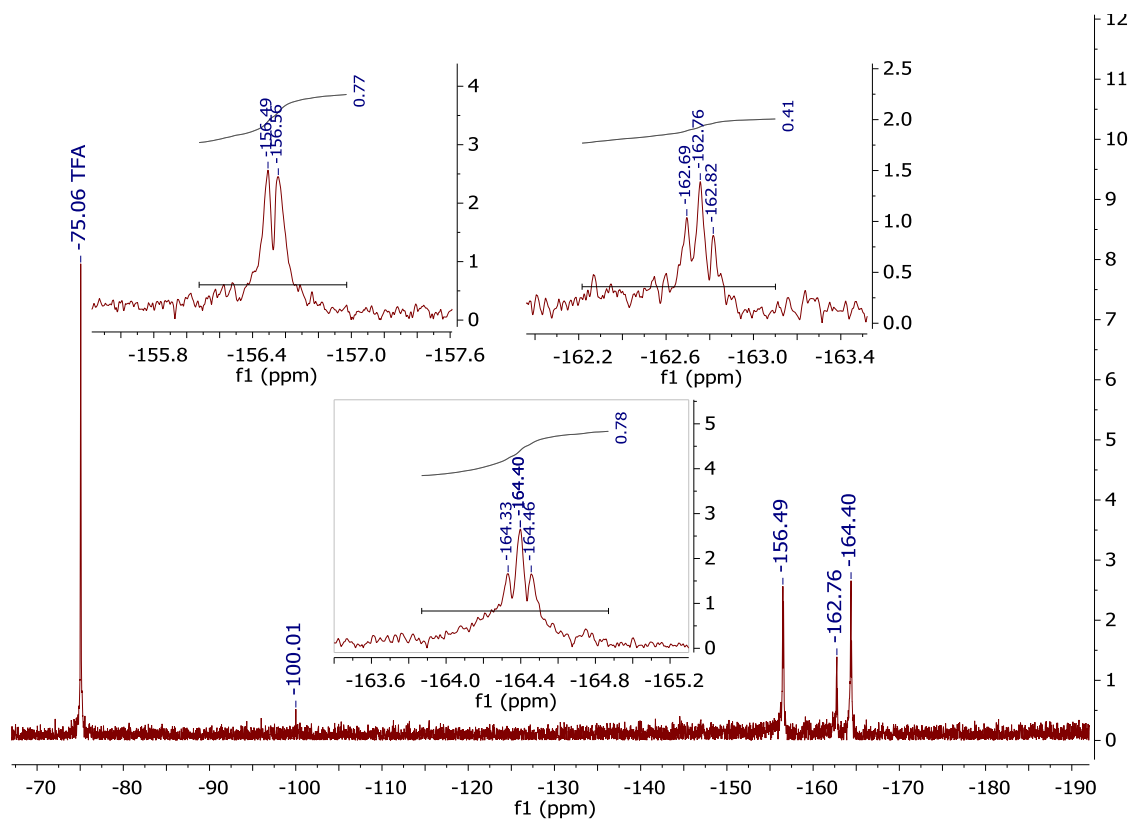
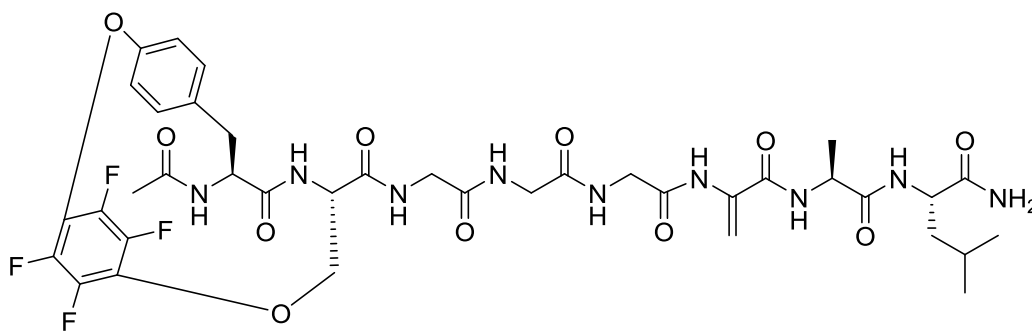


Figure SI39. ¹⁹F NMR spectrum of compound **16** as recorded in H₂O/MeCN-d₃ 1:1 at room temperature.

Product 17.



Isolated mass: 3.4 mg (14%).

QToF LC/MS: Calculated m/z : 879.32, observed m/z : 880.29 $[M+H]^+$. Retention time: 2.633 min. Elemental composition: $C_{38}H_{45}F_4N_9O_{11}$.

QToF MS/MS:

Calculated m/z : 752.22 $[b7-(OH)+H]^+$, 611.16 $[b5+H]^+$, 554.13 $[b4+H]^+$, 497.11 $[b3+H]^+$, 440.09 $[b2+H]^+$ Da.

Observed m/z : 752.19 $[b7-(OH)+H]^+$, 611.14 $[b5+H]^+$, 554.12 $[b4+H]^+$, 496.17 $[b3+H]^+$, 440.07 $[b2+H]^+$ Da.

^{19}F NMR (376 MHz, $H_2O/MeCN-d_3$ 1:1) δ -159.46 (m, 2F), -163.63 (m, 2F).

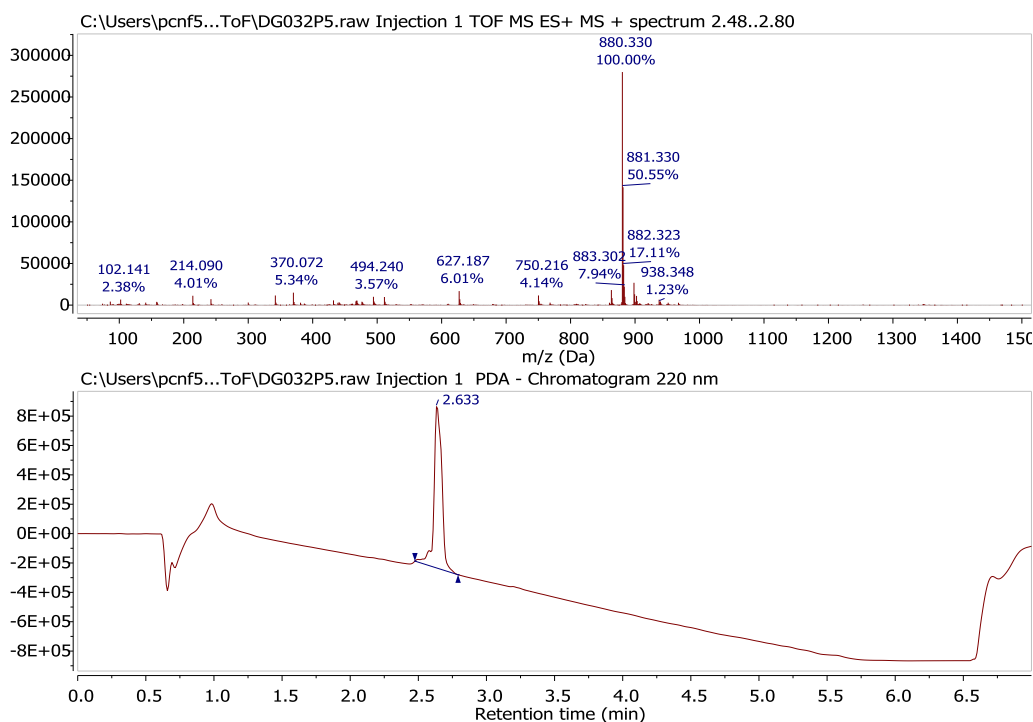


Figure SI40. Structure, high resolution QToF-LC/MS trace at $\lambda=220$ nm and composition of isolated compound 17.

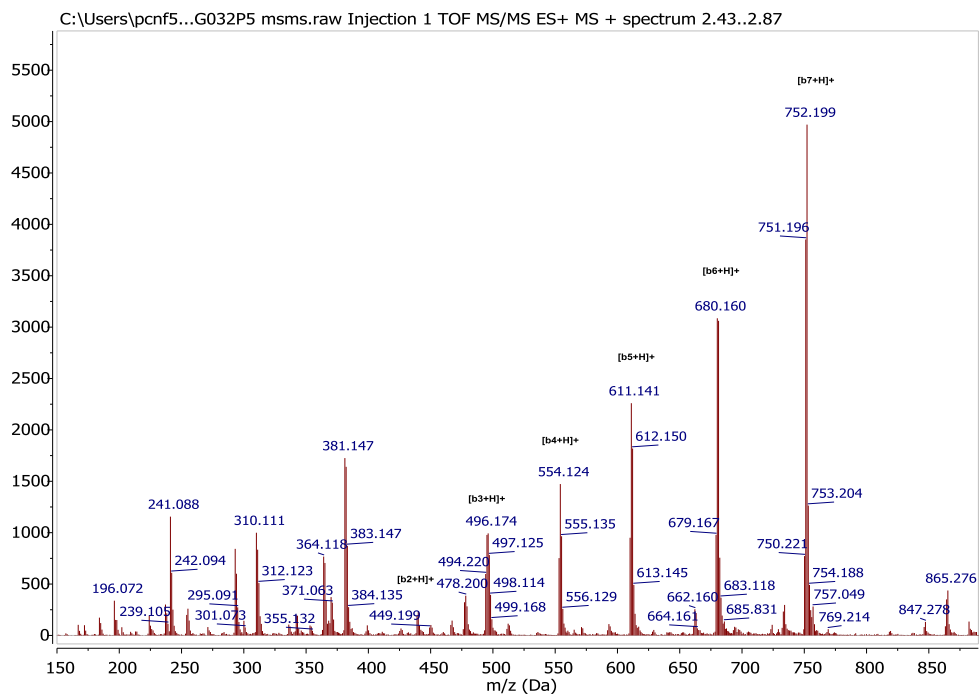


Figure SI41. MS/MS analysis of compound **17** showing its characteristic rupture pattern and the assignment of the main ions observed.

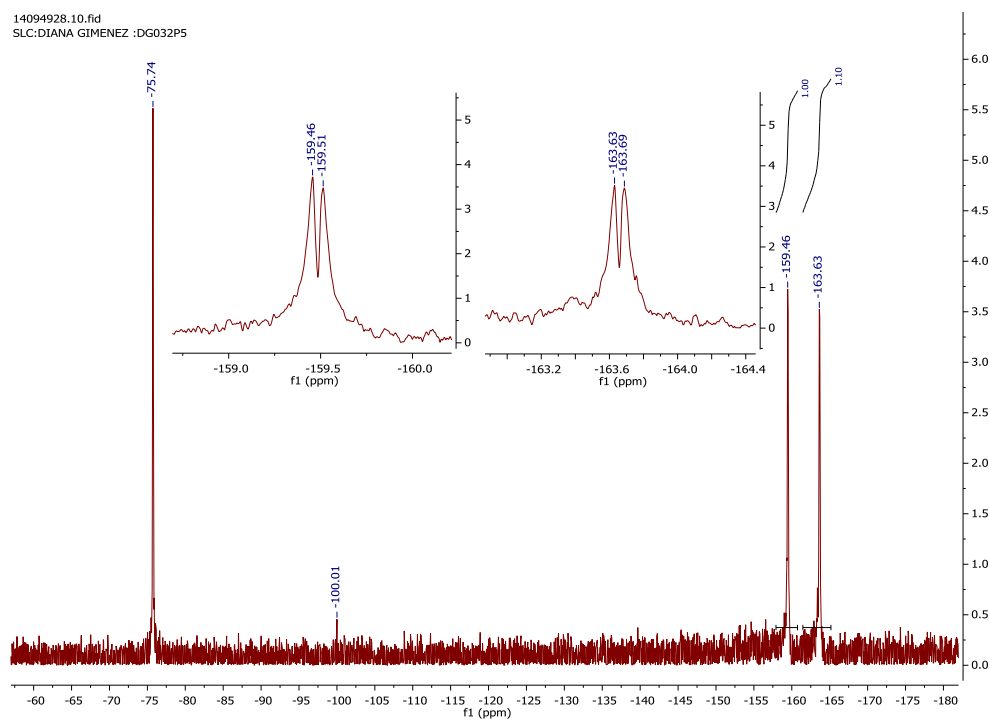
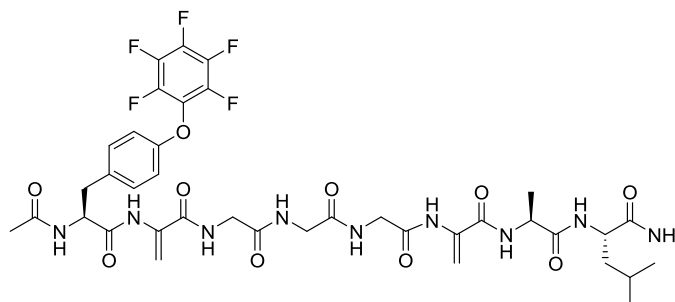


Figure SI42. ¹⁹F NMR spectrum of compound **17** as recorded in H₂O/MeCN-d₃ 1:1 at room temperature.

Product 18.



Isolated mass: 2.2 mg (9%).

QToF LC/MS: Calculated m/z : 881.31, observed m/z : 882.32 $[M+H]^+$. Retention time: 2.633 min. Elemental composition: $C_{38}H_{44}F_5N_9O_{10}$.

QToF MS/MS:

Calculated m/z : 753.21 $[b7+H]^+$, 682.17 $[b6+H]^+$, 613.15 $[b5+H]^+$, 556.13 $[b4+H]^+$, 499.11 $[b3+H]^+$, 495.53 $[z7+H]^+$, 384.20 $[y5+H]^+$, 312.36 $[z4+H]^+$ Da.

Observed m/z : 754.19 $[b7+H]^+$, 683.15 $[b6+H]^+$, 613.13 $[b5+H]^+$, 556.11 $[b4+H]^+$, 499.10 $[b3+H]^+$, 495.22 $[z7+H]^+$, 382.14 $[y5+H]^+$, 310.11 $[z4+H]^+$ Da.

^{19}F NMR (376 MHz, $H_2O/MeCN-d_3$ 1:1) δ -156.24 (d, $J = 23.56$ Hz, 2F), -161.81 (t, $J = 23.40$ Hz, 1F), -163.74 (m, 2F).

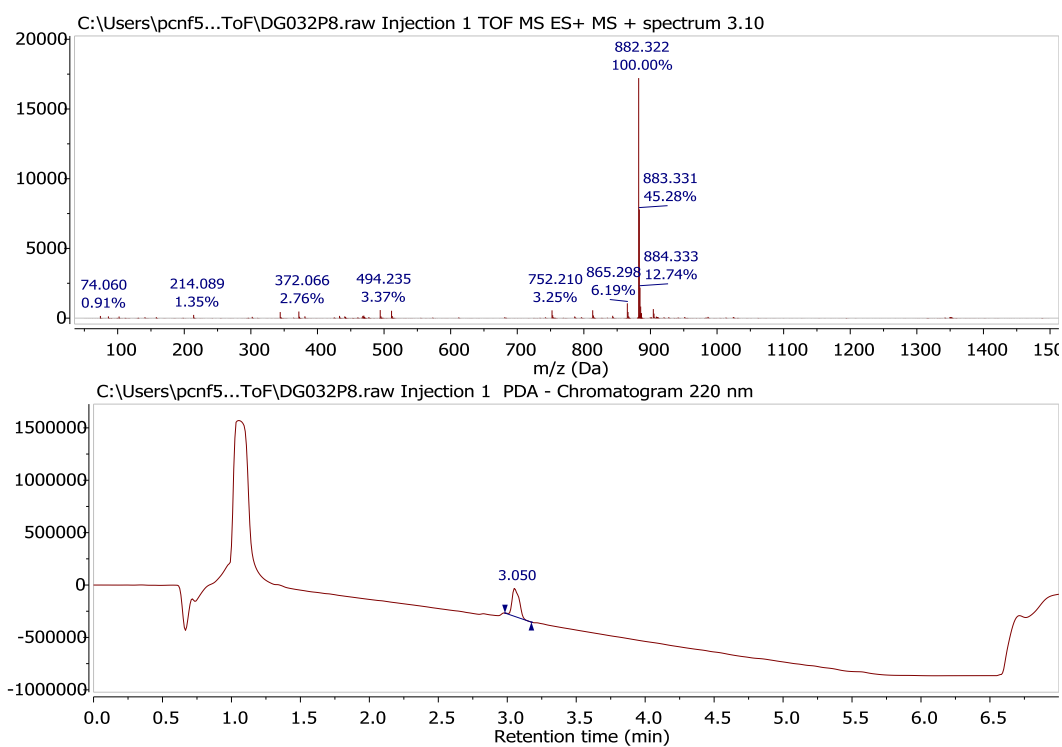
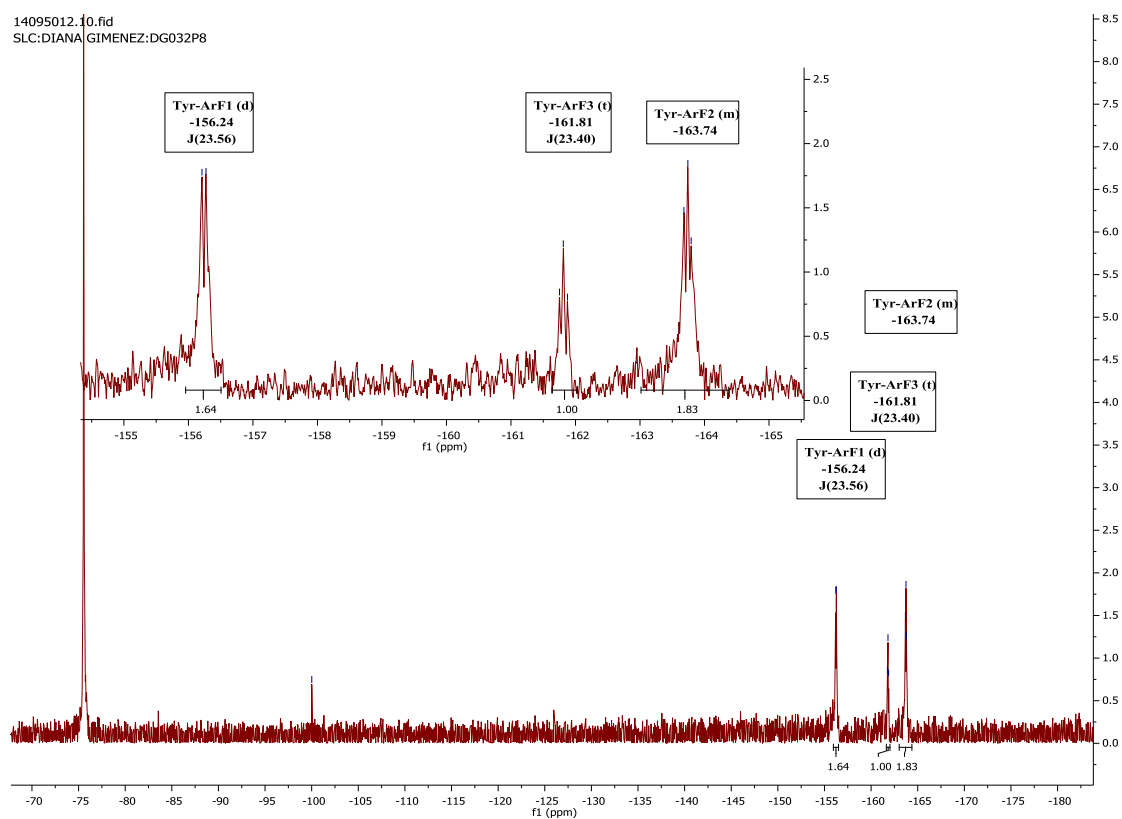
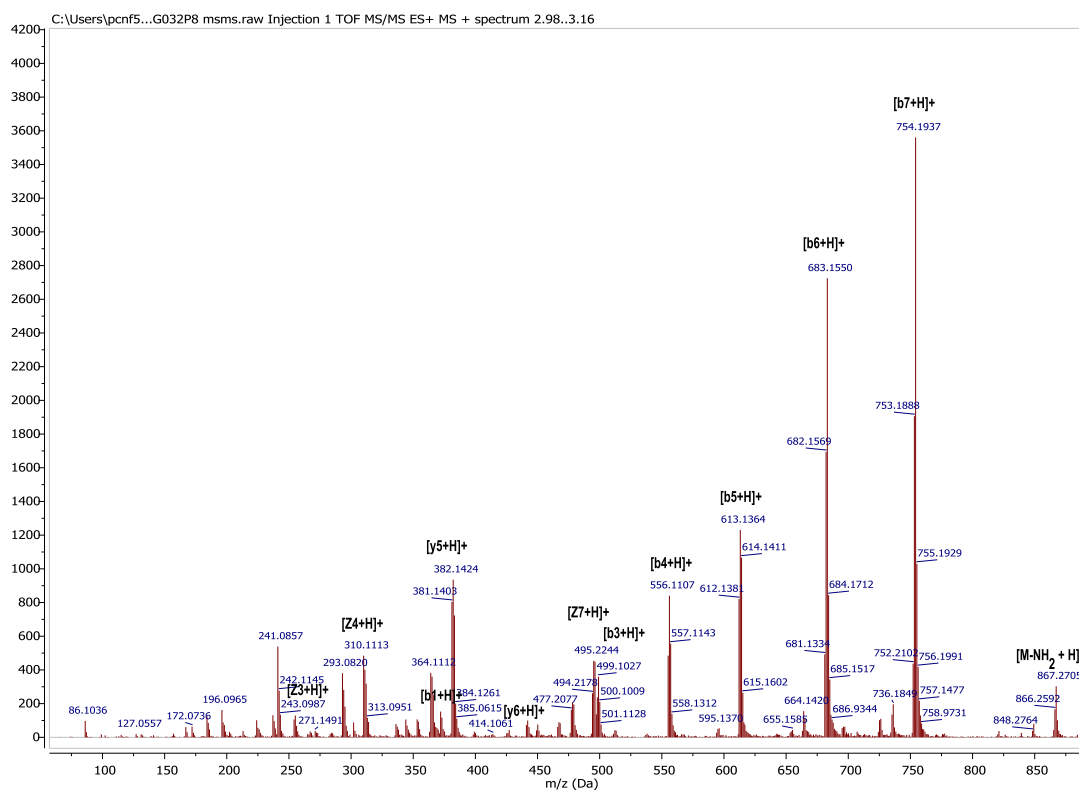
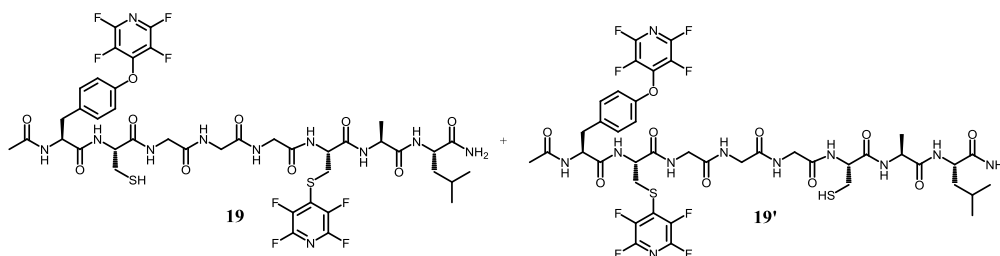


Figure SI43. Structure, high resolution QToF-LC/MS trace at $\lambda=220$ nm and composition of isolated compound **18**.



Product 19 (Mixture of regioisomers).



Isolated mass: 3.2 mg (11%).

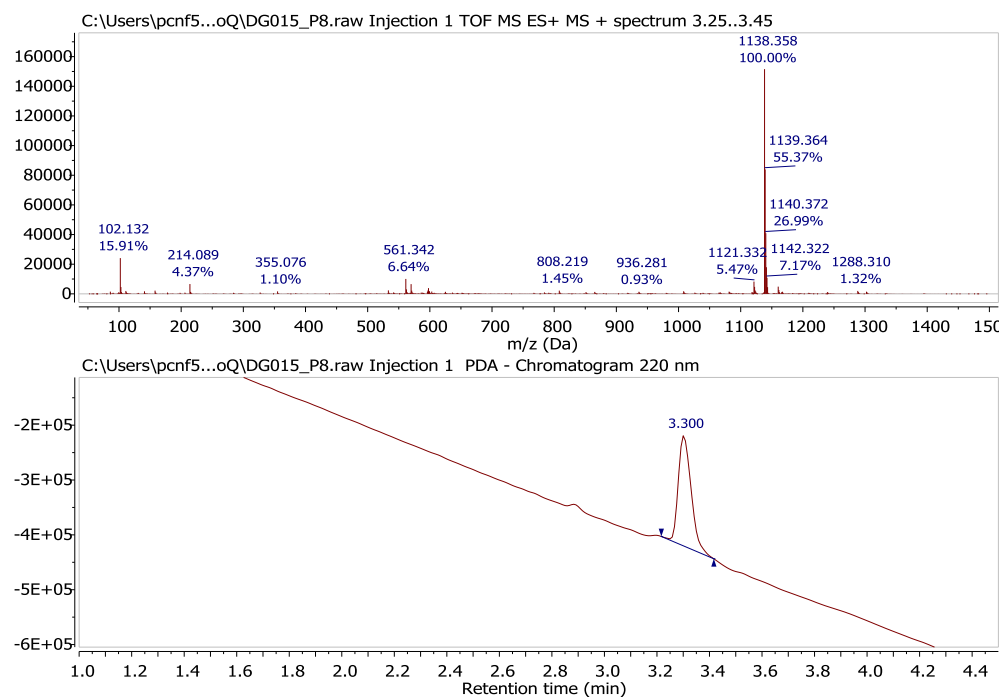
QToF LC/MS: Calculated m/z : 1081.28, observed m/z : 1138.35 [2M+TFA+H]²⁺. Retention time: 3.300 min. Elemental composition: C₄₂ H₄₇ F₈ N₁₁ O₁₀ S₂.

QToF MS/MS:

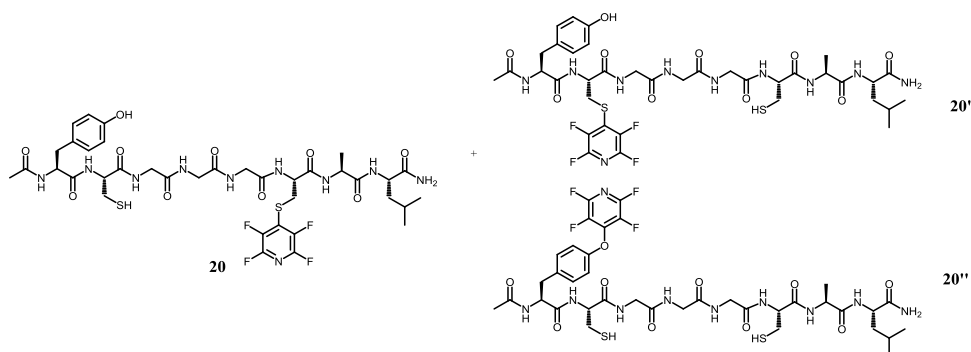
Calculated m/z : 938.64 [2(b6/b'6)+TFA+H]²⁺, 919.18 [(b7/ b'7)+TFA-4/Pyr+H]⁺, 848.15 [b6/ b'6+ TFA-4/Pyr+H]⁺, 778.61 [2b'4+ TFA+H]²⁺, 722.59 [2b'3+ TFA +H]²⁺, 686.60 [2b5 + TFA +H]²⁺, 664.57 [2b'3+ TFA +H]²⁺, 629.62 [2b4 + TFA +H]²⁺, 480.15 [2b5 +-4/Pyr+H]²⁺, 423.13 [2b4 +-4/Pyr+H]²⁺ Da.

Observed m/z : 939.24 [2(b6/b'6)+TFA+H]²⁺, 920.56 [b7 /b'7)+TFA-4/Pyr+H]⁺, 849.17 [b6/b'6)+TFA-4/Pyr+H]⁺, 779.14 [2b'4+TFA+H]²⁺, 723.14 [2b'3+TFA+H]²⁺, 687.23 [2b5 +TFA+H]²⁺, 664.12 [2b'3+TFA+H]²⁺, 630.18 [2b4 +TFA+H]²⁺, 481.13 [2b5+-4/Pyr+H]²⁺, 424.08 [2b4 +-4/Pyr+H]²⁺ Da.

¹⁹F NMR (376 MHz, H₂O/MeCN-d₃ 1:1) δ -91.57 (m, 2F), -93.40 (m, 2F), -137.69 (m, 2F), -156.12 (m, 2F).



Product 20 (Mixture of regioisomers).



Isolated mass: 3.1 mg (13%).

QToF LC/MS: Calculated m/z : 932.29, observed m/z : 1048.30 $[M+TFA+H]^+$. Retention time: 3.008 min. Elemental composition: $C_{37}H_{48}F_4N_{10}O_{10}S_2$.

QToF MS/MS:

Calculated m/z : 918.19 $[b7/b'7/b''7+TFA+H]^+$, 847.15 $[b6/b'6/b''6+TFA+H]^+$, 595.16 $[b5+TFA+H]^+$, 538.46 $[b4+TFA+H]^+$, 481.41 $[b3+TFA+H]^+$, 423.46 $[b4+H]^+$ Da.

Observed m/z : 920.21 $[b7/b'7/b''7+TFA+H]^+$, 849.17 $[b6/b'6/b''6+TFA+H]^+$, 596.17 $[b5+TFA+H]^+$, 538.15 $[b4+TFA+H]^+$, 478.07 $[b3+TFA+H]^+$, 424.08 $[b4+H]^+$ Da.

^{19}F NMR (376 MHz, $H_2O/MeCN-d_3$ 1:1) δ -91.65 (m, 2F), -93.49 (m, 2F), -137.74 (m, 2F), -156.21 (m, 2F).

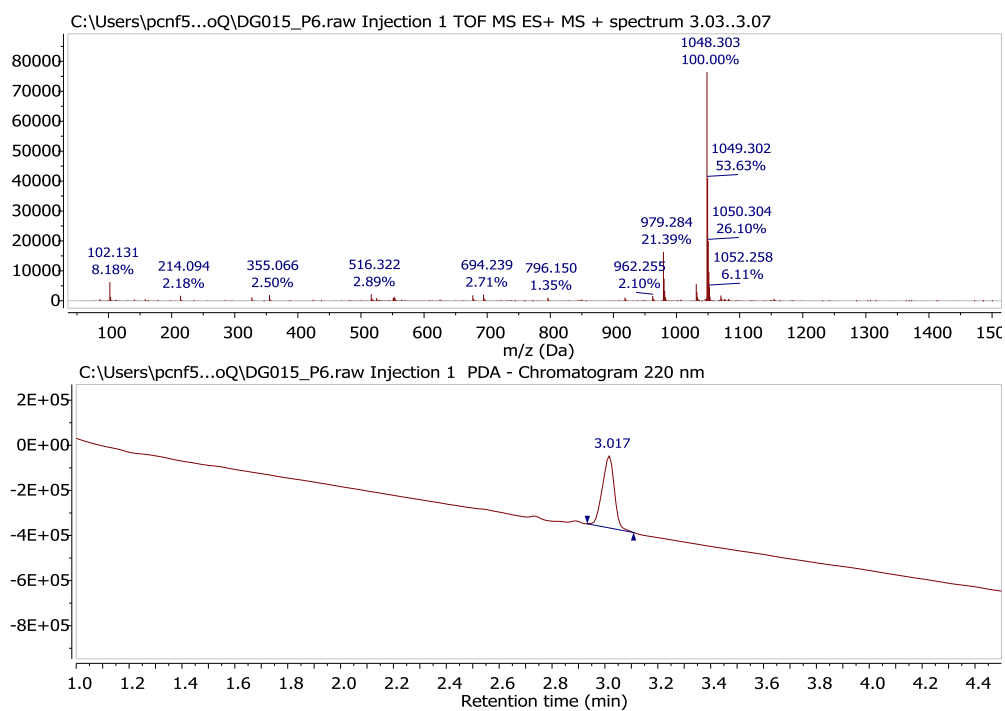


Figure SI49. Structure, high resolution QToF-LC/MS trace at $\lambda=220$ nm and composition of isolated compound **20**.

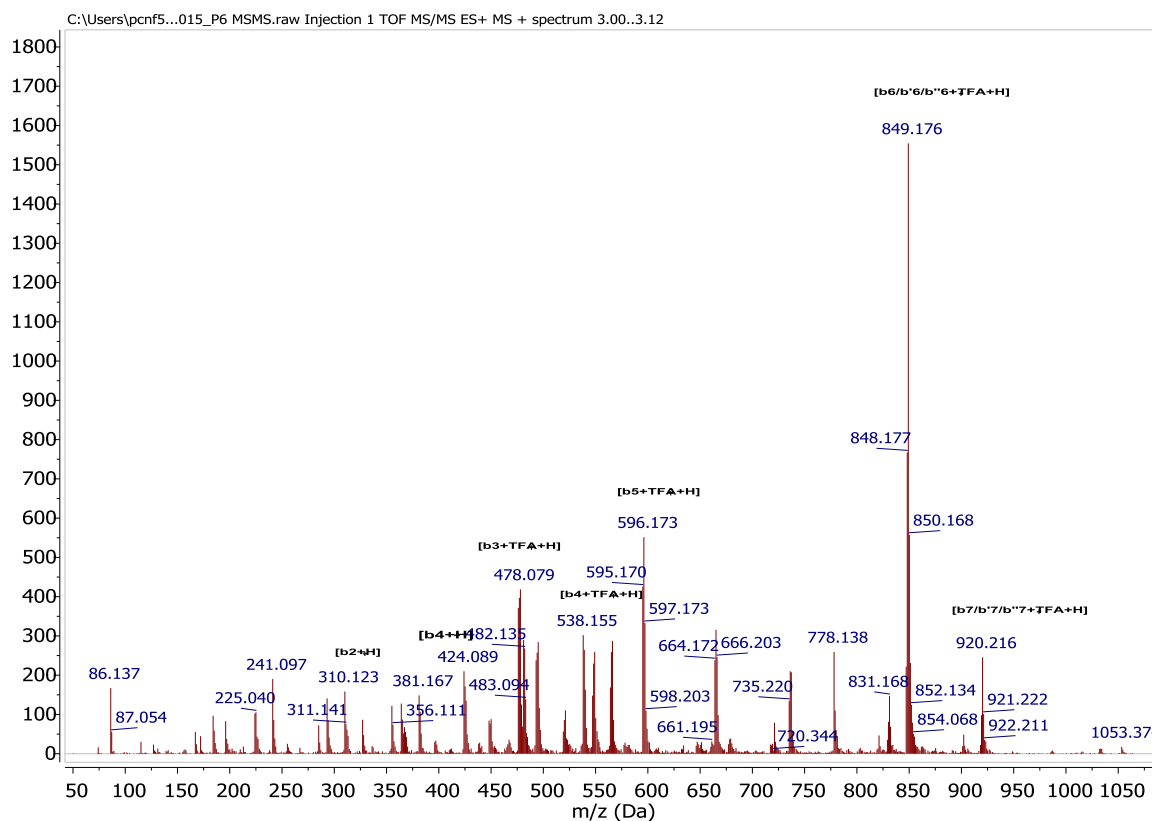


Figure SI50. MS/MS analysis of compound **20** showing its characteristic rupture pattern and the assignment of the main ions observed.

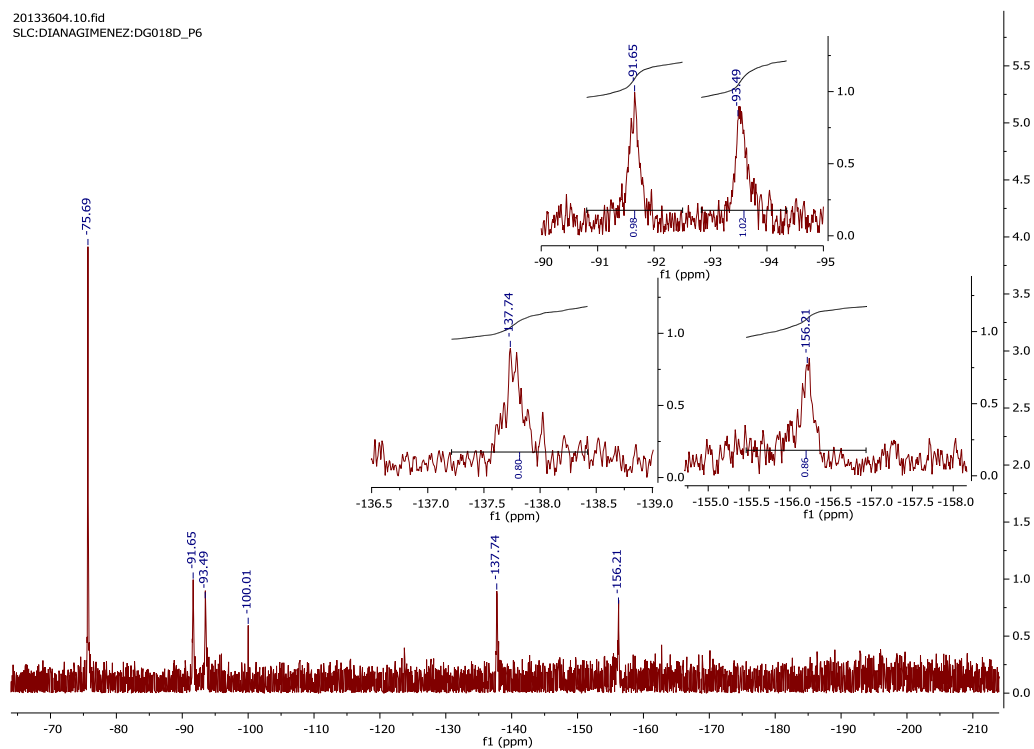
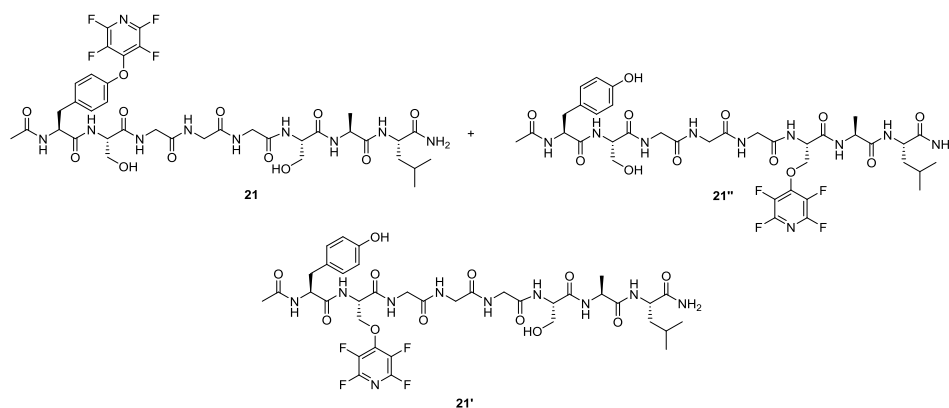


Figure SI51. ^{19}F NMR spectrum of compound **20** as recorded in $\text{H}_2\text{O}/\text{MeCN-d}_3$ 1:1 at room temperature.

Product 21 (Mixture of regioisomers).



Isolated mass: 6.5 mg (27%).

QToF LC/MS: Calculated m/z : 900.34, observed m/z : 901.34 $[M+H]^+$. Retention time: 2.667 min. Elemental composition: C₃₇ H₄₈ F₄ N₁₀ O₁₂.

QToF MS/MS:

Calculated m/z : 772.24 $[b7/b'7/b''7+H]^+$, 754.24 $[b7/b'7/b''7-H_2O+H]^+$, 701.20 $[b6/b'6/b''6+H]^+$, 683.20 $[b6/b'6/b''6-H_2O+H]^+$, 614.17 $[b5/b5''+H]^+$, 557.45 $[b4/b4''+H]^+$, 421.15 $[z'3+H]^+$, 403.15 $[z'3-H_2O+H]^+$ Da.

Observed m/z : 773.21 $[b7/b'7/b''7+H]^+$, 755.20 $[b7/b'7/b''7-H_2O+H]^+$, 702.18 $[b6/b'6/b''6+H]^+$, 683.16 $[b6/b'6/b''6-H_2O+H]^+$, 614.15 $[b5/b5''+H]^+$, 557.13 $[b4/b4''+H]^+$, 419.16 $[z'3+H]^+$, 401.15 $[z'3-H_2O+H]^+$ Da.

¹⁹F NMR (376 MHz, H₂O/MeCN-d₃ 1:1) δ -91.64 (m, 2F), -97.10 (m, 2F), -156.16 (m, 2F), -165.96 (m, 2F).

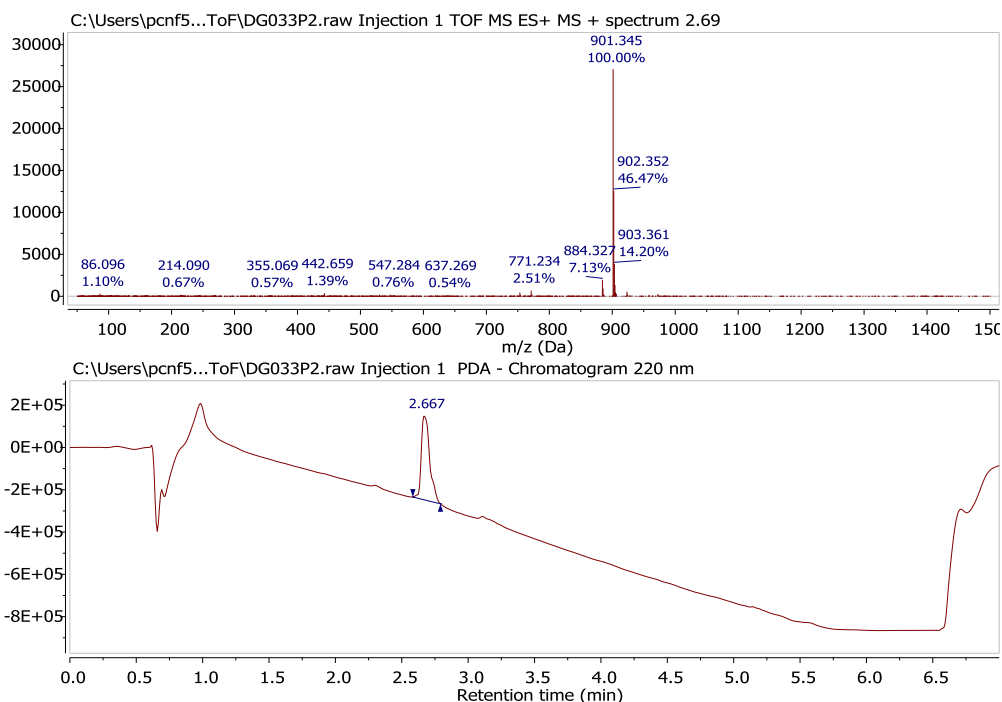


Figure SI52. Structure, high resolution QToF-LC/MS trace at $\lambda=220$ nm and composition of isolated compound **21**.

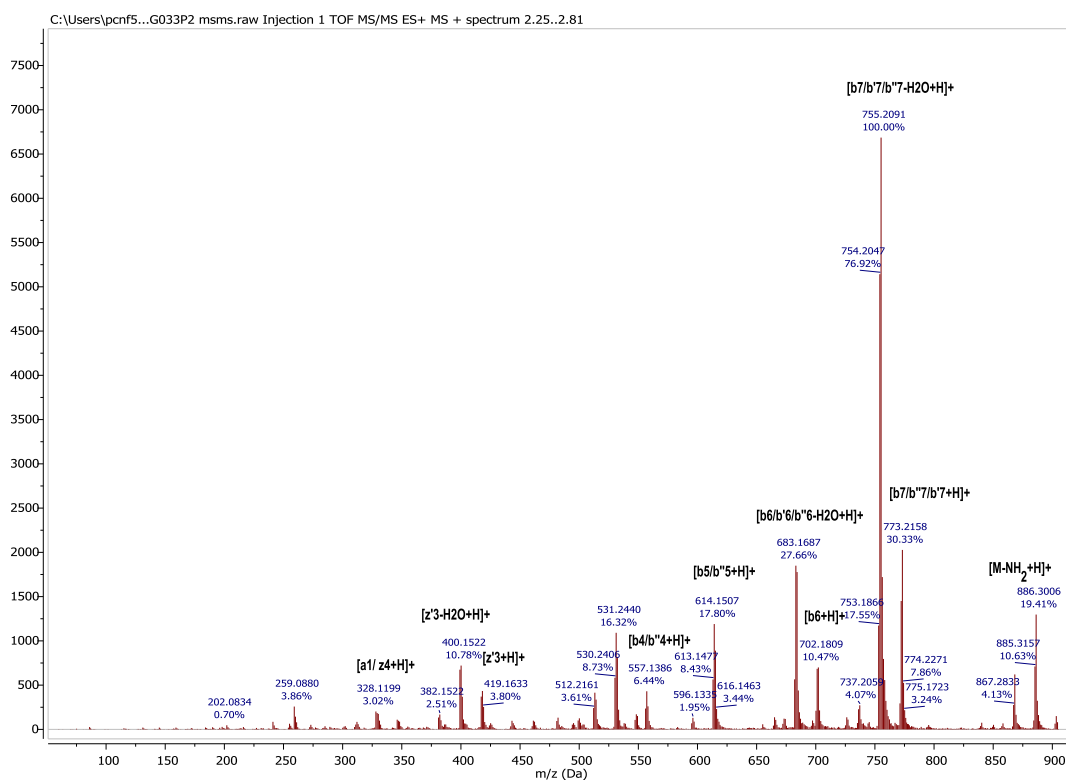


Figure SI53. MS/MS analysis of compound **21** showing its characteristic rupture pattern and the assignation of the main ions observed.

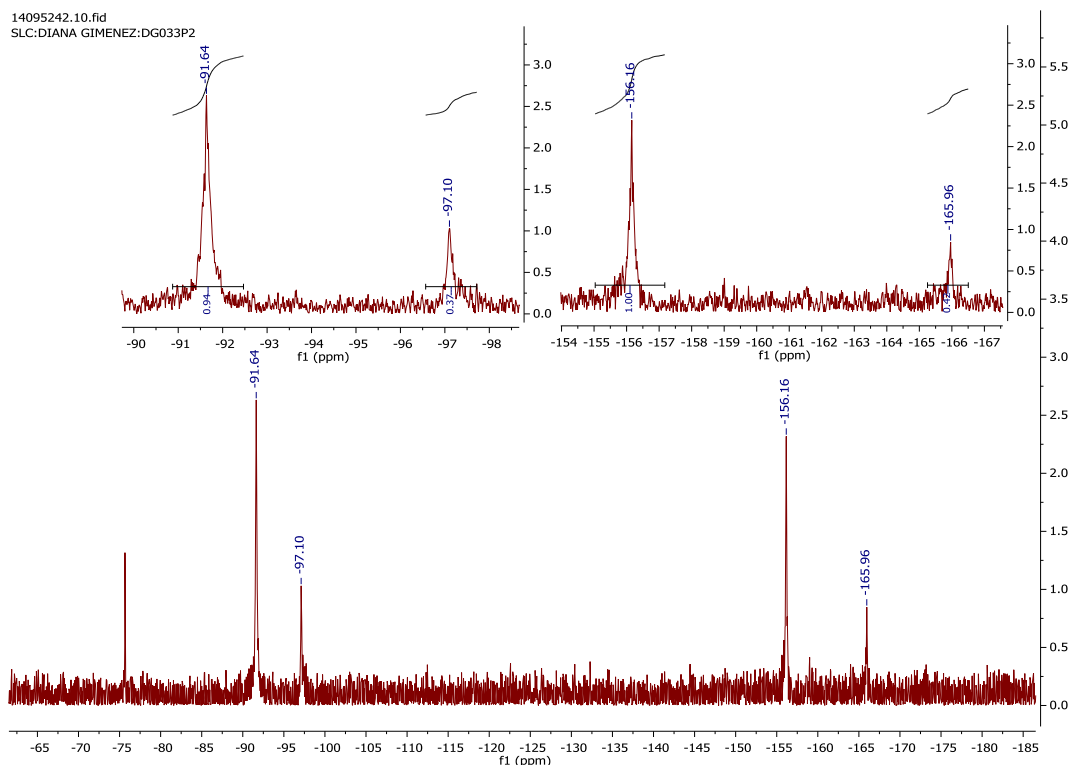
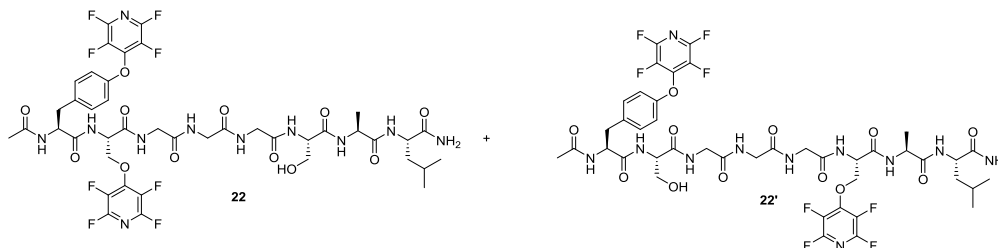


Figure SI54. ^{19}F NMR spectrum of compound **21** as recorded in $\text{H}_2\text{O}/\text{MeCN}-d_3$ 1:1 at room temperature.

Product 22 (Mixture of regioisomers).



Isolated mass: 2.7 mg (9 %).

QToF LC/MS: Calculated m/z : 1049.33, observed m/z : 1050.34 $[\text{M}+\text{H}]^+$. Retention time: 2.667 min. Elemental composition: $\text{C}_{42}\text{H}_{47}\text{F}_8\text{N}_{11}\text{O}_{12}$.

QToF MS/MS:

Calculated m/z : 921.23 $[\text{b}7/\text{b}'7+\text{H}]^+$, 903.22 $[\text{b}7/\text{b}'7-\text{H}_2\text{O}+\text{H}]^+$, 903.22 $[\text{b}7/\text{b}'7-4\text{fPyr}+\text{H}]^+$, 850.19 $[\text{b}6/\text{b}'6+\text{H}]^+$, 833.19 $[\text{b}6/\text{b}'6-\text{H}_2\text{O}+\text{H}]^+$, 683.57 $[\text{b}7/\text{b}'7-4\text{fPyr}+\text{H}]^+$, 613.18 $[\text{b}'5+\text{H}]^+$ Da.

Observed m/z : 922.20 $[\text{b}7/\text{b}'7+\text{H}]^+$, 904.19 $[\text{b}7/\text{b}'7-\text{H}_2\text{O}+\text{H}]^+$, 755.21 $[\text{b}7/\text{b}'7-4\text{fPyr}+\text{H}]^+$, 850.17 $[\text{b}6/\text{b}'6+\text{H}]^+$, 833.16 $[\text{b}6/\text{b}'6-\text{H}_2\text{O}+\text{H}]^+$, 680.23 $[\text{b}7/\text{b}'7-4\text{fPyr}+\text{H}]^+$, 614.15 $[\text{b}'5+\text{H}]^+$ Da.

^{19}F NMR (376 MHz, $\text{H}_2\text{O}/\text{MeCN}-d_3$ 1:1) δ -91.63 (m,2F), -93.39 (m,2F), -156.17 (m,2F), -159.31 (m,2F).

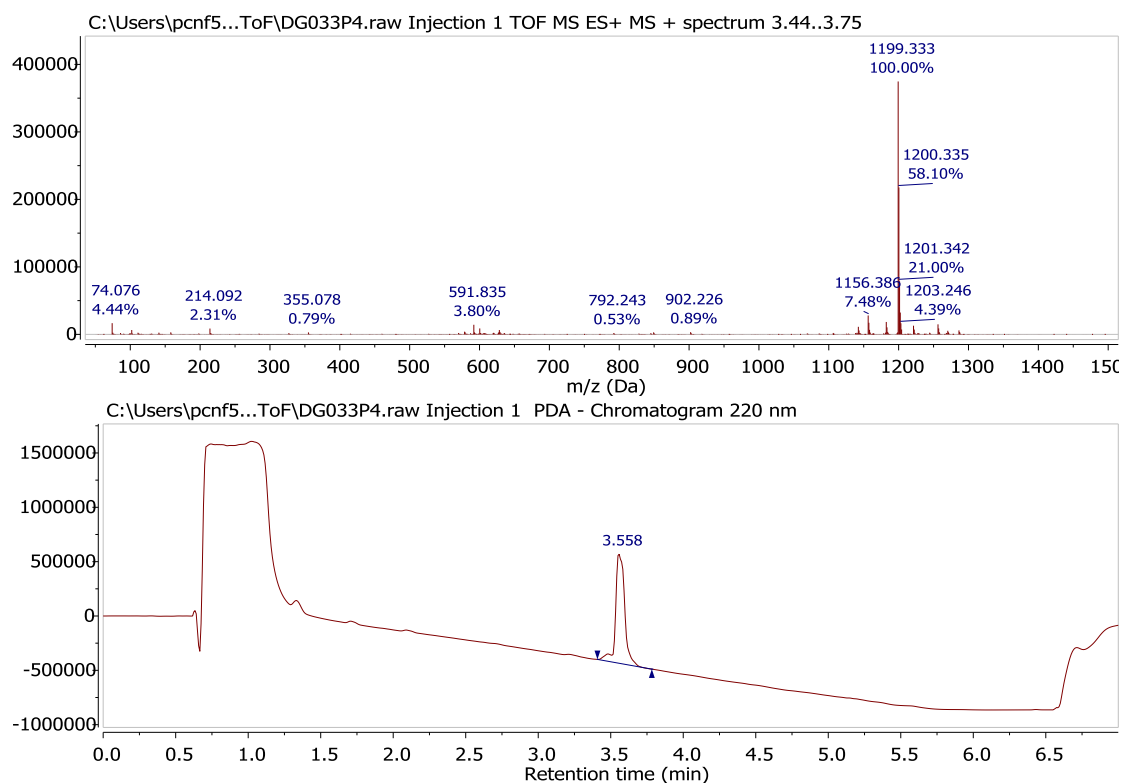


Figure SI58. Structure, high resolution QToF-LC/MS trace at $\lambda=220$ nm and composition of isolated compound **23**.

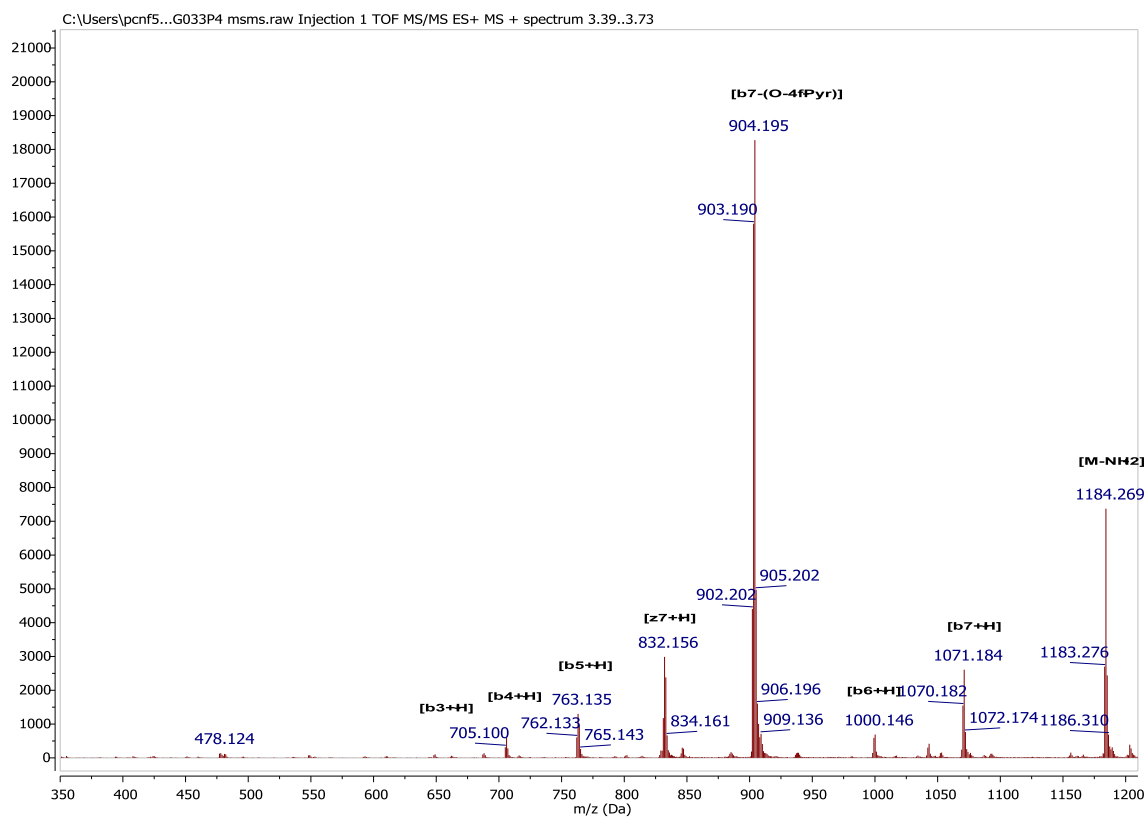


Figure SI59. MS/MS analysis of compound **23** showing its characteristic rupture pattern and the assignation of the main ions observed.

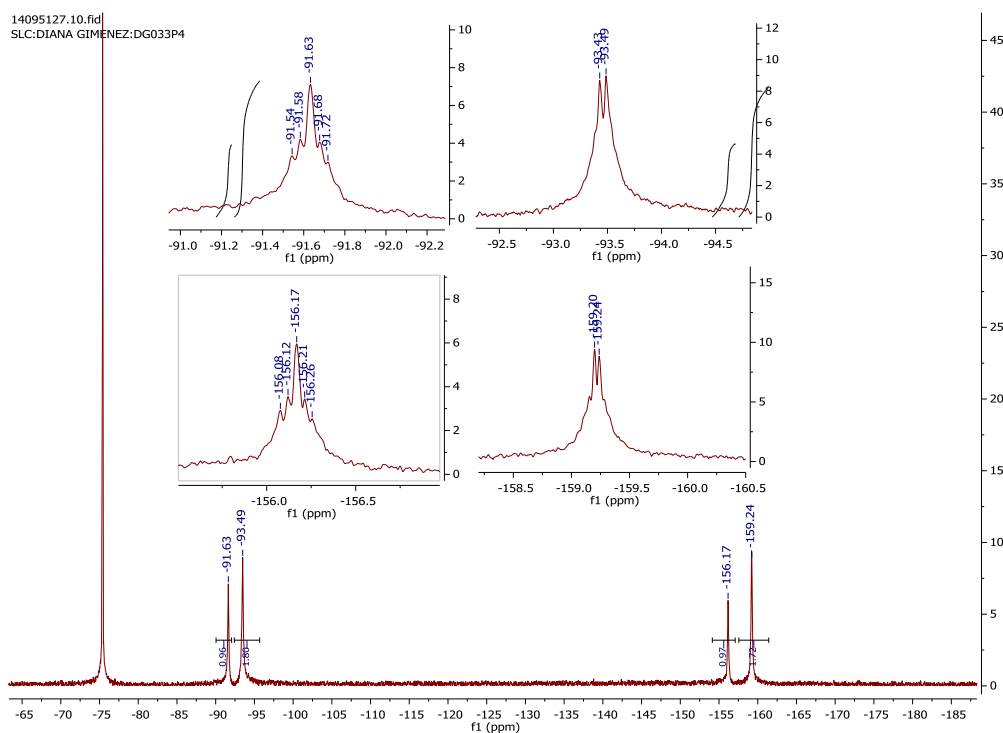


Figure SI60. ^{19}F NMR spectrum of compound **23** as recorded in $\text{H}_2\text{O}/\text{MeCN}-d_3$ 1:1 at room temperature.

Effect of perfluoro-tagging over Vasopresin and Oxytocin bio-stability:

General procedure for solution phase peptide tagging

Commercially available C-terminal amide oxytocin (**24**) and vasopressin (**25**) were purchased from Cayman Chemical Company and Apollo Scientific Ltd. respectively, and used as starting materials without further purification. In both cases 10 mg of the starting products were dissolved in 5 mL of DMF to which another 5 mL of a freshly made stock solution of DIPEA 50 mM in DMF was then added. Solutions were then placed in argon flushed syringes, and 25 equivalents of either pentafluoropyridine or tetrafluoropyridazine were slowly added. The systems were then allowed to react while vigorously shaking at room temperature for 4.5 h. After removal of DMF and volatiles under vacuum, the remaining oily residue was dissolved in $\text{H}_2\text{O}/\text{MeCN}$ (10 mL) and freeze-dried. Crude materials were characterised by LC/MS (ESI+) to confirm the presence of the desired products and further purified by semi-preparative HPLC (as described previously). Final pure compounds were further characterised by ^{19}F -NMR (2 mg/mL in CD_3CN), high resolution LC/MS-QToF and ion directed tandem mass spectrometry (MS/MS) in order to confirm the tagging positions at the tyrosine and N-terminus positions.

LC/MS analysis:

Oxytocin (**24**) arylation using pentafluoropyridine (**1**) and tetrafluoropyridazine (**3**) :

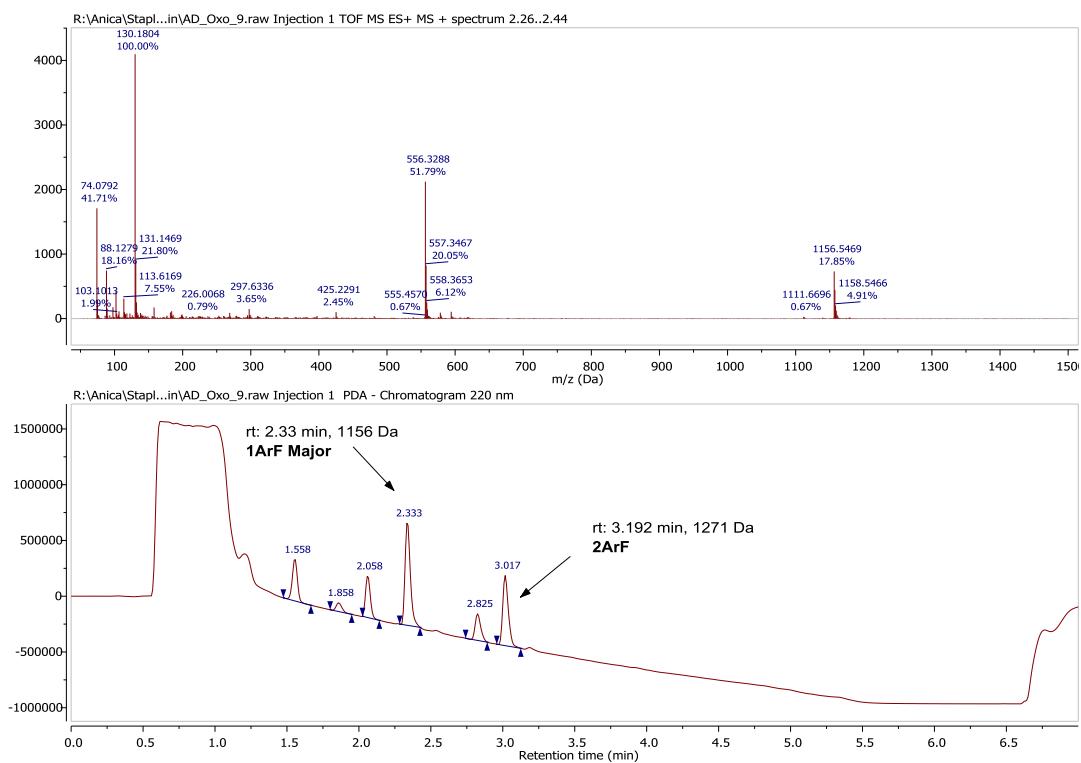


Figure SI61. LC/MS trace at $\lambda=220$ nm of crude reaction of Oxytocin with pentafluoropyridine (1) in the presence of DPEA as a base.

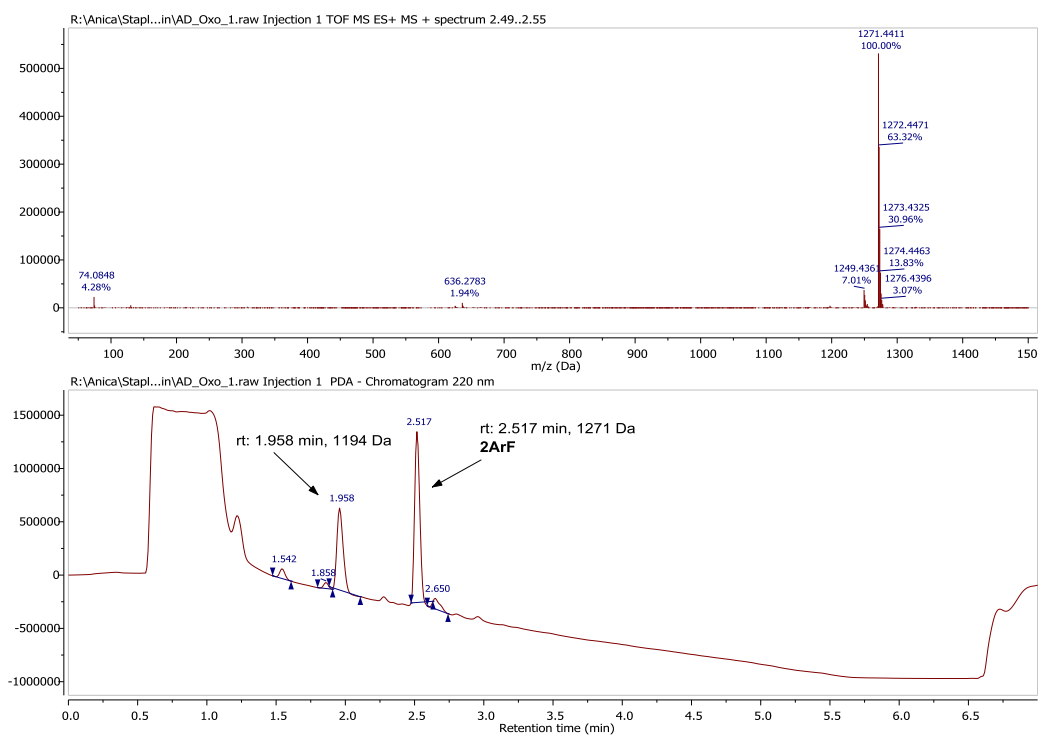


Figure SI62. LC/MS trace at $\lambda=220$ nm of crude reaction of Oxytocin with tetrafluoropyridazine (3) in the presence of DIPEA as a base.

Vasopressin (**25**) arylation using pentafluoropyridine (**1**) and tetrafluoropyridazine (**3**) :

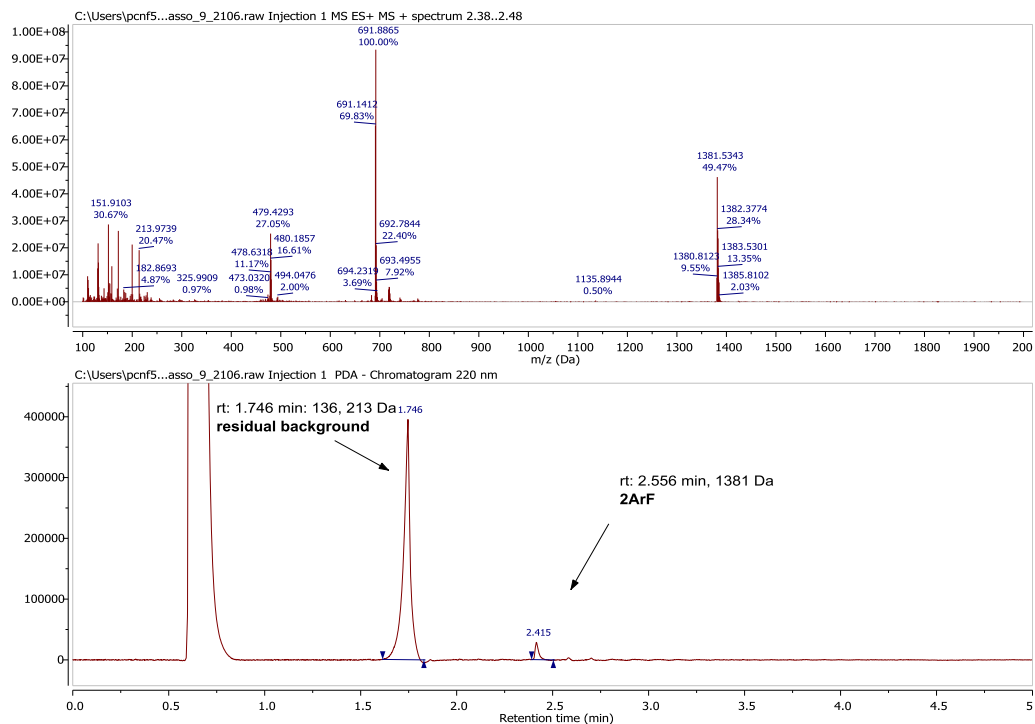


Figure SI63. LC/MS trace at $\lambda=220$ nm of crude reaction of Vasopressin with pentafluoropyridine (**1**) in the presence of DIPEA as a base.

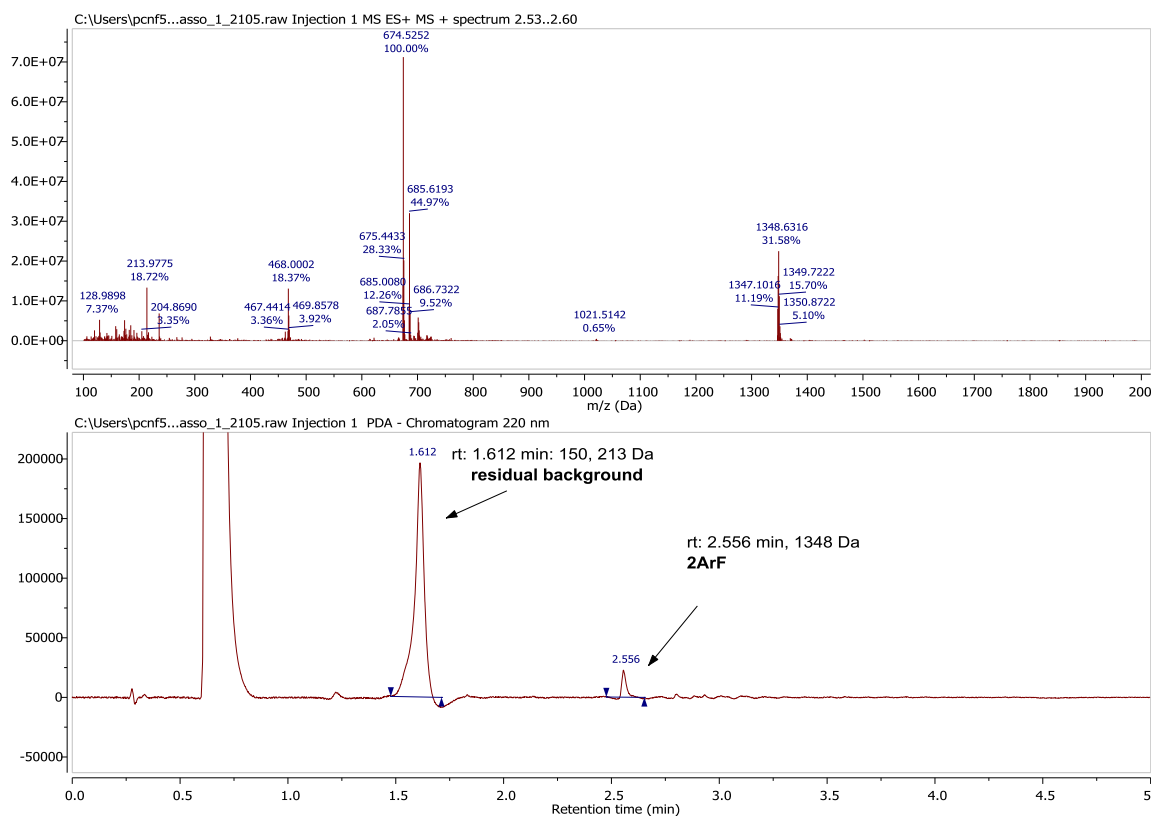
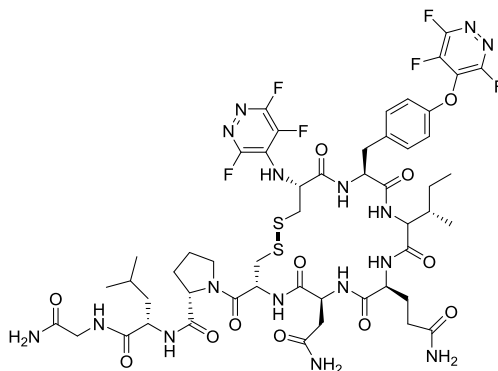


Figure SI64. LC/MS trace at $\lambda=220$ nm of crude reaction of Vasopressin with tetrafluoropyridazine (**3**) in the presence of DIPEA as a base.

Characterization of tetrafluoropyridazine-tagged analogues 26 and 27

Compound 26



Isolated mass: 4.6 mg (36%).

QToF LC/MS: Calculated m/z : 1270.43, observed m/z : 1271.42 $[M+H]^+$. Retention time: 2.858 min. Elemental composition: $C_{51} H_{64} F_6 N_{16} O_{12} S_2$.

QToF MS/MS:

Calculated m/z : 1198.38 $[b8+H]^+$, 1085.30 $[b7+H]^+$, 988.25 $[b6+H]^+$, 960.25 $[a6+H]^+$, 284.18 $[y3+H]^+$ Da.

Observed m/z : 1199.38 $[b8+H]^+$, 1086.29 $[b7+H]^+$, 989.25 $[b6+H]^+$, 961.25 $[a6+H]^+$, 285.19 $[y3+H]^+$ Da.

^{19}F NMR (376 MHz, $MeCN-d_3$): δ -88.15 (1F), -89.18 (1F), -95.84 (1F), -102.08 (1F), -140.29 (1F), -151.91 (1F).

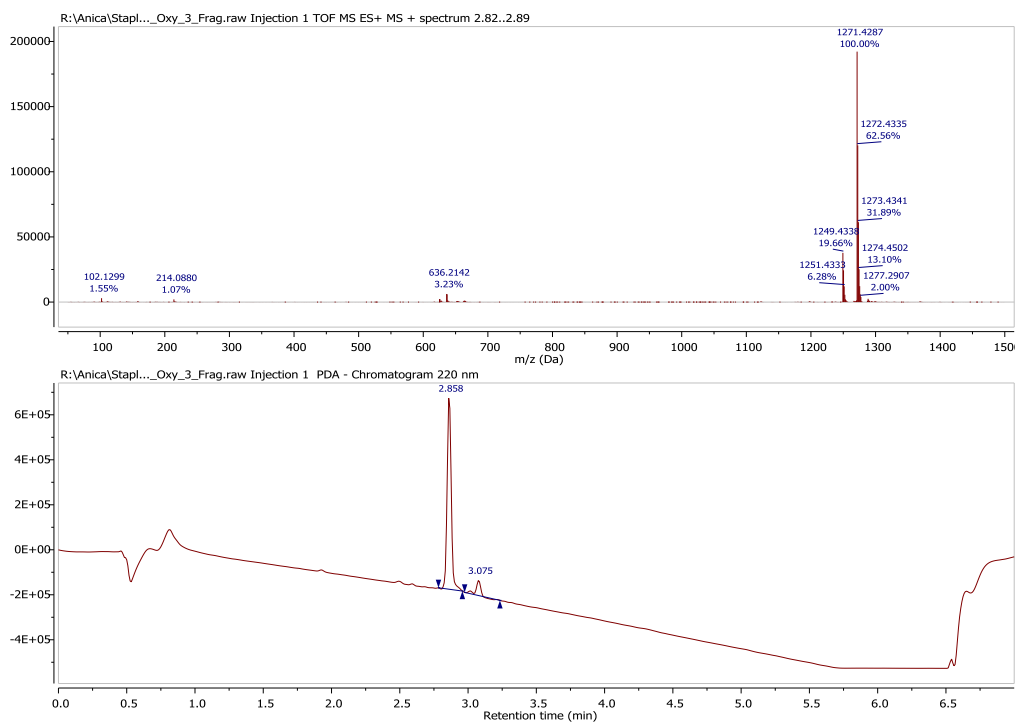


Figure SI65. Structure, high resolution QToF-LC/MS trace at $\lambda=220$ nm and composition of isolated compound **26**.

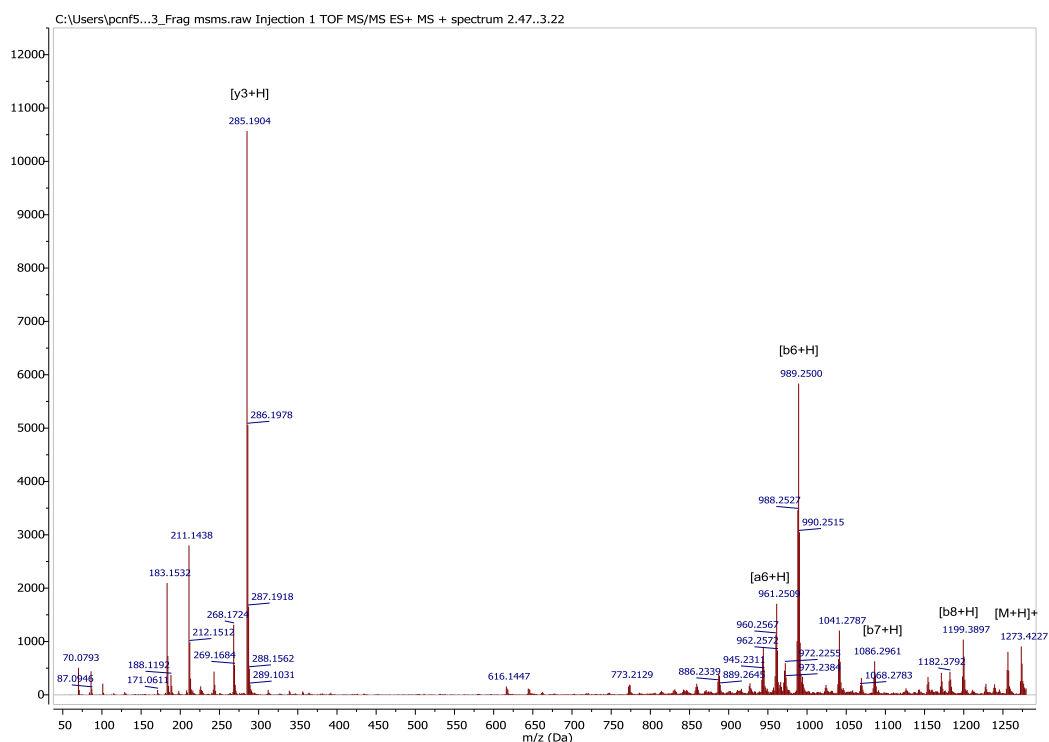


Figure SI66. MS/MS analysis of compound **26** showing its characteristic rupture pattern and the assignment of the main ions observed.

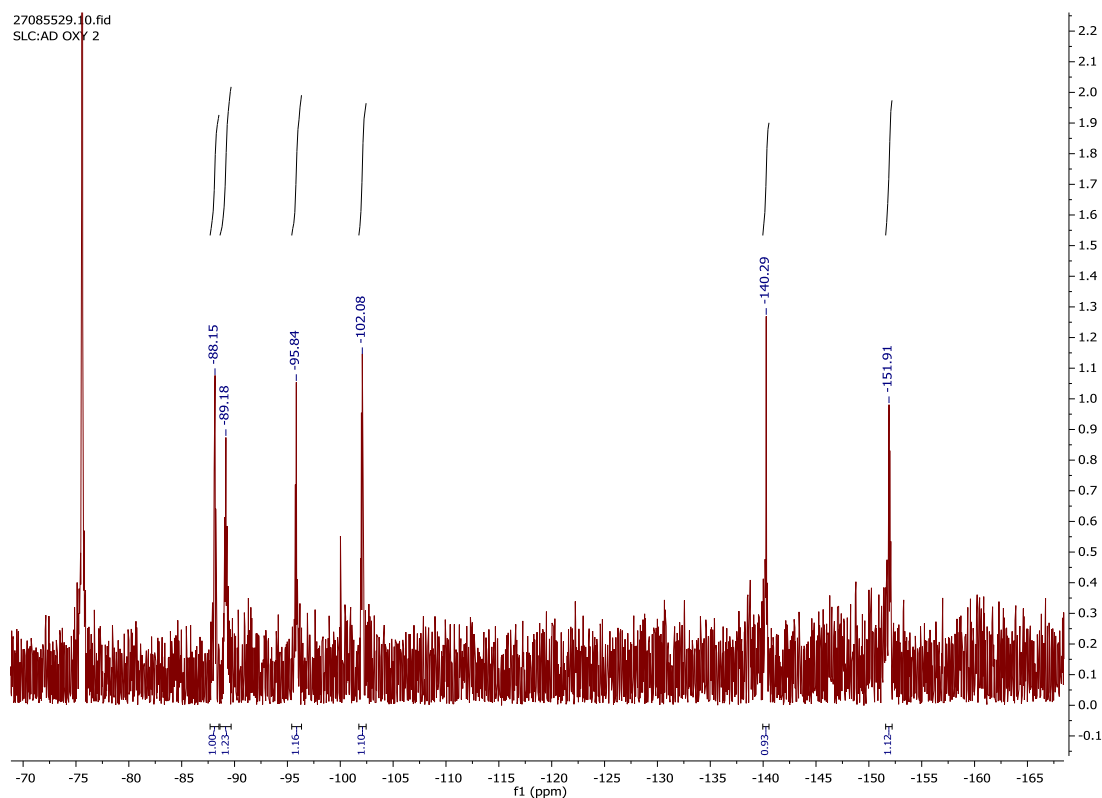
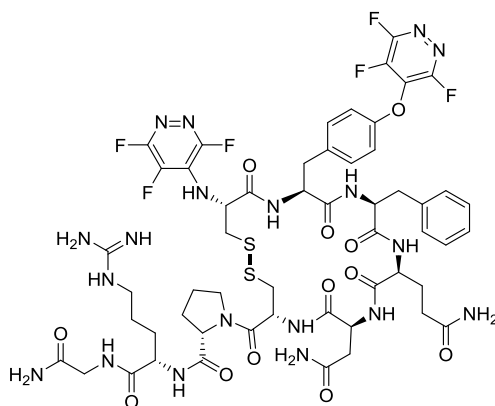


Figure SI67. ^{19}F NMR spectrum of compound **26** as recorded in MeCN-d_3 at room temperature.

Compound 27



Isolated mass: 5.4 mg (43%).

QToF LC/MS: Calculated m/z : 1347.42, observed m/z : 1348.43 $[\text{M}+\text{H}]^+$. Retention time: 2.300 min. Elemental composition: $\text{C}_{54}\text{H}_{63}\text{F}_6\text{N}_{19}\text{O}_{12}\text{S}_2$.

QToF MS/MS:

Calculated m/z : 1022.23 $[\text{b}_6+\text{H}]^+$, 920.23 $[\text{b}_5+\text{H}]^+$, 806.19 $[\text{b}_4+\text{H}]^+$, 786.34 $[\text{z}_7-\text{NH}_3+\text{H}]^+$, 678.13 $[\text{b}_3+\text{H}]^+$, 531.06 $[\text{b}_2+\text{H}]^+$, 503.06 $[\text{a}_3+\text{H}]^+$, 327.19 $[\text{y}_3+\text{H}]^+$, 310.18 $[\text{y}_3+\text{NH}_3+\text{H}]^+$, 213.12 $[\text{y}_2-\text{NH}_3+\text{H}]^+$ Da.

Figure SI69. MS/MS analysis of compound **27** showing its characteristic rupture pattern and the assignation of the main ions observed.

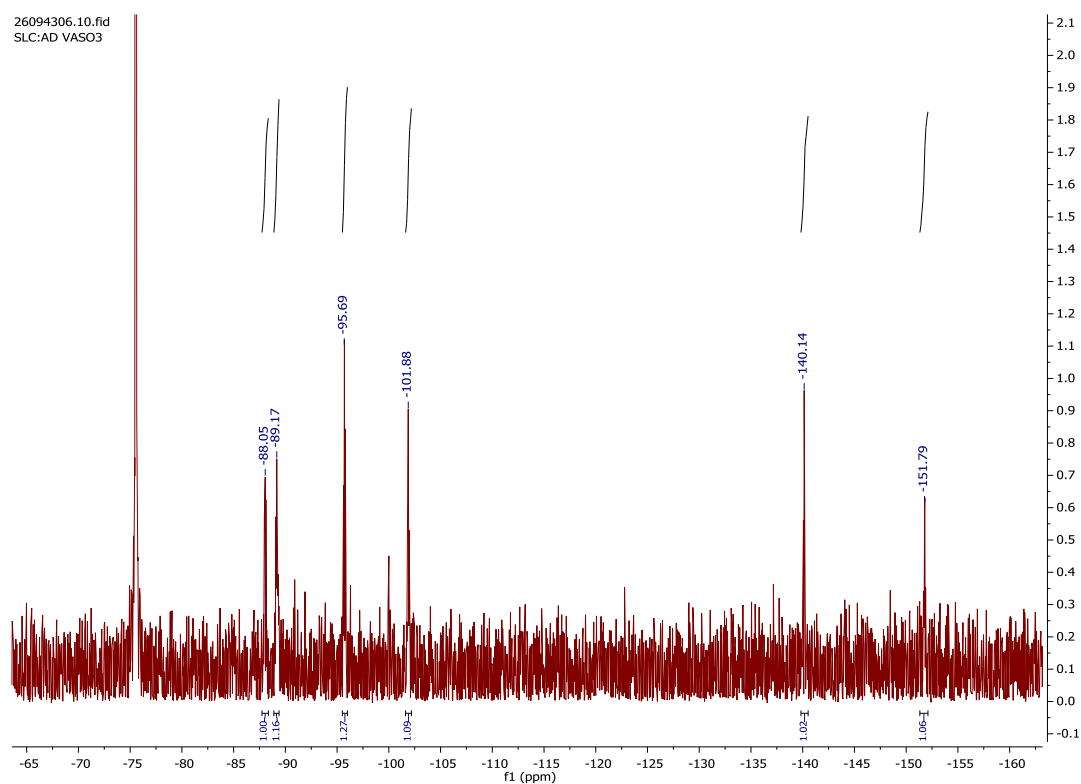


Figure SI70. ^{19}F NMR spectrum of compound **27** as recorded in MeCN-d_3 at room temperature.

General procedure for in vitro digestion using Chymotrypsin

For bio-stability assays α -chymotrypsin, from bovine pancreas, was purchased from Sigma-Aldrich. For digestion, peptides were dissolved in a stock solution of Tris buffer (25mM, pH: 7.6) up to a concentration of 1 mg/mL concentration. Simultaneously a freshly made stock solution of enzyme in the same chilled buffer was prepared. The samples were immediately prepared by mixing in an eppendorf an aliquot of 100 μL of peptide solution with the corresponding amount of enzyme stock solution to lead a final peptide to enzyme ratio of 25:1. The sample mixtures were then incubated in a thermally controlled water bath at 20°C for a minimum of 24 h. During the incubation time, 15 μL aliquots of sample mixture were withdrawn at different times, quenched at once with 15 μL of 30% MeCN/TFA solution and analyzed by analytical reverse phase HPLC, employing a X-Bridge C_{18} column (5.3 μm , 4.6 x 100 mm, 40°C) in a Pelkin-Elmer 200 series lc system supplied with auto-sampler, UV/Vis detector and a Peltier column oven. In all samples a linear gradient rising from eluent A (95:5:0.05% H_2O :MeCN:TFA) to 100% of eluent B (5:95:0.03% H_2O :MeCN:TFA) during $t=30$ min plus 5 min of isocratic B elution was applied at a constant flow rate of 1 mL/min. Detection was performed at $\lambda=220$ nm. In order to properly analyze the evolution of digested peptide, and due to the fact that in some cases close proximity did not permit a direct integration of well resolved

peaks, the signals corresponding to both peptide and enzyme in the raw chromatograms were baseline corrected and then fitted into separate Gaussian equations using Origin8 software. The area enclosed by each function was taken as the peak neat integrated area. The ratio of non-digested peptide is then estimated as:

$$\textit{Peptide Ratio} = \frac{[\textit{Peptide Area/Enzyme Area}]_t}{[\textit{Peptide Area/Enzyme Area}]_{t=0}}.$$

For each peptide a minimum of two independent assays were performed, and the final Peptide Ratio vs Incubation time analyzed in terms of an exponential decay behavior where:

$$\textit{Peptide Ratio} = y_0 + Ae^{-kt}$$

allowing the comparison of the resulting fitted models. Note that due to enzyme aggregation, the proposed method may be only valid for the short initial times window.

In order to discard possible peptide degradation during experimental time, control samples were run by subjecting each peptide to the same procedure and conditions using the corresponding volume of Tris buffer instead of enzyme solution. In any case degradation of the starting materials was observed.

In vitro bio-stability of non-tagged Oxytocin 24

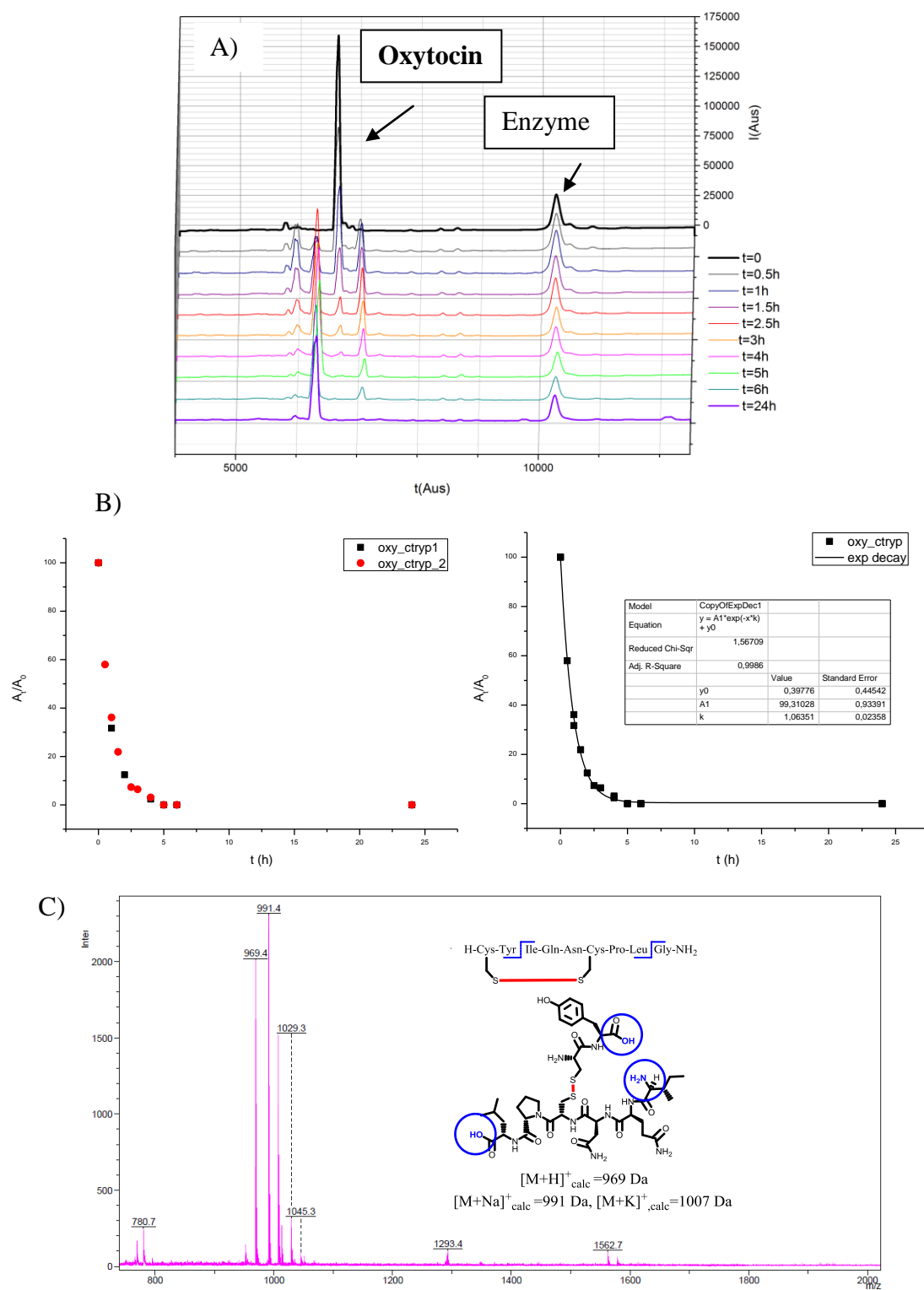


Figure SI71. A) HPLC traces showing the progression of parent oxytocin (24) digestion in the presence of chymotrypsin ($\lambda = 220$ nm). B) Experimental points (n=2) and exponential fit showing the ratio of non-digested peptide left in the sample with the incubation time. C) Maldi-ToF analysis of the final digested products after 24h of incubation.

In vitro bio-stability of perfluoro-tagged Oxytocin **26**

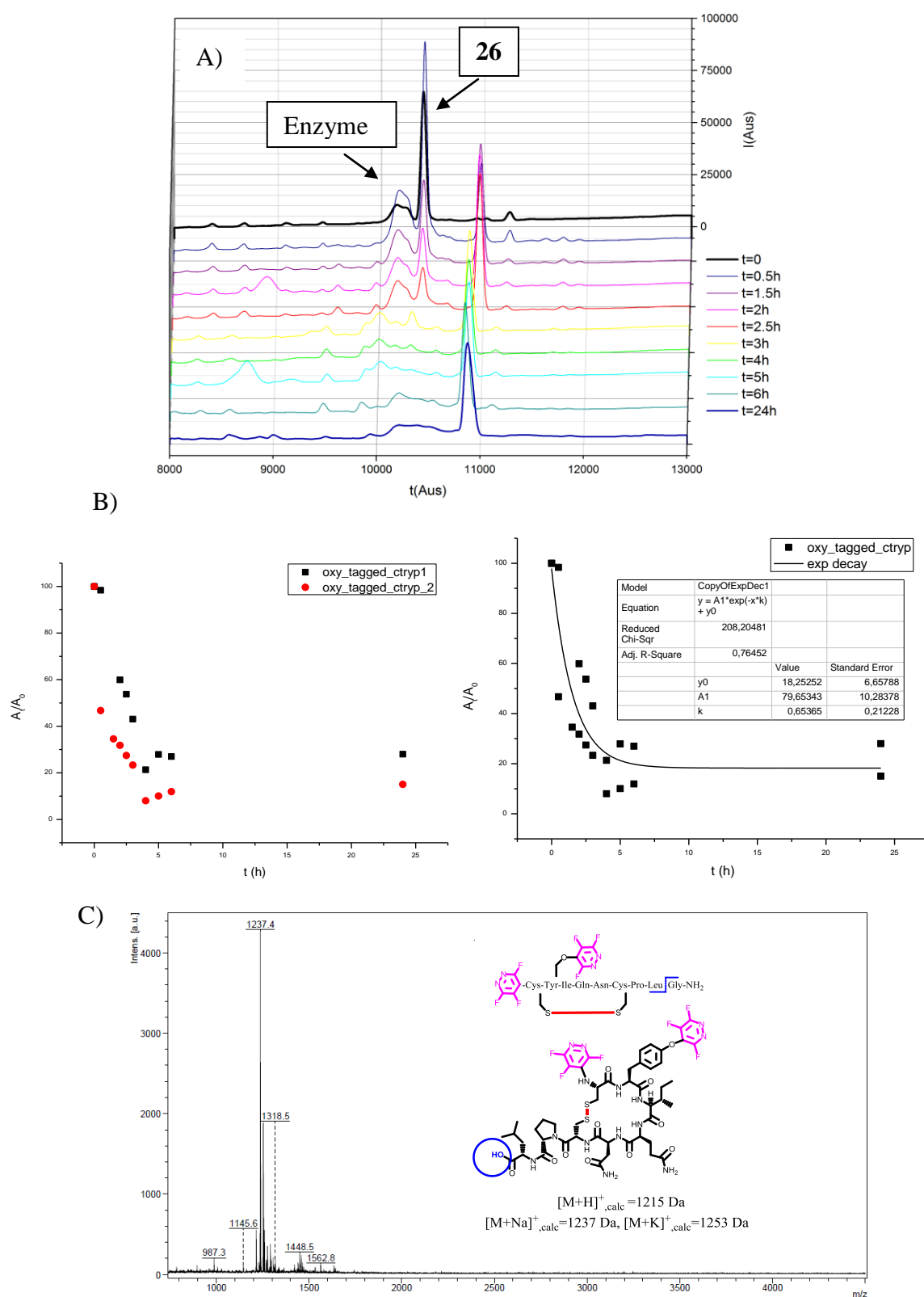


Figure SI72. A) HPLC traces showing the progression of perfluoro-tagged oxytocin (**26**) digestion in the presence of chymotrypsin ($\lambda = 220$ nm). B) Experimental points (n=2) and exponential fit showing the ratio of non-digested peptide left in the sample with the incubation time. C) Maldi-ToF analysis of the final digested products after 24h of incubation.

In vitro bio-stability of non-tagged Vasopressin 25

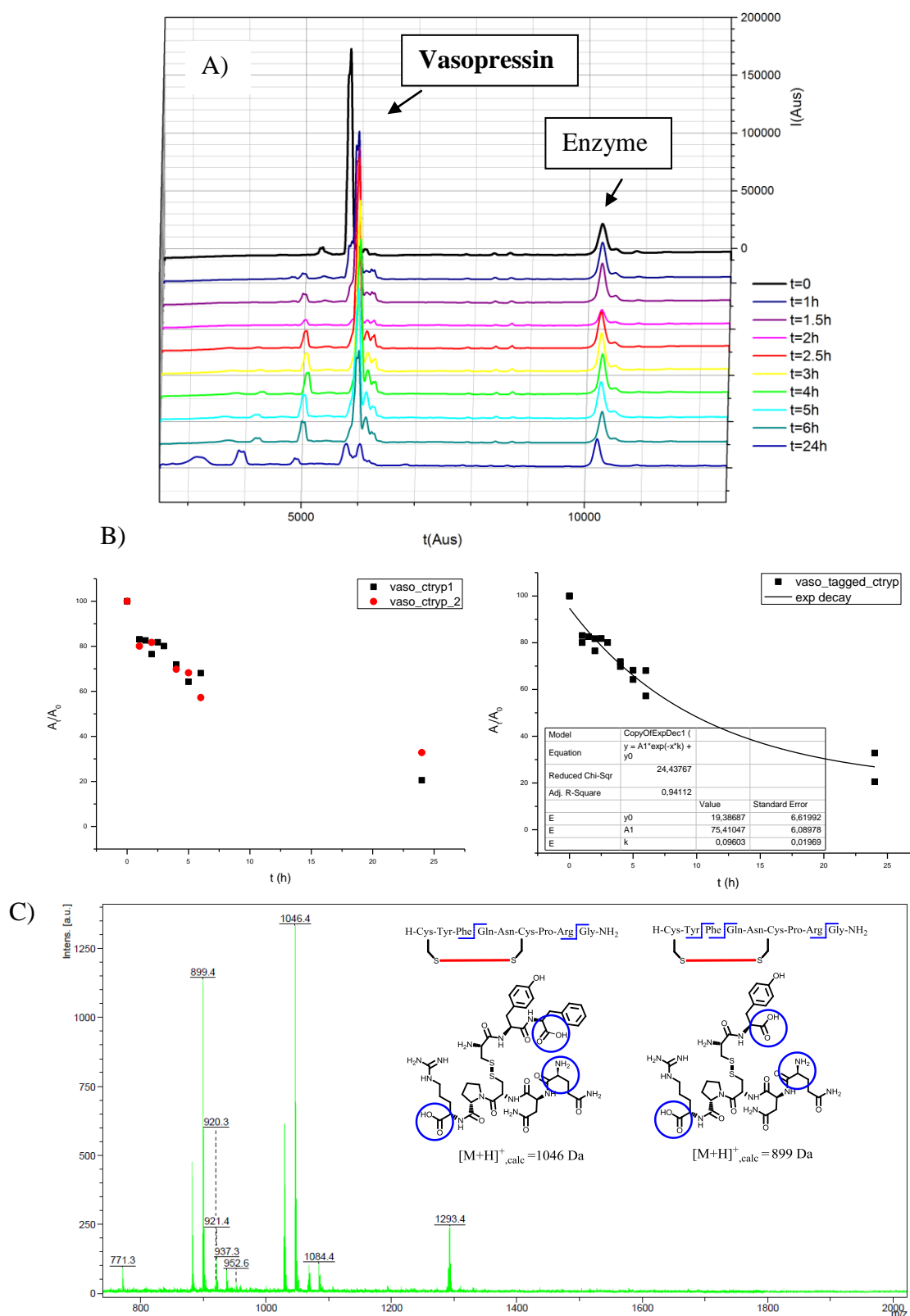


Figure SI73. A) HPLC traces showing the progression of parent vasopressin (**25**) digestion in the presence of chymotrypsin ($\lambda = 220$ nm). B) Experimental points (n=2) and exponential fit showing the ratio of non-digested peptide left in the sample with the incubation time. C) MALDI-ToF analysis of the final digested products after 24h of incubation.

In vitro bio-stability of perfluoro-tagged Vasopressin 27

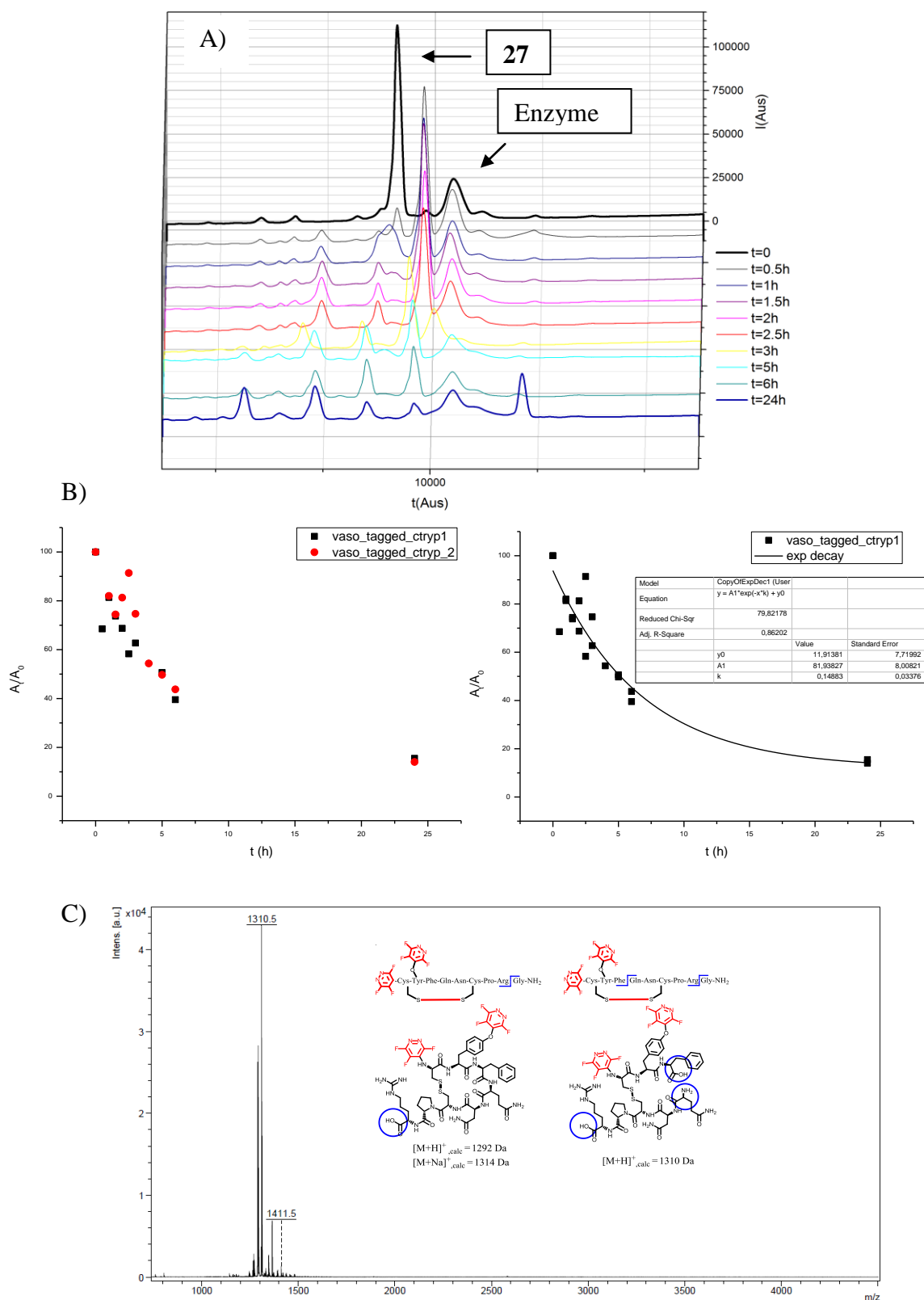
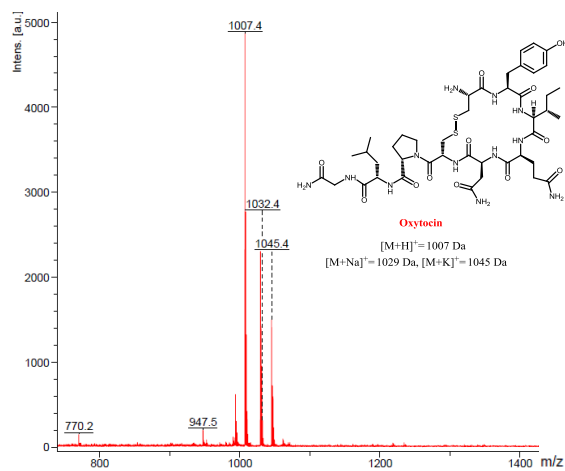
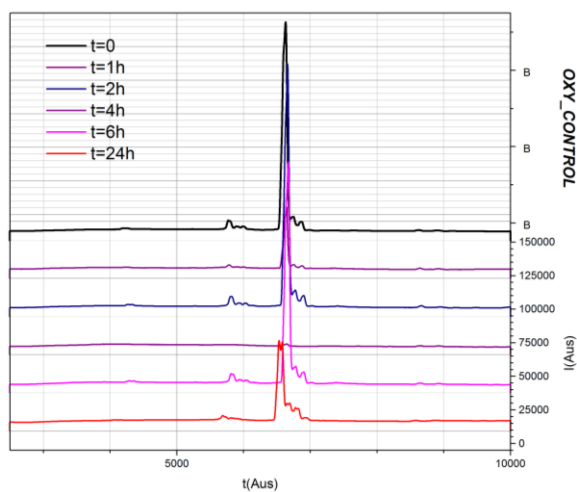


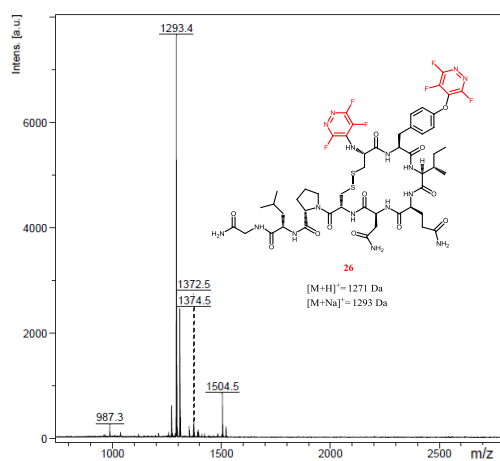
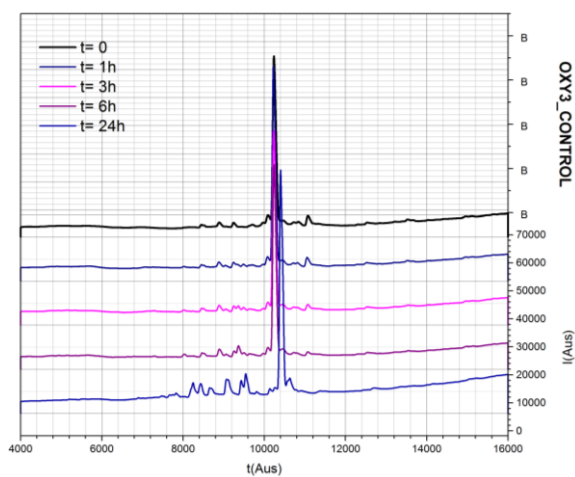
Figure SI74. A) HPLC traces showing the progression of perfluoro-tagged vasopressin (**27**) digestion in the presence of chymotrypsin ($\lambda = 220$ nm). B) Experimental points (n=2) and exponential fit showing the ratio of non-digested peptide left in the sample with the incubation time. C) Maldi-ToF analysis of the final digested products after 24h of incubation.

Control digestions (no enzyme):

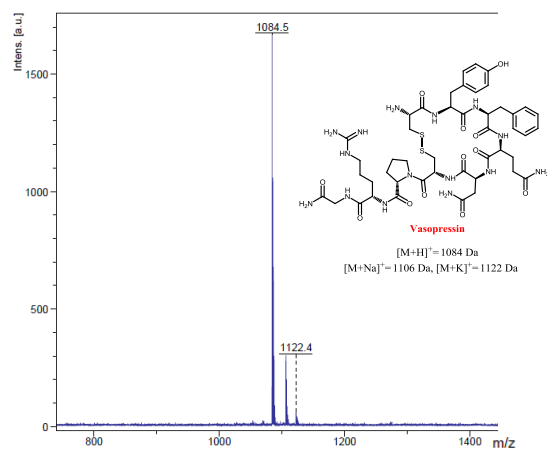
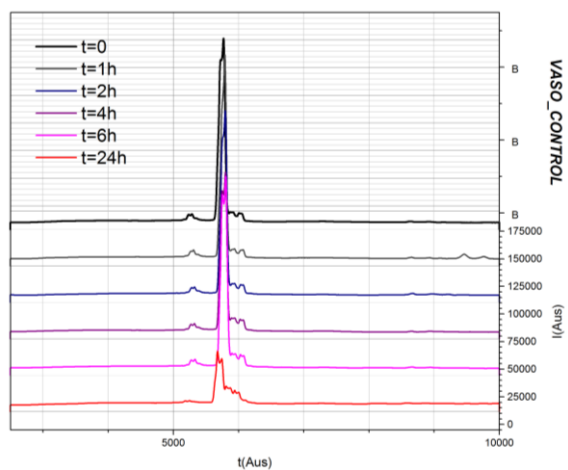
A)



B)



C)



D)

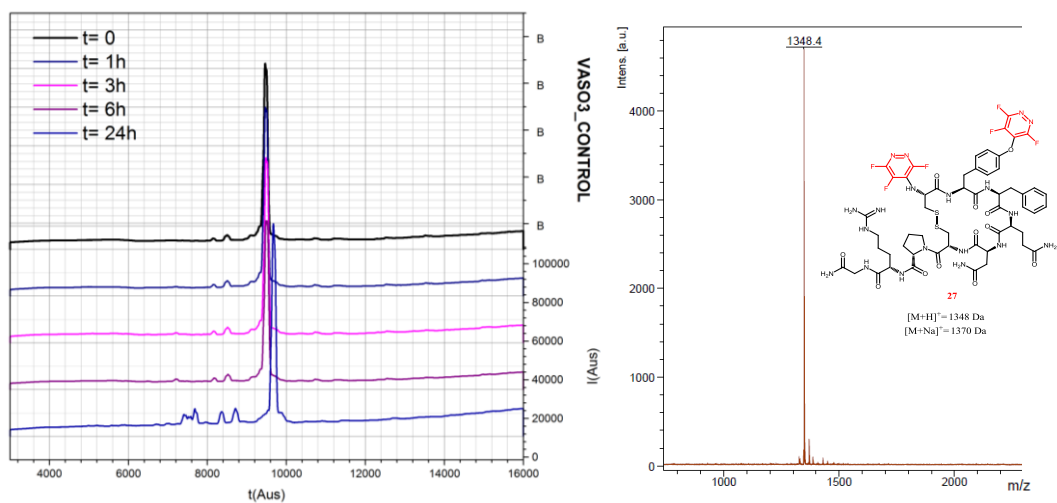


Figure SI75. Control reactions showing the HPLC trace progression and the final Maldi-ToF analysis after 24 h of incubation at 20°C in the absence of chymotrypsin. A) parent oxytocin **24**, B) “tagged” analogue **26**, C) parent vasopressin **25** and D) “tagged” vasopressin **27**.